THE UNIVERSITY of EDINBURGH

This thesis has been submitted in fulfilment of the requirements for a postgraduate degree (e.g. PhD, MPhil, DClinPsychol) at the University of Edinburgh. Please note the following terms and conditions of use:

Probing Spatial and Subunit-dependent Signalling by the NMDA Receptor

by

Sean McKay, BSc

A thesis submitted for The degree of Doctor of Philosophy
at The University of Edinburgh
August 2014

College of Medicine and Veterinary Medicine
University of Edinburgh
Supervisor: Professor Giles Hardingham
2nd Supervisor: Professor David Wyllie

Declaration

I hereby declare that the majority of the following work is my own, with the contributions of others indicated where appropriate. This work has bot been submitted for any other degree or professional qualification.

Sean McKay

Abstract

NMDARs are ligand-gated cation channels which are activated by the neurotransmitter glutamate. NMDARs are essential in coupling electrical activity to biochemical signalling as a consequence of their high Ca^{2+} permeability. This Ca^{2+} influx acts as a secondary messenger to mediate neurodevelopment, synaptic plasticity, neuroprotection and neurodegeneration. The biological outcome of NMDAR activation is determined by a complicated interrelationship between the concentration of Ca^{2+} influx, NMDAR location (synaptic vs. extrasynaptic) as well as the subtype of the GluN2 subunit. Despite the recognition that NMDAR mediated physiology is multifaceted, tools used to study subunit and location dependent signalling are poorly characterized and in other cases, non-existent. Therefore, the aim of this thesis is to address this issue.

Firstly, I assessed the current pharmacological approach used to selectively activate extrasynaptic NMDARs. Here, synaptic NMDARs are first blocked with MK-801 during phasic activation and then extrasynaptic NMDARs are tonically activated. This approach relies on the continual irreversible blockade of synaptic NMDARs by MK-801 yet contrary to the current dogma, I demonstrate this blockade is unstable during tonic agonist exposure and even more so when physiologically relevant concentrations of Mg^{2+} are present. This confines a temporal limit in which selective activation of extrasynaptic NMDARs can occur with significant consequences for studying synaptic vs. extrasynaptic NMDAR signalling.

Dissecting subunit-dependent signalling mediated by the two major GluN2 subunits in the forebrain, GluN2A and GluN2B, has been advanced significantly by selective GluN2B antagonism yet a reciprocal GluN2A selective antagonist has been lacking. Utilizing novel GluN2A-specific antagonists, I demonstrate a developmental upregulation of GluN2A-mediated NMDA currents which concurrently dilutes the contribution of GluN2B-mediated currents. Moreover, I tested the hypothesis that the C-terminus of GluN2A and GluN2B are essential in controlling the developmental switch of GluN2 subunits utilizing knock-in mice whereby the C-terminus of GluN2A is replaced with that of GluN2B. Surprisingly, the exchange of the C-terminus does not impede the developmental switch in subunits nor the proportion of NMDARs at synaptic vs extrasynaptic sites. However, replacing the C-terminus of GluN2A with that of GluN2B induces a greater neuronal vulnerability to NMDA-dependent excitotoxicity.

Collectively, this work enhances our understanding of the complex physiology mediated by the NMDAR by determining how pharmacological tools are best utilized to study the roles of NMDAR location and subunit composition in addition to revealing the importance of the GluN2 C-terminus in development and excitotoxicity.

Table of Contents

Chapter 5: The role of the GluN2 C-termini in the expression of GluN2 subtypes, excitotoxicity and neuroprotection..110

Abbreviations

AMPAR	AMPA receptor
CaMKII	Ca2+/calmodulin-dependent protein kinase II
CREB	c-AMP response element binding protein
CNS	central nervous system
DAPI	4',6-diamidino-2-phenylindole
DIV	days in vitro
GluR	glutamate receptor
ifenprodil	4-[2-[4-(cyclohexylmethyl)- 1-piperidinyl]-1-hydroxypropyl]phenol
LTD	long-term depression
LTP	long term potentiation
MAGUK	membrane-associated guanylate kinase
mEPSC	miniature excitatory postsynaptic current
mGluR	metabotropic glutamate receptor
MK-801	(+)-5-methyl-10,11-dihydro-5H-dibenzo [a,d] cyclohepten-5,10-imine
NMDA	N-methyl-D-aspartate
NMDAR	NMDA receptor
GluN2A-/-	GluN2A knockout (mouse)
GluN2B/-	GluN2Bknockout (mouse)
GluN2A$^{(2BCTR)}$	GluN2A-2B-C-terminal swap
GluN2B$^{(2ACTR)}$	GluN2B-2A-C-terminal swap
NVP-AAM077	(R)-[(S)-1-(4-Bromo-phenyl)-ethylamino]-(2,3-dioxo-1,2,3,4-
pDNA	plasmid DNA
PKA	cAMP-dependent protein kinase A

PSD	postsynaptic density
TTX	tetrodotoxin
VGCC	voltage-gated calcium channel

Chapter 1

Introduction

Introduction

Glutamate is the major excitatory neurotransmitter in the mammalian central nervous system (CNS). At the postsynaptic membrane, glutamate can activate a host of receptors as summarized in **Figure 1.1**.

```
                        ┌─────────────────────┐
                        │ Glutamate Receptors │
                        └─────────────────────┘
                                   │
              ┌────────────────────┴────────────────────┐
    ┌───────────────────┐                    ┌───────────────────────┐
    │ Ionotropic Glutamate│                  │ Metabatropic Glutamate│
    │     Receptors       │                  │       Receptors        │
    └───────────────────┘                    └───────────────────────┘
```

| Ionic Permeability: $Na^+ > Ca^{2+}$ | Ionic Permeability: $Ca^{2+} > Na^+$ | G_q Type | $G_{i/o}$ Type |

| Kainate Receptors | NMDA Receptors | Group I -mGluR$_1$ - mGluR$_5$ | Group II & III |

| AMPA receptors containing GluA2 subunit | AMPA receptors lacking GluA2 subunit | | |
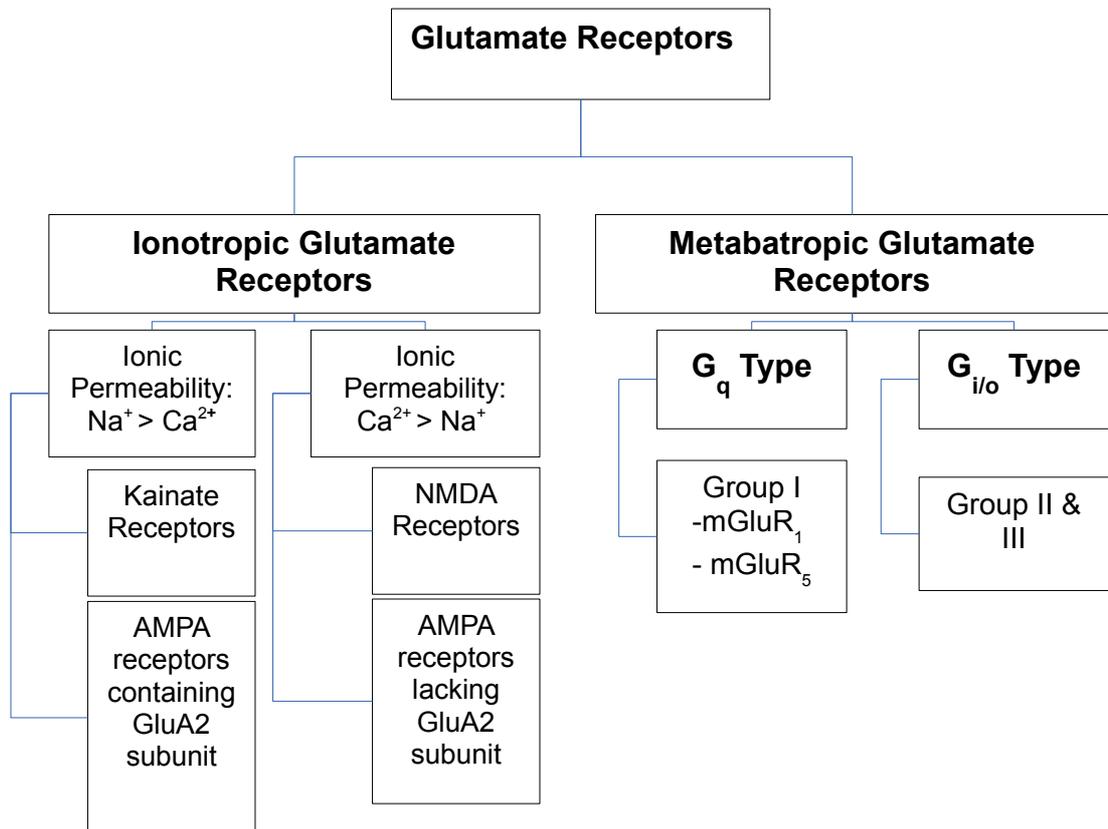
Figure 1.1: Summary of receptors activated by the neurotransmitter glutamate. The receptors can largely be split into groups where one class conducts ions on activation of glutamate (ionotropic) and the other relays chemical messengers (metabotropic).

GluA2-containing AMPA receptors and kainate receptors are highly permeable to Na^+ and are thus suited to generating fast excitatory transmission in accordance with the Hodgin-Huxley model (Destexhe et al. 1995). Activation of NMDA

receptors (NMDARs), AMPA receptors lacking the GluA2 subunit, and group I metabotropic receptors all cause an increase in post-synaptic Ca^{2+} levels. This is noteworthy as Ca^{2+} can act as a secondary messenger in order regulate a wide array of brain functions; the divalency, ionic radius and complex electron shell configuration of Ca^{2+} makes it suited to induce conformational changes in proteins (Bading 2013).

Ca^{2+} signalling by NMDARs is now well established to be involved in important physiological functions such as learning and memory in addition to pathological conditions such as stroke and neurodegenerative diseases (Giles E Hardingham & Bading 2010). Furthermore, in recent years, it has become ever more apparent that the dysregulation of NMDARs is involved in a number of epileptic and neuropsychiatric disorders (Lakhan et al. 2013).

The aim of this thesis is to aid in elucidating the complex signalling by NMDARs with particular focus on spatial and subunit-specific signalling by the NMDAR. Therefore, this introduction will cover the following regarding the NMDAR: structure and how it relates to its function; temporal and spatial patterns of subunit expression during development; pharmacology; neuroprotective and neuronal death signalling; learning & memory, and finally, its role in diseases.

1.1 The Relevance of NMDAR Structure in Relation to its Function

1.1.1 NMDA subunit structure

In the forebrain, most NMDARs are tetrameric ion channels consisting of two GluN1 subunits and two GluN2 subunits. The arrangement of the subunits has previously been contentious; evidence existed for an adjacent/"1/1/2/2" (Balasuriya et al. 2013) or alternating/"1/2/1/2" (Riou et al. 2012) subunit configuration. However, the recent determination of the X-ray crystal structure of the NMDAR unequivocally confirms the subunit arrangement is alternate (Lee et al. 2014). The structure of the NMDAR subunit is illustrated in **Figure 1.2**; a brief summary of each component shall be given below and elaborated on in further sections where necessary.
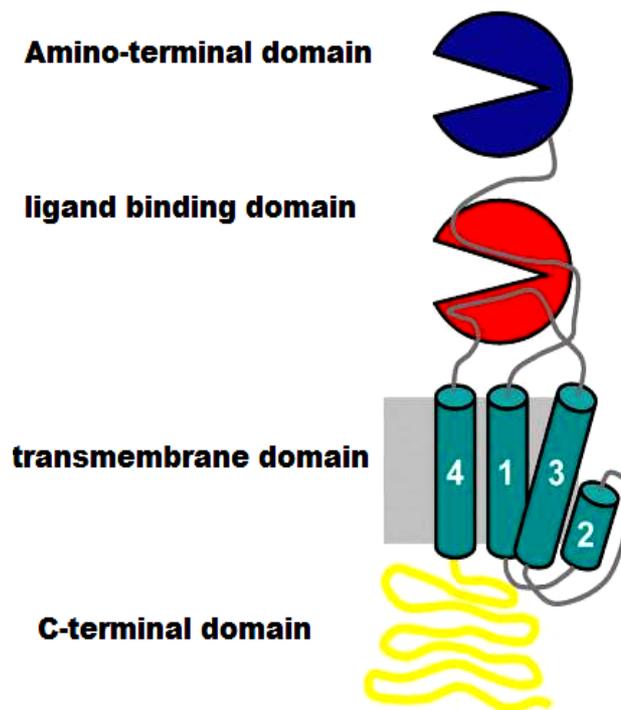
Figure 1.2: Structure of the NMDAR subunit. Image from (Wyllie et al. 2013)

The amino-terminal domain (ATD) largely provides sites for allosteric modulation. For example, Zn^{2+} and H^+ are endogenous allosteric modulators which bind to the GluN2 ATD (Karakas et al. 2011; Furukawa 2012). The ligand binding domain provides an agonist site for glycine or D-serine to bind to GluN1 or glutamate to bind to GluN2. The transmembrane domain and adjacent amino acids largely determine the biophysical properties of the NMDAR. Lastly, the primary function of the CTD is to couple Ca^{2+} to intracellular signalling and regulate trafficking of the NMDAR via post-translational modifications cascades in addition to being essential for correct gating of the NMDAR.

The GluN1 and GluN2 subunits can be modulated by a variety of endogenous molecules and ions as illustrated in **Figure 1.3.A.** This complex regulation in part explains the physiology of the NMDAR which shall now be elaborated on below.

1.1.2 The NMDA receptor as a co-incidence detector

The NMDAR is a ligand-gated ion channel as it requires the binding of glycine/D-serine to the GluN1 subunit and glutamate binding to the GluN2 subunit; occupation of all four binding sites induces a conformational change in the receptor. However, at resting membrane potentials (-60 mV to -70 mV), there is very little ion flow in the open state of the channel as the channel pore is blocked by Mg^{2+}. Post-synaptic depolarization, largely through the activation of AMPA and kainate receptors, can alleviate this Mg^{2+} block. Therefore, to permit ion flow, the NMDAR requires synchronization of pre-synaptic release of glutamate and post-synaptic depolarization hence why it is known as a co-incidence detector (**Figure 1.3.B**). Although Ca^{2+}/Na^+ influx intracellularly is the most studied ion conductance of the NMDAR, there is also a K^+ efflux. This K^+ efflux can enhance presynaptic Ca^{2+} transients and neurotransmitter release, induced by local depolarization at the synaptic cleft, which is a candidate mechanism for promoting spike time dependent plasticity (Shih et al. 2013).
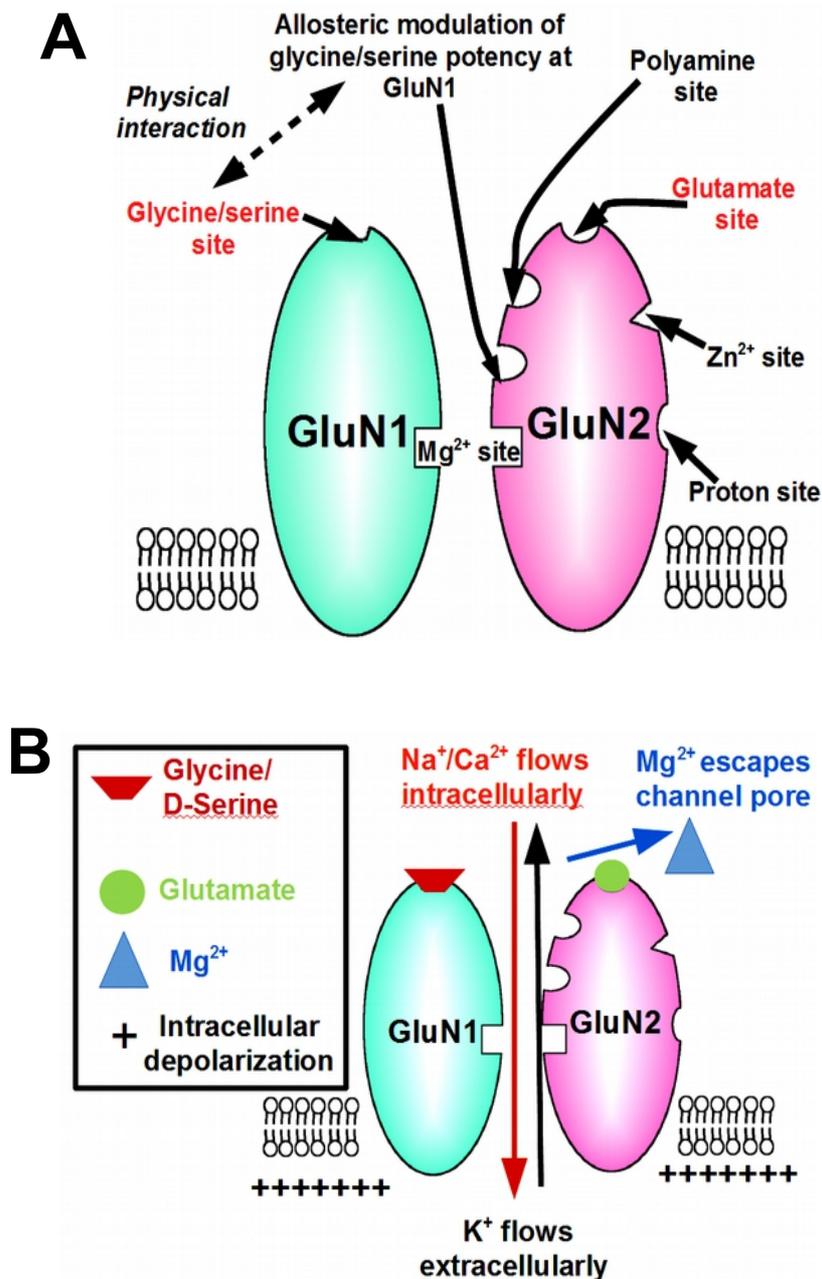
Figure 1.3: A) Illustration of agonist and modulatory sites on the GluN1 and GluN2 subunits. **B)** Schematic showing how the NMDAR operates as a co-incidence detector. Presynaptic release of glutamate is required so glutamate can bind to the GluN2 subunit and if glycine/D-serine is also bound to the GluN1 subunit, a conformational change results in the NMDAR channel opening. However, intracellular depolarization is also required to alleviate the Mg^{2+} block of the channel pore. Therefore, to permit the flow of cations, the NMDAR requires presynaptic release of glutamate and postsynaptic depolarization.

It should be noted that it was recently reported that the NMDARs may have the capacity to function independently of ion influx and act purely as a metabotropic receptor (Nabavi et al. 2013; Kessels et al. 2013). This conclusion was partly derived from the observation that competitive antagonists acting at the GluN1 and GLuN2 agonist sites can block long-term depression (LTD) but open channel channel blocker failed to do so. However, this hypothesis has since been refuted by reports that open channel blockers do indeed block LTD emphasizing the classical role of Ca^{2+} influx in mediating synaptic plasticity(Babiec et al. 2014).

1.1.3 GluN1 subunit

Both GluN1 subunits of the tetramer must be bound by either glycine or D-serine in order for the NMDAR channel to open. The purpose of this obligatory agonist binding site is not well understood. Levels of glycine and D-serine in the extracellular fluid of the cortex are high enough to saturate NMDARs (Matsui et al. 1995) leading some to suggest the agonist site may be saturated *in vivo*. However, this fails to take into account the release, uptake and metabolism of these amino acids. For example, by co-expressing the glycine transporter (GLYT1) with NMDA receptors in oocytes, it was observed glycine concentrations could decrease from a saturating concentration to $< EC_{50}$ in a matter of seconds (Supplisson & Bergman 1997). Furthermore, $GlyT1^{+/-}$ have enhanced NMDAR:AMPAR ratio in CA1 in pyramidal neurons suggesting glycine uptake is critical for regulating synaptic NMDAR activation (Tsai et al. 2004; Gabernet et al. 2005).

Recently, using enzymes which degrade either D-serine or glycine, it has been proposed that D-serine activates synaptic NMDARs whereas glycine activates extrasynaptic NMDARs (Papouin et al. 2012). However, while serine racemase knock-out (SR-KO) mice have clear deficits in LTP due to their inability to synthesise serine, NMDAR synaptic potentials are preserved in these mice

suggesting some overlap of glycine and serine at the synapse (Rosenberg et al. 2013).

The GluN1 subunit has 3 regions of alternative splicing, one at the N-terminus and two at the C-terminus, which can result in 8 different isoforms. The isoforms can result in different trafficking mechanisms (Horak & Wenthold 2009) and functional differences such as altering NMDA receptor dependent regulation of gene expression (Bradley et al. 2006). The alternative splicing is developmentally and regionally regulated but despite this, the GluN1-1a subtype is the most widely expressed in the CNS and is the canonical subtype (Cull-Candy et al. 2001).

1.1.4 GluN2 subunit

1.1.4.1 GluN2 subunit: amino terminal domain, ligand binding domain and transmembrane domain

There are 4 genes, G*rin2a-d,* which encode for four GluN2 subunits (A-D). Incorporation of different subunits alters the biophysical properties of the channels as summarized in T**able 1.1.**

When considering NMDAR sensitivity to Mg^{2+}, Ca^{2+} permeability and single-channel conductance, NMDARs containing GluN2A/GluN2B subunits are biophysically similar as are GluN2C/GluN2D. This can largely be attributed to 2A/2B having a serine residue (Ser632 in GluN2A) at the intracellular side of the third membrane-associated domain whereas 2C/2D have a leucine residue (Leu657 in GluN2D) (Siegler Retchless et al. 2012). This single amino acid difference dramatically alters the Mg^{2+} block, Ca^{2+} permeability and single channel conductance of the NMDAR.

	GluN2A	GluN2B	GluN2C	GluN2D
GluN1 agonist potency	↑	↑↑	↑↑↑	↑↑↑↑
GluN2 agonist potency	↑	↑↑	↑↑↑	↑↑↑↑↑
Deactivation rate	↑↑↑↑	↑↑↑	↑↑	↑
Zinc inhibition	Nanomolar affinity	Micromolar affinity	-	-
Polyamine Potentiation	↑ glycine affinity	↑ glycine affinity ↑current	-	-
Allosteric site for modulation of GluN1 agonist potency	Present	-	-	-
Mg^{2+} sensitivity	Higher		Lower	
H^+ sensitivity	Higher		Lower	
Ca^{2+} permeability	Higher		Lower	
Conductance	50/40 pS		35/18 pS	

Table 1.1: Incorporation of different GluN2 subunits alters the biophysical properties of NMDARs. Adapted from (Wyllie et al. 2013)with additional information from (Zhang et al. 1994; Rachline et al. 2005)

1.1.4.2 GluN2 Subunit: the CTD of GluN2A and GluN2B

The extracellular and transmembrane domains are highly conserved (69%) between GluN2A and GluN2B. However, when considering the C-terminal domain region, it is poorly conserved with only 29% homology (Ryan et al. 2008). Although deletion of GluN2A and GluN2B CTDs can alter channel conductance and gating, switching the CTDs between GluN2A and GluN2B does not alter the properties of the chimera channels (Maki et al. 2012; Punnakkal et al. 2012). It can therefore be concluded that the divergence of the CTD between GluN2A and GluN2B does not contribute to subunit-specific gating properties but is an essential structural component in order for the NMDAR to function correctly. On the other hand, there is an abundance of evidence which supports the hypothesis that the divergence of the CTDs allows the different subunits to couple to different intracellular signalling cascades; a brief summary of these is given in **Table 2** with many being elaborated in subsequent sections where necessary.

Protein Type	Example	Physiological function
Membrane-associated guanylate kinases (scaffolding proteins)	SAP-102 & PSD-95 (Elias et al. 2008)	SAP-102 can traffick both GluN2B & GluN2A whereas PSD-95 can only traffick GluN2A. Both stabilize NMDARs at the synapse. As they both have structurally similar PDZ domains, they both can have the potential to couple NMDARs to similar proteins. However, they undergo different post translational modification ; e.g only PSD-95 is palmitoylated.
Tyrosine kinases and phosphatases	Fyn & Src (Prybylowski et al. 2005) (Yang et al. 2012)	Phosphorylation of Tyr1472 at GluN2B prevents clathrin adaptor protein AP-2 binding to YEKL motif: ultimately reduces endocytosis
	STEP (Braithwaite et al. 2006)	Antagonizes actions of tyrosine phoshporylation.
Serine/threonine kinases and phosphatases	PKA (Cerne et al. 1993)	PSD-95 associates with A kinase anchoring proteins allowing PKA to increase NMDA currents.
	PKC (Gardoni et al. 2001) (Liao et al. 2001)	Phosphorylation of GluN2A (ser-1416) and GluN2B (ser1303/1323) enhances NMDA currents.
	CK2 (Sanz-Clemente et al. 2010)	Phosphorylation of ser1480 disrupts interaction of GLuN2B with PSD-95/SAP-102
	DAPK (Tu et al. 2010) CaMKII (Liao et al. 2001)	Phosphorylates ser1303 of GluN2B CTD and enhances NMDA currents
	PP1 and calcineurin (Wang et al. 1994)	Antagonizes the actions of PKA and PKC.
Palmitoylation	- (Hayashi et al. 2009)	Can enhance NMDA stability at membrane by enhancing Fyn phosphorylation. At other sites, leads to increase accumulation in golgi apparatus and decreased surface expression.

Table 1.2: A summary of post-translational modifications of GluN2A and GluN2B CTDs.

1.1.6 The GluN3 subunit

The physiological role of the GluN3 subunit is less well known than the GluN2 subunit. Diheteromeric GluN1-GluN3 NMDARs are gated exclusively by glycine, have no Mg^{2+} block and are only permeable to Na^+ and K^+. However, they may be incorporated into a triheteromeric NMDAR with another GluN2 subunit. This dramatically alters the property of the NMDAR by acting as a dominant-negative modulator of the GluN2 subunit; a reduction in Mg^{2+} block and Ca^{2+} influx is a defining feature (Pachernegg et al. 2012). In layer 2/3 visual cortical neurons, GluN3A forms a triheteromeric NMDAR with GluN2B presynaptically ; the reduced Mg^{2+} block enhances spontaneous and evoked glutamate release which is critical for spike timing-dependent LTD (Larsen et al. 2011). Interestingly, in forebrain regions, GluN3A declines during development as GluN2A increases so it is feasible that GluN3A limits synaptic development. Indeed, knockout of GluN3A accelerates synaptic maturation (Henson et al. 2012) whereas overexpression delays maturation (Roberts et al. 2009). Whether spike timing-dependent LTD synchronizes this developmental break remains an interesting and open question.

1.1.7 Triheteromeric (GluN2A-GluN2B) NMDARs

Much of the research regarding GluN2 containing NMDARs has assumed the tetramer is composed of GluN2 subunits of the same subtype. However, recent evidence suggests this may not be the case. For example, at hippocampal synapses in culture (Tovar et al. 2013) and *in vitro* slices (Gray et al. 2011; Rauner & Köhr 2011), it has been reported that there is a prominent population of triheteromeric NMDARs containing GluN1, GluN2A and GluN2B subunits. Their existence may explain the recent rejection of a well researched hypothesis that one diheteromeric GluN2 population may induce LTP and another population may induce LTD (Shipton & Paulsen 2014). This shall be elaborated on in further sections.

Due to the difficulty of isolating triheteromeric NMDARs, little is known about their structure and how it relates to their function at the molecular level. However, an elegant approach to rectify this has recently been established by (Hansen et al. 2014). When assessing glutamate deactivation time course after a 5 ms glutamate pulse, triheteromeric GluN2A-GluN2B NMDARs are 1.8-fold slower than that of GluN1/GluN2A diheteromers but 5.5-fold faster than that of GluN1/GluN2B diheteromers; this suggests GluN2A largely determines the decay kinetics of triheteromeric GluN2A-GluN2B NMDARs. Additionally, GluN2A-GluN2B NMDARs have a distinct pharmacological profiles which shall be discussed below.

As discussed above, the CTD of GluN2A and GluN2B have diverged significantly. If the assumption is made that during Ca^{2+} influx, both CTDs of the two GluN2 subunits are exposed to the same Ca^{2+} concentrations in a triheteromeric NMDAR, it is feasible that functions such as synaptic plasticity could be determined by the Ca^{2+} affinity of the proteins coupled to the CTDs.

It is clear that further research into the structure of triheteromeric NMDARs is critical in order to fully understand the complex physiology of NMDARs.

1.2 Temporal and spatial patterns of NMDAR subunit expression during development

As discussed above, incorporation of different GluN2 and GluN3 subunits can dramatically alter the properties of NMDARs. As shown in **Figure 1.4,** GluN2 and GluN3 subunits change their temporal and spatial patterns during development in the rodent brain. They also show distinct spatial expression patterns depending on the brain region. For example , GluN2C and GluN2D are expressed strongly in the hindbrain during development and adulthood whereas in the forebrain, GluN2A and GluN2B are more strongly expressed.
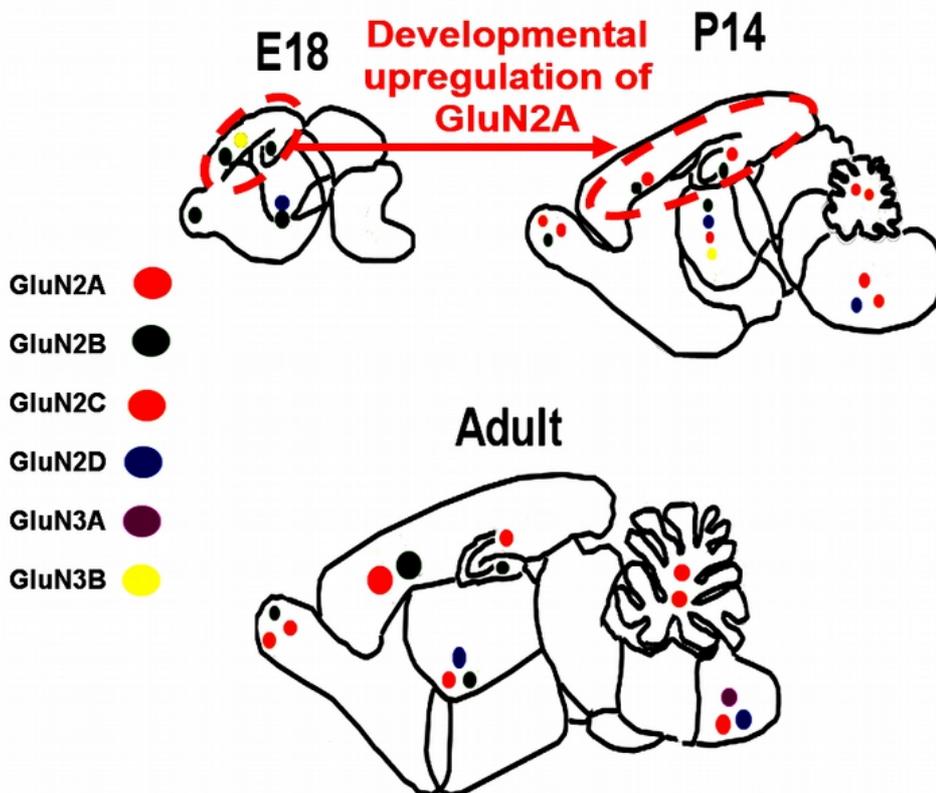
Figure 1.4: temporal and spatial patterns of NMDAR subunit expression during development. Note the developmental upregulation of GluN2A in the hippocampus and cortex. Adapted from (Paoletti et al. 2013)

From this point on, this thesis will focus on the forebrain region. The reason being that this brain region can undergo widespread excitotoxicity during a stroke or traumatic brain injury in addition to being a critical location for neurodegenerative diseases such as A1zheimer's disease. Secondly, the hippocampus is the most widely studied structure regarding synaptic plasticity which is currently the best candidate molecular mechanism underlying learning and memory. Lastly, the data presented in this thesis was derived using cortical cultures as a model to study subunit-dependent and spatial signalling by the NMDAR; cortical and hippocampal cultures have been used extensively for this purpose (Hardingham & Bading 2010).

1.2.1 Temporal expression of GluN2 subunits in hippocampus and cortex

At early stages in development, both in the cortex and the hippocampus, GluN2B is the dominant GluN2 subunit expressed. However, during development there is upregulation of GluN2A. This has been noted at the mRNA level (Watanabe et al. 1992; Monyer et al. 1994), at the protein level in synaptosomal preparations (Portera-Cailliau et al. 1996) and by co-immunoprecipitation with GluN1 (Sheng et al. 1994). By injecting oocytes with mRNA prepared from P1 and adult whole rat brains, (Williams et al. 1993) could detect a decrease in the sensitivity of NMDARs to the GluN2B selective antagonist ifenprodil. This drop in GluN2B antagonism could be recapitulated in developing rat cortical cultures (Tovar & Westbrook 1999; Ilyin et al. 1996; M-A Martel et al. 2009), developing mouse hippocampal cultures (Thomas et al. 2006) or in acutely dissociated parietal cortical neurons from young and old rats (Kew et al. 1998). In hippocampal and cortical slices, there is a developmental increase in the speed of NMDA EPSC decay kinetics (Carmigoto & Vicini 1992) indicating an increase in GluN2A at the synapse and this correlates very well with a drop in the sensitivity of EPSCs to GluN2B antagonism (Kirson & Yaari 1996). Furthermore, elegant studies implementing single-cell RT-PCR have correlated an increase in GluN2A mRNA with a drop in ifenprodil sensitivity

(Hoffmann et al. 2002) and an increase in EPSC decay kinetics (Flint et al. 1997) at the single cell level. Altogether, the change in biophysical properties and drop in ifenprodil sensitivity of the NMDAR EPSC in a variety of preparations suggest GluN2A containing NMDARs are incorporated into the synapse during development. This is commonly known as the "GluN2B to GluN2A "switch". However, as discussed, there is now evidence for a strong triheteromeirc GluN2A-GluN2Bs so the upregulation of GluN2A may not be as binary as once thought ; it is perhaps best to hypothesise the GluN2A upregulation as an incorporation.

Studies implementing immunoprecipation agree that the upregulation of GluN2A is incorporated into diheteromeric and triheteromeric GluN2A-GluN2B NMDARs but the ratio at which this occurs is not clear (Al-Hallaq et al. 2007; Sheng et al. 1994; Luo et al. 1997). However, as stated above, at hippocampal synapses in culture (Tovar et al. 2013) and *in vitro* slices (Gray et al. 2011; Rauner & Köhr 2011), it has been reported that there is a prominent population of triheteromeric GluN2A-GluN2B NMDARs at the synapse. Furthermore, overexpression of GluN2A has been noted to decrease lateral diffusion of GluN2B containing NMDARs suggesting GluN2A forms a triheteromer with GluN2B thus stabilizing the receptor at the synapse (Groc et al. 2006).

1.2.2 Molecular mechanisms underlying GluN2A upregulation

The developmental increase in *Grin2a* mRNA described above is an excellent candidate mechanism to explain the developmental upregulation of GluN2A containing NMDARs. However, transcriptional control of GluN2 subunit expression could also occur by a downregulation of *Grin2b*. Indeed, the repressor element 1 silencing transcription factor (REST) is essential for epigenetically reducing G*rin2b* transcription and if REST is genetically knocked-out, there is a deficit in the developmental switch in subunits (Rodenas-Ruano et al. 2012). Such a phenomenon would not explain the rapid switching in GluN2 subunits in minutes, discussed

below, due to the time scale of epigenetic modelling.

A striking observation is that in neuronal cultures, where the network activity is artificially created and is somewhat oscillatory in nature, the developmental switch in GluN2 subunits still occurs. This suggests that a specific electrical input is not necessary for this developmental process to occur. However, in young hippocampal slices predominately expressing GluN2B, there can be a rapid upregulation of GluN2A at the synapse within minutes by a LTP induction protocol which is also reversible (Bellone & Nicoll 2007). Although it is debatable whether such protocols are physiologically relevant, it is of great interest that that subunits can switch in such a time scale. Such protocols have been used as an assay to determine the molecular mechanisms involved in the upregulation of GluN2A; mGluR5 and NMDAR activation were found to be essential (Matta et al. 2011). In the CA1 region of the hippocampus, in mGluR5 knock-out mice, there is an incomplete reduction in the developmental switch of NMDA subunits suggesting there are overlapping signalling cascades involved in the switch with mGluR5 signalling being prominent.

A variety of post-translational modifications have been proposed to be involved in the developmental switch in subunits. Casein kinase II (CK2) phosphorylates ser1480 of the GluN2B which drives endocytosis; this kinase activity increases during the time window of the developmental switch and is critical in the increase of GluN2A at the synapse (Sanz-Clemente et al. 2010). The molecular mechanism underlying the enhanced endocytosis involves phosphorylation of S1480 disrupting the interaction PSD-95/SAP102 with the PDZ domain of the GluN2B CTD (Chung et al. 2004). This has the consequence of Y1472 being able to be dephosphorylated and AP-2 binding to the YEKL motif thus promoting GluN2B endocytosis. Furthermore, the N-terminal of SAP-102 binds to a non PDZ binding site on the GluN2B CTD where it promotes lateral diffusion of NMDARs to perisynaptic

endocytic zones (Chen et al. 2012).

Additionally, CK2 can be regulated by Ca^{2+} influx through the NMDAR albeit indirectly via CaMKII. Ca^{2+}/calmodulin-dependent protein kinase II (CaMKII) binds to the Glu2NB CTD in the region 1290-1309 (Strack et al. 2000) where it can promote the phosphorylation of ser1480 by CK2 (Chung et al. 2004). However, CK2 is a constitutively active kinase (Olsten & Litchfield 2004) so CaMKII cannot regulate CK2 via its kinase activity; it has been proposed that CaMKII forms a trimolecular complex with CK2 and the PDZ domain of the GluN2B CTD and promotes CK2 phosphorylation of ser1480 via physical interaction (Sanz-Clemente et al. 2013). It should be noted that inhibiting synaptic activity, blocking NMDARs or blocking CaMKII does not block basal ser1480 phosphorylation entirely but reduces it to around 50%. Furthermore, inhibition of CaMKII failed to prevent the developmental switch in subunits induced by an LTP protocol (Matta et al. 2011).

It is also interesting to note that dark rearing rats from birth can result in an increase in the phosphorylation of the GluN2B CTD at ser1303 which correlates with a delay in the upregulation of GluN2A in the visual cortex and retina; even more remarkable, only 6 hours of light can reverse both the delayed expression of GluN2A and the increased phosphorylation of ser1303 (Giannakopoulos et al. 2010). Ser1303 is a target for PKC, DAPK and CaMKII; although these experiments do not prove that CaMKII phosphorylation of Ser1303 delays the switch, it is intriguing to note that dark rearing increases CaMKII expression in the retina (Xue et al. 2001).

SAP-102 is expressed predominately in the neonatal brain with an increase of PSD-95 expression occurring in the first several months post birth; SAP-102 somewhat mirrors the temporal expression of GluN2B and PSD-95 mirrors that of GluN2A. Whereas SAP-102 is critical in synaptogenesis where it can promote the trafficking of both GluN2B and GluN2A NMDARs, PSD-95 is critical after synaptogenesis

where it maintains the developmental switch of GluN2 subunits; the molecular basis for this may be that PSD-95 only promotes the trafficking of GluN2A NMDARs (Elias et al. 2008).

Blockade of NMDARs and AMPARs has been reported to increase GluN2A expression within hours with no effect on GluN2B expression in culture (von Engelhardt et al. 2009). As TTX could not reproduce this effect, it must be presumed the effect is due to blocking miniature synaptic events which can tonically suppress local dendritic protein synthesis (Sutton et al. 2006). Nevertheless, this phenomenon has yet to be explored in any great detail.

To summarize, there is evidence that the upregulation of GluN2A is controlled by both transcriptional and post-translational mechanisms. One possible mechanism to test the role of post-translational mechanisms is to subject both GluN2B and GluN2A to the same regulation; this can be achieved by genetically replacing the GluN2A CTD with that of GluN2B. Such an approach is utilized in **chapter 5** where I determine if the developmental upregulation of GluN2A is impeded.

1.2.3 The physiological outcome of GluN2A upregulation

During a synaptic event, a diheteromeric GluN2B-NMDAR carries approximately twice the charge of a diheteromeric GluN2A-NMDAR (Erreger et al. 2005). Furthermore, per unit of charge, GluN2B-NMDARs carry more Ca^{2+} that GluN2A-NMDARs (Sobczyk, et al. 2005). Lastly, the GluN2B CTD has a higher affinity for CAMKII than the GluN2A CTD; there is ever increasing evidence that CAMKII is necessary for certain forms of synaptic plasticity (see (Nicoll & Roche 2013 for a review; **section 1.5** for a greater discussion on synaptic plasticity). Altogether, the difference in Ca^{2+} permeability and CAMKII affinity results in GluN2B-NMDARs having a lower threshold for the induction of long-term potentiation (LTP) compared

to GluN2A-NMDARs.

Consequently, the developmental upregulation of GluN2A will increase the threshold for LTP induction. However, importantly, the GluN2A:GluN2B ratio is not fixed and can be modified by neural activity; the modification of synaptic plasticity itself is known as metaplasticity (see Abraham 2008 for a review). For example, monocular deprivation in mice leads to a decrease in the GluN2A:GluN2B ratio in the visual cortex which juxtaposes in a lowering of LTP induction (Chen & Bear 2007, Philpot et al. 2007). Genetic deletion of GluN2A disrupts the modification of the LTP threshold during monocular deprivation thus confirming the GluN2A:GluN2B dictates the threshold for LTP (Cho et al. 2009).

It has also been demonstrated that the divergence of the GluN2A and GluN2B CTD has resulted in different forms of plasticity and behaviours (Ryan et al. 2013) which would be absent if the upregulation of GluN2A failed to occur. In agreement, genetic deletion of either the whole GluN2A subunit or the CTD alone resuls in impaired spatial working memory (Bannermann et al. 2008)

The upregulation of GluN2A has also been noted to alter synaptogenesis (see **section 1.2.4.1**) and excitotoxicity (**see section 1.4.3 & chapter 5**).

1.2.4 Spatial expression of NMDARs at the neuronal level during development

1.2.4.1 Synaptogenesis

Although it is beyond the scope of this thesis to discuss the complex physiology underlying synaptogenesis, nevertheless, a basic appreciation of this phenomenon is required to appreciate NMDAR signalling during development.

During the first postnatal week, dendritic shafts are covered with filopodia which protrude and retract with a life time of approximately 10 minutes where synapses can form. However, predominately during the second developmental week, if a filopodia comes into contact with a developing axon, a complex cross-stalk signalling process can take place which can result in the development of a dendritic spine (Calabrese et al. 2006). This complex signalling can involve cell-adhesion proteins and chemically released transmitters. During this time period, NMDARs largely switch from predominately existing outside the synapse or "extrasynaptic NMDARs (exNMDARs)" to predominately existing at the synapse or "synaptic NMDARs (synNMDARs)". This switch in NMDAR membrane location is also recapitulated in neuronal cultures (Tovar & Westbrook 1999; M-A Martel et al. 2009) where spines are noted to increase rapidly between DIV 10 and DIV 14 (Boyer et al. 1998).

NMDARs have been proposed to control synaptogenesis. For example, overexpression of GluN2B increases spine motility whereas GluN2A overexpression was noted to stop synapse number and growth in organotypic hippocampal slices (Gambrill & Barria 2011). However, knocking down both AMPAR and NMDAR mediated synaptic transmission in a single neuron *in vivo* failed to alter spine development arguing that ionotropic glutamatergic synaptic transmission is not required for spine development (Lu et al. 2013). This observation is consistent with pharmacological silencing of network activity in culture which failed to alter dendritic spine formation or density (Harms & Craig 2005; Kossel et al. 1997). Additionally, a well defined genetic programme required for synapse assembly can operate without network activity (Valor et al. 2007). However, it is important to stress that tetrodotoxin is the most common pharmacological approach to silence neuronal activity; this approach still permits miniature synaptic events to occur. Nevertheless, the observations from Lu et al are striking and would certainly warrant

further investigations to determine if compensations from metabotropic glutamate receptors had occurred.

1.2.4.2 Surface mobility of NMDAR

By blocking synaptic NMDARs with MK-801, which has very slow off rate, it was observed that the recovery of this blockade could only be explained by the movement of NMDARs from outside the synapse into the synapse (Tovar & Westbrook 2002). Under high resolution imaging, it has been observed that GluN2B containing NMDARs are more mobile than GluN2A, with GluN2A spending a greater time at the synapse; as stated above, overexpression of GluN2A decreases the mobility of GluN2B possibly because of the formation of triheteromeric GluN2A-GluN2B NMDARs (Groc et al. 2006). Interestingly, after endocytosis, the GluN2B CTD is trafficked through recycling endosomes whereas the GluN2A is sorted into late endosomes destined for degradation; the GluN2A CTD can be "rescued" from degradation if it forms a heterodimer with GluN2B (Tang et al. 2010). Therefore, it is interesting to speculate that in a triheteromeric GluN2A-GluN2B NMDAR, the GluN2B subunit prolongs the half-life of the receptor whereas the GluN2A subunits promotes stability at the synapse.

It has been reported that GluN2A containing NMDARs are preferentially targeted to the synapse via a mechanism involving the CTD (Steigerwald et al. 2000) but this finding could not be recapitulated in subsequent studies (Thomas et al. 2006). Furthermore, a loss of ifenprodil sensitivity is observed at extrasynaptic sites in culture (M-A Martel et al. 2009) and hippocampal slices (Harris & Pettit 2007). The latter study does not report the mobility of NMDARs previously reported by Tovar & Westbrook with a possible explanation that NMDAR mobility is an artefact of the culture system; further work is needed to determine if NMDARs form stable pools or are mobile *in vivo*. Lastly, D-Serine has been proposed to slow the mobility of

GluN2A containing NMDARs whereas glycine to slow the mobility of GluN2B in cultures (Papouin et al. 2012).

To summarize, it is evident that NMDARs switch from predominately extrasynaptic to synaptic during the second developmental week which juxtaposes with a developmental upregulation of GluN2A. In **chapter 5**, the role of the GluN2 C-terminus in this process will be investigated.

1.3 NMDAR pharmacology

The drugs used to alter NMDAR properties pertaining to this thesis are summarized in **table 1.3.**

Drug	Site of Action	Mechanism of Action	Selectivity against GluN2A or GluN2B
Memantine	Channel Pore	Non-competitive/requires channel to be open	**X**
(+) MK-801	Channel pore	Non competitive/requires channel to be open	**X**
Protons	M3-S2 linker region of GLuN2	Negative allosteric modulation	
Ifenprodil	Amino-terminal domain of GluN2	Negative allosteric modulator	If used at 3 µM, selectively inhibits a 100% diheteromeric GluN2B population by 80%
Zinc	Amino-terminal domain of GluN2	At nanomolar concentrations : allosteric modulation of proton sensitivity.	At nanomolar concentrations, selectively inhibits diheteromeric GluN2A population with a maximum of 70%
NVP-AAM077	Agonist binding site on GluN2 subunit	Competitive antagonist	~5-fold more selective for GluN2A than GluN2B
TCN 201 & TCN 213	For TCN 201: GluN1-GluN2A interface	Allosterically modulates agonist affinity at GluN1 subunit. Modulation can be superseded by increasing agonist concentration.	TCN 213 (30 µM) and TCN 201 (10 µM) selectively inhibit GluN2A over GluN2B.

Table 1.3 : Summary of NMDAR antagonists relevant to this thesis. See (Paoletti & Neyton 2007) for an extensive review.

1.3.1 (+)/- MK-801

MK-801 was developed as an anticonvulsant and was later found to be an NMDAR antagonist (Wong et al. 1986). MK-801 is "use dependent" meaning it only blocks NMDARs which are in the open state induced by agonist binding (Huettner & Bean 1988). Both by patch clamp recordings (Huettner & Bean 1988) and by radioligand binding assays (Reynolds & Miller 1988) it was noted that Mg^{2+} inhibits MK-801 binding. This suggests that MK-801 has an overlapping binding site with Mg^{2+} somewhere in the channel pore. This was later confirmed by site directed mutagenesis where mutations, such as N616Q in the M2 loop of the GluN1 subunit, abolished inhibition by both Mg^{2+} and MK-801 (Kashiwagi et al. 2002) .

MK-801 has a very slow off-rate as it requires the NMDAR channel to be open ; in other words, the recovery from the MK-801 block is also use dependent. This, combined with a reported time constant for recovery of 92±106min (mean±SD) (Huettner & Bean 1988) led to MK-801 being labelled as an "irreversible antagonist." However, the time constant calculated was determined using 30 μM NMDA; if a higher concentration of NMDA was used then the open probability of the NMDAR would increase ultimately resulting in a decrease in the time constant. Furthermore, the large standard deviation suggests some cells had a faster recovery than others perhaps because of insufficient washout of MK-801. Critically, although it is established Mg^{2+} inhibits MK-801 binding, the effects of Mg^{2+} on the dissociation of MK-801 had yet to be investigated; the determination of this will be the main focus of **chapter 3** and the relevance of this eluded to the upcoming sections regarding establishing the role of the NMDAR in mediating excitotoxicity.

As MK-801 is extremely potent, unlike Mg^{2+}, MK-801 is not suitable to discriminate between 2A/2B and 2C/2D subunit types. At pH 7.6, all four subunits have an IC_{50} in the range of 9–38 nM (Dravid et al. 2007). MK-801 also shows antagonism at

nicotinic acetylcholine receptors (nACHRs) (Briggs & McKenna 1996; Ramoa et al. 1990) in addition to inhibiting serotonin (Iravani et al. 1999) and dopamine (Clarke & Reuben 1995) transporters.

1.3.2 Protons

Protons are an endogenous negative allosteric modulator of NMDARs(Traynelis et al. 1995; Low et al. 2003) . Polyamines (Traynelis et al. 1995) and zinc (Low et al. 2000) (in an allosteric modulator manner) enhance proton sensitivity.

1.3.3 Memantine

Memantine is also an open channel blocker of the NMDAR ; the N616Q mutation described above also abolishes memantine potency confirming it has an overlapping binding site with both Mg^{2+} and MK-801 (Kashiwagi et al. 2002). Unlike MK-801, memantine has a very high off-rate in the absence of Mg^{2+} and is the main proposed reason why it is well tolerated clinically compared to antagonists with a slower off rate (Chen et al. 1992). In the presence of Mg^{2+}, memantine preferentially inhibits GluN2C/GluN2D over GluN2A/GluN2B under steady state glutamate application (Kotermanski & Johnson 2009). Additionally, Otton et al. 2011 demonstrate that inhibition of GluN2A containing NMDARs by memantine is drastically reduced in the presence of Mg^{2+}.

It will be elaborated in a further section regarding the therapeutic uses of memantine, and the proposed mechanisms, but it should be stressed that memantine has off-target effects including antagonism at 5-HT(3) receptors (Rammes et al. 2001) and nACHRs (Aracava et al. 2005; Buisson & Bertrand 1998) with additional agonist action at dopaminergic (D_2) receptors (Seeman et al. 2008).

1.3.4 Ifenprodil

Ifenprodil is an allosteric modulator with a 400-fold selectivity for GluN2B (IC_{50} = 0.34 μM) over GluN2A (IC_{50} = 146 μM) (Williams 1993). Ifenprodil is commonly used at 3 μM which inhibits GluN2B containing NMDAR by 80%. At higher concentrations, it has been noted that ifenprodil has an IC_{50} of 10 μM at presynaptic P/Q type Ca^{2+} channels (Delaney et al. 2012) but as ifenprodil has been used at 3 μM throughout this thesis, the effects will be negligible. Ifenprodil inhibits triheteromeric NMDARs by approximately 30% under constant agonist exposure (Hatton & Paoletti 2005; Hansen et al. 2014).

1.3.5 NVP-AAM077

NVP-AAM077 was originally characterized in a heterologous *Xenopus* oocyte system expressing human NMDARs. NVP-AAM077 was found have a >100 fold preference for inhibiting NMDARs containing GluN2A over GluN2B (Auberson et al. 2002). However, this and other studies Liu et al. (2004a), failed to take into consideration that as GluN2A and GluN2B have different affinities for glutamate, and as NVP-AAM077 acts as a competitive antagonist, its potency is dependent on the concentration of glutamate present at the NMDAR.

To resolve this, IC_{50} values for NVP-AAM077 were calculated at the EC_{50} values for glutamate at the GluN1/GluN2A and GluN1/GluN2B NMDARs for rat NMDARs ; NVP-AAM077 was found to be only ~5-fold more selective for GluN2A than GluN2B when glutamate is at the respective EC_{50} (Frizelle et al. 2006; Neyton & Paoletti 2006). Repeating this more robust approach to determine selectivity at human NMDARs would be fruitful as it would determine if there is any species difference in NVP-AAM077 potency.

The importance of the above in selectively blocking GluN2A containing NMDARs is elegantly demonstrated by the implementation of GluN2A knockout mice. In matureGluN2A$^{-/-}$ CA1 pyramidal cells, NVP-AAM077 block of approximately 20% of an EPSC is observed when used at 50nM but if increased 8-fold to 400nM, it blocks approximately 60% (Berberich et al. 2005). Therefore, despite NVP-AAM077 at 400 nM being unsuitable to selectivity inhibit GluN2A, it has been used at this concentration to investigate synaptic plasticity and excitotoxicity which shall be elaborated in a subsequent section. Additionally, NVP-AAM077 acts as an antagonist at GluN2C and GluN2D containing NMDARs (Feng et al. 2004).

1.3.6 Zinc

In the nanomolar range, zinc acts as an allosteric modulator to inhibit GluN2A containing NMDARs with little antagonism of GluN2B containing NMDARs (Paoletti et al. 1997). At higher concentrations, zinc acts as an NMDAR channel blocker where it antagonizes both diheteromeric GluN2A and GluN2B containing NMDARs. In the nanomolar range, maximal inhibition by zinc has been determined to be 80% for a diheteromeric GluN2A population and 14% for GluN2A-GluN2B triheteromeric NMDARs (Hatton & Paoletti 2005). Such a loss of zinc antagonism at GluN2A-GluN2B NMDARs was not reported by (Hansen et al. 2014); at pH 7.3, a maximum inhibition of 59% and 49% maximum inhibition was observed for diheteromeric GluN2A and triheteromeric GluN2A-GluN2B NMDARs respectively. Interestingly, a triheteromeric population containing one WT GluN2A and one GluN2A with the zinc binding site mutated had a marked decrease in zinc potency compared to triheteromeric GluN2A-GluN2B NMDARs. To explain such an observation, it is clear further research is needed to explain zinc modulation fully.

1.3.7 TCN 201 and TCN 213

TCN 201 and TCN 213 were identified as selective antagonists for GluN2A containing NMDARs by a Ca^{2+} imaging screen (Bettini et al. 2010). Subsequently, TCN 201 and TCN 213 were found to allosterically modulate, via the GluN2A subunit, glycine/D-serine binding at the GluN1 subunit (McKay et al. 2012; Edman et al. 2012; Hansen et al. 2012). Therefore, the IC_{50} of these compounds are dependent on the concentration of either glycine or D-serine at the NMDAR. Further studies revealed that Val783 in the S2 segment of the agonist binding site on GluN2A subunit is critical in the binding of TCN 201 (Hansen et al. 2012).

The main focus of **chapter 4** will be determining the ability of these compounds to antagonize endogenously expressed GluN2A-containing NMDARs in rat cortical cultures.

1.4 Neuroprotective and neuronal death signalling

Although on the surface it seems paradoxical that NMDARs can mediate both neuroprotection and neuronal death, the subsequent section will discuss the complex signalling by NMDARs which makes this possible.

1.4.1 Excitotoxicity mediated by NMDARs

1.4.1.1 Introduction to excitotoxicity

Over 50 years ago, (Lucas & Newhouse. 1957) observed that subcutaneous doses of glutamate caused widespread degeneration in the inner retina of mice. Additionally, subcutaneous doses of glutamate was noted to cause degeneration in the hypothalamus of rats (Olney 1969) and Olney coined the term "excitotoxicity" to describe the toxic effects of glutamate. Further *in vitro* studies of retinal slices demonstrated that NMDAR activation alone was sufficient to induce excitotoxicity and could be blocked by NMDAR antagonists (Olney et al. 1986). Furthermore, occlusion of the carotid artery induces ischemic conditions and causes excitotoxicity in the hippocampus; focal infusion of an NMDAR antagonist into the hippocampus before this insult dramatically reduces excitotoxicity (Simon et al. 1984). Altogether, this suggests NMDARs are the predominate glutamate receptor that mediate excitotoxicity *in vivo.*

Neuronal *in vitro* cultures were noted to recapitulate the excitotoxicity of *in vivo* and *in vitro* slice studies (Choi 1987a; Choi et al. 1987b; Choi et al. 1988) permitting dissection of the molecular mechanisms underlying excitotoxicity. Subsequent studies utilizing high tonic glutamate or NMDA has revealed that excitotoxicity is controlled via complex and interrelated signalling cascades summarized in **Figure 1.5.**
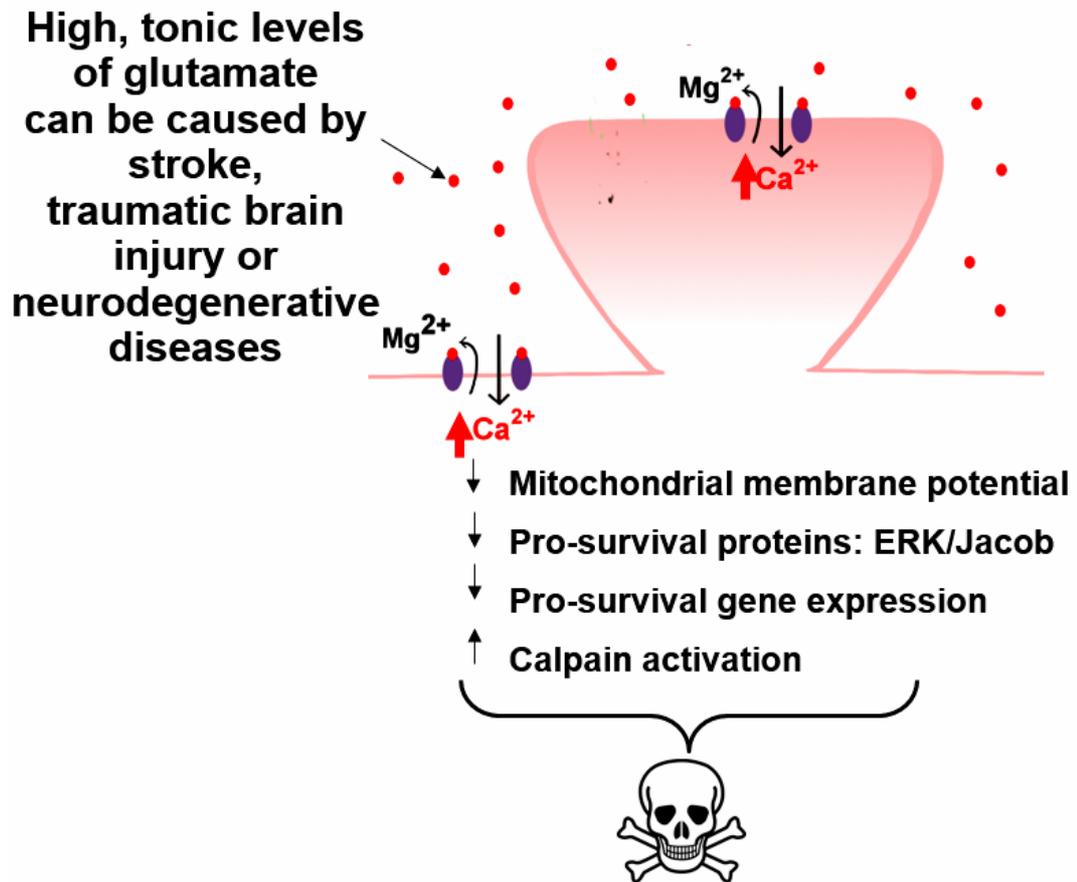
Figure 1.5: **Signalling cascades induced by high tonic glutamate.** High tonic glutamate can result from ischemic insults, traumatic brain injury or certain neurodegenerative diseases. High tonic glutamate leads to a Ca^{2+} influx that activates pro-death signalling cascades. This includes a collapse of the mitochondrial membrane potential, a decrease in the activity of pro-survival gene expression/protein activity and finally, an increase in the activity of calpains. Such signalling can lead to neuronal apoptosis.

1.4.1.2 Spatial signalling of NMDARs and excitotoxicity

Of great interest was the Ca^{2+} source specificity in mediating excitotoxicity. This was first addressed by (Tymianski et al. 1993) where it was noted that although depolarization and bath application of glutamate could evoke similar Ca^{2+} somatic influxes, glutamate preferentially induced excitotoxicity. Similarly, depolarization

and bath glutamate was found to activate transcription of *c-fos* but via different promoter elements (Bading et al. 1993). Furthermore, it was demonstrated that cytoplasmic and nuclear Ca^{2+} must be thought as distinct biochemical compartments in neurons as they can control distinct transcriptional pathways (Hardingham et al. 1997). Ca^{2+} influx via synaptic activation of NMDARs promotes further Ca^{2+} release from intracellular stores resulting in a nuclear Ca^{2+} wave sufficient to activate CREB-mediated transcription without the need for cytoplasmic proteins (Hardingham et al. 2001). However, bath/tonic application of glutamate which activates both synaptic and extrasynaptic NMDAR results in CREB shut-off which is a key mediator of excitotoxicity (Hardingham et al. 2002). As synaptic activity strongly activated synNMDARs and promoted CREB activation, it was proposed that exNMDARs may preferentially shut-off CREB. However, there is a temporal difference between synaptic activation of synNMDARs and tonic activation of both synNMDARs and exNMDARs.

To further test the hypothesis that exNMDARs are preferentially coupled to excitotoxicity, it would be necessary to isolate the two spatial populations and measure a key component of excitotoxicity. To pharmacologically isolate exNMDARs, (Hardingham et al. 2002) drove synaptic activity in the presence of MK-801 to block synNMDARs; once this blockade was complete and MK-801 washed out, exogenous glutamate could be added to preferentially activate exNMDARs. This approach is shown graphically in **Figure 1.6.**
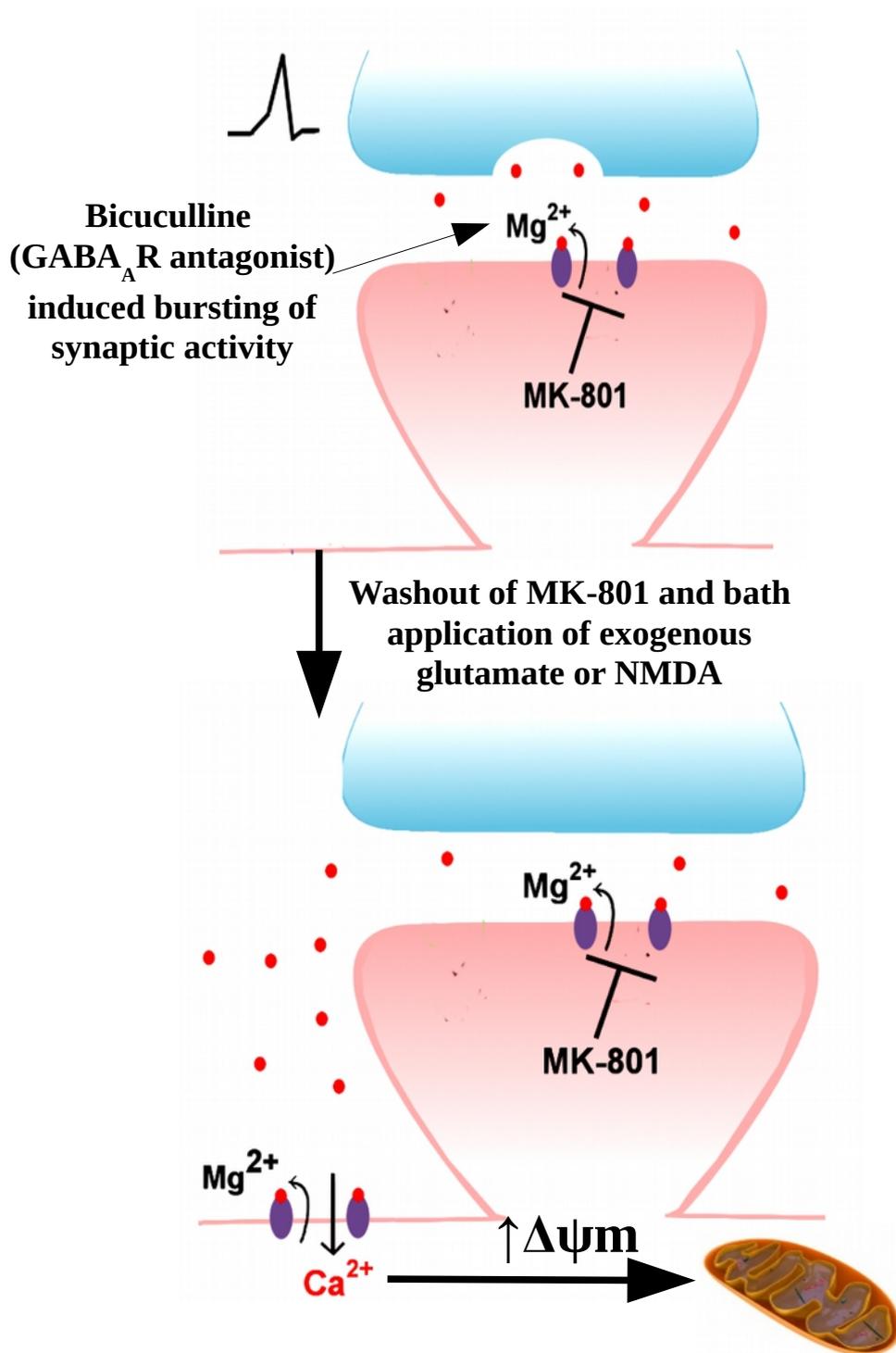
Figure 1.6: Blockade of synNMDARs with MK-801. SynNMDARs can selectively be blocked by promoting bursts of synaptic activity in the presence of MK-801. After washout of MK-801, exNMDARs can be selectively activated by bath applying exogenous glutamate of NMDA. Selective activation of exNMDARs is sufficient to depolarize mitochondria.

Measuring for depolarization of mitochondrial membrane potential, a key factor in excitotoxicity (Qiu et al. 2013), juxtaposed with the above approach revealed details of spatial signalling by NMDARs. Firstly, synaptic activity fails to impact on the mitochondrial membrane potential which is in agreement with synaptic activity being neuroprotective (discussed below). Secondly, selective activation of exNMDARs was sufficient to depolarize mitochondria suggesting exNMDARs may indeed preferentially couple to excitotoxicity. Furthermore, utilizing an electron probe micro-analyzer, (Stanika et al. 2009) determined that although bath application of NMDA caused 3.6 times more Ca^{2+} in the cytoplasm compared to synaptic activation by bicuculline, at the mitochondria there was 155-fold increase in Ca^{2+}; this confirms that is not simply the Ca^{2+} load that dictates Ca^{2+} mediated mitochondrial dysfunction.

One possible explanation for this phenomenon is that although mitochondria are strongly expressed in dendrites where they play a critical role in spine development and plasticity, they are very rarely expressed in dendritic spines or filopodia (Li et al. 2004). Therefore, as mitochondria are largely located extrasynaptically, they may be better spatially located to buffer toxic Ca^{2+} influx during an excitotoxic insult.

It is important to stress that the above experiments do not prove that exNMDARs exclusively mediate excitotoxicity but rather there is strong evidence to suggest exNMDARs may preferentially couple to excitotoxicity. As discussed prior, memantine is an open channel blocker with an off-rate which is suitable for blocking high tonic levels of glutamate but spares blocking physiological levels of synaptic activity (Lipton 2006). Recent studies claim memantine preferentially blocks exNMDARs (Xia et al. 2010; Okamoto et al. 2009) yet the design of these experiments do not support this conclusion; exNMDARs were isolated using the MK-801 approach discussed above and 10 μM memantine was found to strongly block tonic activation of these receptors. However, if the experiment was repeated

with attempting to block both synaptic and extrasynaptic NMDARs under tonic activation then a similar level of block would be observed (Wrighton et al. 2008; Wroge et al. 2012; this thesis). Therefore, from these studies, it is evident that memantine would only preferentially block exNMDARs if synaptic activity was preserved at the synapse whilst simultaneously there was high tonic glutamate at extrasynaptic sites; to what extent this occurs *in vivo* is not clear. Furthermore, it is now established that memantine can block low frequency-evoked synaptic NMDARs in Mg^{2+}-free ACSF utilizing autaptic cultures (Wroge et al. 2012). Furthermore, in low 0.1 mM Mg^{2+}, memantine can block NMDAR-EPSCs at high, but not low, frequency-evoked synaptic NMDARs (Wild et al. 2013). To summarize, the neuroprotective effects of memantine should not solely be attributed blocking exNMDARs but rather the temporal profile of glutamate activating both synNMDARs and exNMDARs should be considered.

The hypothesis that exNMDARs are preferentially coupled to excitotoxicity is not absolute; evidence exists for synaptic NMDARs exclusively mediating excitotoxicity (Wroge et al. 2012; Papouin et al. 2012) whilst additionally, it has been proposed that co-activation of both synaptic and extrasynaptic NMDARs mediate excitotoxicity (Zhou et al. 2013) as summarized in **Figure 1.7**. The studies of Wroge *et al* and Zhou *et al.* utilized MK-801 to block synNMDARs in an attempt to selectively activate exNMDARs. However, rather than measure immediate effects such as mitochondrial depolarization, they attempted to induce neuronal death itself. This of course requires synNMDARs to be selectively blocked by MK-801 for a greater length of time yet it is unclear if MK-801 would stably block synNMDARs under these conditions. If MK-801 is proven to be unstable, it would subsequently be difficult to interpret the results of Wroge *et al* and Zhou *et al.*

Therefore, an attempt to resolve the conflicting hypotheses regarding source specificity in NMDAR-dependent excitotoxicity will be made in **chapter 3** by

determining the stability of the MK-801 block under tonic agonist exposure and physiologically concentrations of Mg^{2+}.
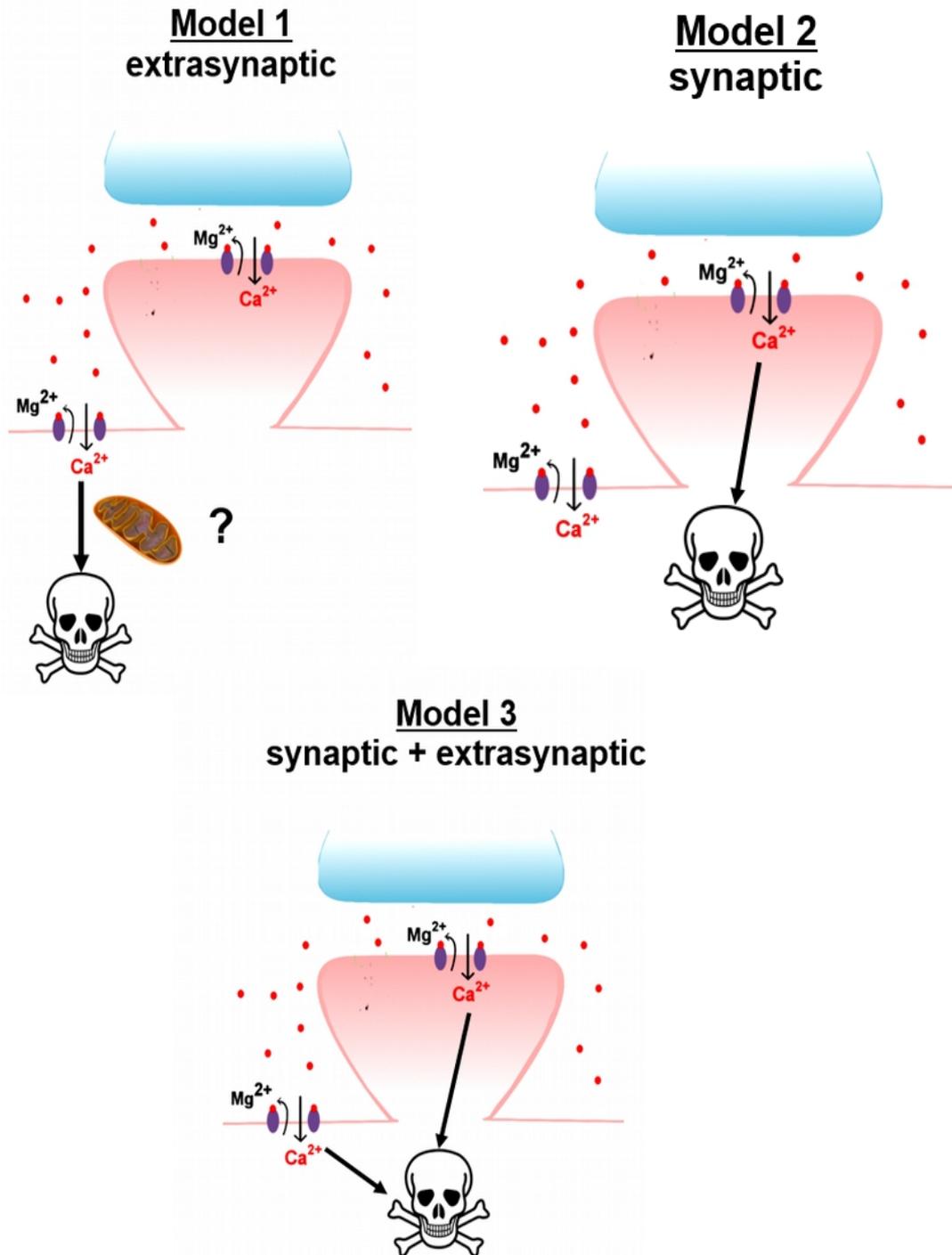
Figure 1.7: Source specificity in NMDAR-dependent excitotoxicity. NMDAR mediated excitotoxicity can theoretically occur by three distinct spatial routes: synNMDARs alone, exNMDARs alone or a combination of synNMDARs and exNMDARs.

1.4.2 Neuroprotective signalling by synaptic activity

The concept that NMDAR activation under physiological conditions may be beneficial was first proposed by Olney; he noted that NMDAR antagonists administered subcutaneously to rats could induce large vacuoles containing mitochondria in posterior cingulate neurons (Olney et al. 1989). Subsequently, it was demonstrated perinatal antagonism of NMDARs could induce widespread apoptosis (Ikonomidou et al. 1999) and exacerbate neuronal death induced by head trauma (Pohl et al. 1999). Great strides in the last 15 years have dissected out the molecular mechanisms underlying neuroprotective signalling by synaptic activity as summarized in **Figure 1.8**.
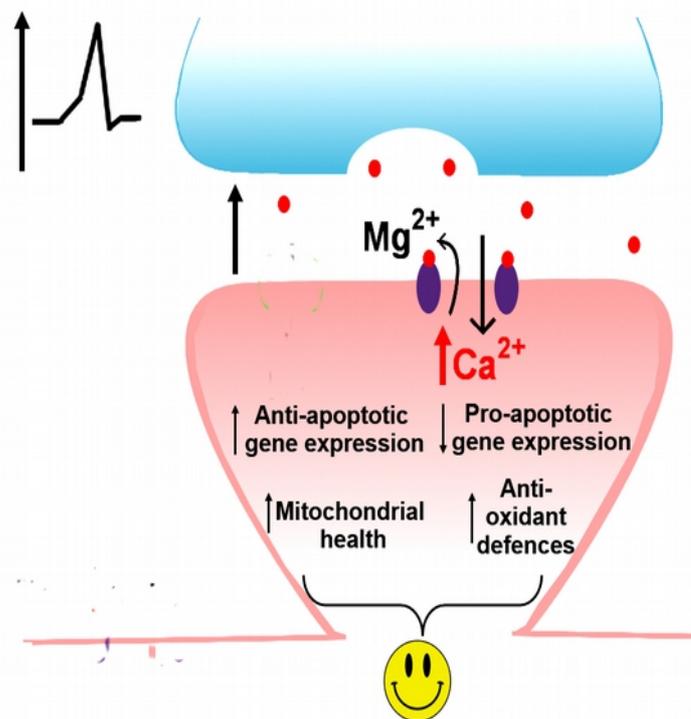
Figure 1.8: Synaptic activity is neuroprotective. Increasing synaptic activity promotes Ca^{2+} influx at synNMDARs with little activation of exNMDARs. This temporal and spatial activation promotes anti-apoptotic genes expression, antioxidant defences and mitochondrial health. In addition to promoting survival pathways, synaptic activity also dampens pro death signalling pathways by decreasing pro-apoptotic gene expression.

As discussed in the previous section, synaptic activity results in the activation of CREB via nuclear Ca^{2+}. Specifically, nuclear CaM kinase is activated and phosphorylates CREB at ser133 which in turn promotes the binding of CREB binding protein (CBP); CBP is then subsequently phosphorylated at ser301 by CaMKIV finally permitting the transcription of certain genes which have CRE region (Wu et al. 2001). CREB can regulate "activity-regulated inhibitors of death (AID)" genes which converge to boost mitochondrial health and thus leave neurons less vulnerable to excitotoxicity (Zhang et al. 2009). Only 1 of the 9 AID genes, NPAS4, was found not to be a CREB target gene which stresses the importance of CREB regulated gene expression. Incidentally, NPAS4 has subsequently been shown to be critical in regulating mitochondrial health (Qiu et al. 2013).

Ca^{2+} influx via NMDARs can also activate CREB in a slower, indirect mechanism by activating ERK. Fascinatingly, glutamate uncaging (1Hz, 60 secs) at only 7 dendritic spines can activate ERK sufficiently to detect CREB phosphorylation of ser133 (Zhai et al. 2013). Although the physiological relevance of this is unclear as the experiments were conducted in the absence of Mg^{2+}, it clearly demonstrates that even small synaptic Ca^{2+} transients have the potential to be neuroprotective. Furthermore, when dendritic and somatic Ca^{2+} are buffered, it is still possible to activate ERK by Ca^{2+} influxes via synaptic NMDAR; this suggests a local pool of Ca^{2+} in the direct vicinity of the NMDARs should be thought as biochemically distinct from that in the dendrites and soma (Hardingham et al. 2001a).

In addition to dampening down pro-apoptotic signalling, synaptic activation of CREB can also promote pro-survival gene expressions such as brain-derived neurotrophic factor (BDNF). BDNF is neuroprotective and can mitigate the detrimental effects of blocking synaptic activity (Hansen et al. 2004). Synaptic activity also boosts anti-oxidant defences leaving neurons more resistant to oxidative stress (Papadia et al. 2008).

1.4.3 GluN2 subtype and coupling to neuroprotection and excitotoxicity signalling

It has been reported that, independent of membrane location, GluN2A mediates neuroprotective signalling whilst GluN2B mediates excitotoxicity (Liu et al. 2007a). However, this study derives many of the conclusions from experiments where NVP-AAM077 would not selectively block GluN2A but would also block a significant portion of GluN2B NMDARs. Another study utilizing a more appropriate concentration of NVP-AAM077 concluded that in mature neurons both GluN2A and GluN2B mediate excitotoxicity; an additive effect of ifenprodil and NVP-AAM077 was observed in blocking excitotoxicity (von Engelhardt et al. 2007). Furthermore, in young neurons that predominately express only the GluN2B subunit, NMDARs can still mediate neuroprotective and excitotoxic signalling. This suggests it is the location of the NMDAR/temporal profile of glutamate which dictates whether the NMDAR couples to neuroprotective or excitotoxic signalling in this instance (M-A Martel et al. 2009). GluN2B and GluN2A mediating both neuroprotection and excitotoxicity has also been reported (Stanika et al. 2009).

As previously discussed, the CTD of GluN2A and GluN2B have diverged significantly in order to couple to different signalling cascades; it was hypothesized that any potential differences in excitotoxicity may be down to differences in the CTDs. To address this, chimera constructs were designed where the GluN2A CTD was swapped with that of GluN2NB (named GluN2A$^{2B(CTR)}$) and the reciprocal GluN2B CTD with the GluN2A CTD (named GluN2B$^{2A(CTR)}$). When these constructs were transfected into neurons, it was observed that the GluN2B CTD promoted excitotoxicity whether coupled to the GluN2A or GluN2B subunit (Martel et al. 2012); this suggests both GluN2A and GluN2B can both mediate excitotoxicity but the CTD of GluN2B induces a stronger insult. Furthermore, cultures from

genetically modified mice where the GluN2B CTD had been replaced with that of GluN2A, were created. Under similar Ca^{2+} loads to WT cultures, the GluN2B$^{2(ACTR)}$ cultures were less vulnerable to excitotoxicity, confirming the GluN2B CTD preferentially couples to excitotoxicity. Importantly, such findings were recapitulated *in vivo.* Interestingly, the detrimental effects of the GluN2B CTD could be overcome by increasing concentrations of agonist; this suggests that under high Ca^{2+} influx the CTD becomes irrelevant possibly because the toxic effects of Ca^{2+} at mitochondria is saturated and cannot be further enhanced by intracellular signalling by the NMDAR.

There are several mechanisms by which the CTD of GluN2B may preferentially couple to excitotoxicity. Firstly, a cell-permeable peptide mimetic of the GluN2B PDZ ligand (NA-1/Tat-NR2B9c) disrupts the interaction of the GluN2B CTD and PSD-95 (Aarts et al. 2002). Under excitotoxic conditions, NA-1/Tat-NR2B9c uncouples the GluN2B from nitric oxide production which ultimately has the effect of dampening down pro-death p38 signalling and CREB shut-off (Soriano et al. 2008; Martel et al. 2012). From a clinical perspective, it is promising that NA-1/Tat-NR2B9c has the beneficial effect of not only reducing lesion size but also improving general outcome of non human primates post stroke (Cook et al. 2012). Furthermore, NA-1/Tat-NR2B9c was found to reduce lesion size 12-95 hours after infusion in a phase II aneurysm trial (Hill et al. 2012). Other studies have linked the GluN2B C-terminal domain to excitotoxicity. Death-associated protein kinase 1 (DAPK1) phosphorylates ser1303 on the CTD of GluN2B which increases NMDA currents and thus excitotoxicity; a peptide which blocks DAPK1 interaction with the CTD was shown to be neuroprotective *in vivo* (Tu et al. 2010).

A study utilizing cultures derived from genetically modified mice where the GluN2A CTD had been replaced with that of GluN2B (the opposite genetic modification to that in the Martel (2012) study) will be the focus of **chapter 5**;

evaluating the role of the GluN2 CTD in excitotoxicity and neuroprotection will be expanded here.

1.5 NMDAR-dependent synaptic Plasticity

The earliest evidence that NMDARs are necessary for some forms of memory *in vivo* was derived from a pharmacological approach; administration of NMDAR antagonists prevented spatial learning with no effect on visual learning (Morris et al. 1986). Since then, a great body of work has attempted to elucidate the molecular processes involved in learning & memory; it should be stressed that is beyond the scope of this thesis to discuss in any great detail the intricacies of such processes which will vary greatly between brain regions.

Nevertheless, synaptic plasticity, the ability of synapses to strengthen or weaken their connections, supports Hebbian theory. The two most studied forms of synaptic plasticity are long term potentiation (LTP) and long-term depression (LTD) (Malenka & Bear 2004). NMDAR dependent LTP is induced by a short but high frequency stimulation of a presynaptic pathway ultimately resulting in a high level of Ca^{2+} influx via NMDARs; this postsynaptic Ca^{2+} activates certain kinases which promotes the insertion of AMPAR into the synapse thus causing an increase in synaptic strength. It has been widely proposed that this was AMPAR subunit specific with the GluA1 CTD being critical for this insertion (Kessels & Malinow 2009, Anggono & Huganir 2012). However, replacement of the GluA1 subunit with the GluA2 subunit and even more surprisingly, a kainate receptors (which are not endogenously expressed hippocampal pyramidal neurons), showed normal LTP (Granger et al. 2013). If such findings are replicated, a paradigm shift from the view that changes in the trafficking of GluA1 containing AMPA receptor being the predominant mechanism underlying LTP, may be needed.

On the other hand, NMDAR dependent LTD is achieved by a sustained but lower Ca^{2+} influx via NMDAR; now, this postsynaptic Ca^{2+} favours the activation of phosphatases which promote the retrieval of AMPA receptors at the synapse. It has

been proposed that NMDAR may mediate LTD through a metabotropic mechanism (Nabavi et al. 2013; Kessels et al. 2013) but this has since been refuted (Babiec et al. 2014).

1.5.2 NMDAR subunit-specific contributions to LTP and LTD

A long-standing hypothesis is that due to subtle differences in biophysical properties of GluN2A and GluN2B, coupled to their divergent CTDs, one GluN2 subunit may mediate LTD and the other LTP. However, the data is contradictory especially regarding LTD (Shipton & Paulsen 2014). Much of this controversy is due to the use of the NVP-AAM077 (previously discussed) and confounded by the problem of compensatory mechanisms induced by genetic knock-out of whole subunits. Furthermore, as previously discussed, there is increasing evidence that a triheteromeric GluN2A-GluN2B population exists which was a critical factor not included in the original hypothesis.

As previously discussed, truncating the C terminal domain of GluN2A and GluN2B alters channel gating but reciprocally switching the CTD domains has no effect. Therefore, where genetic truncation of the CTD of GluN2 subunits has resulted in deficits in synaptic plasticity (Sprengel et al. 1998; Moody et al. 2011) it is difficult to determine if this was due to uncoupling of the NMDAR to signalling cascades or changes in the biophysical properties of the NMDAR. To address this, a genetic approach identical to that discussed in **section 1.4.3** was utilized to investigate hippocampal LTP; the C terminal domains of the GluN2A and GluN2B subunits were reciprocally swapped. When the CTD of GluN2A was replaced with GluN2B, no deficits in LTP induced by both theta-burst and theta-pulse stimulations were observed. Conversely, when the CTD of GluN2B was replaced with that of GluN2A, there was now enhanced theta-burst LTP but suppressed theta-pulse LTP (Ryan et al. 2013). This suggests that GluN2B preferentially promotes certain forms of LTP via

its CTD. It has been proposed the GluN2B subunit may have a preferential role in LTP through its interaction with CaMKII (Nicoll & Roche 2013; Halt et al. 2012).

1.6 The role of the NMDA Receptor in Pathological conditions

As discussed heavily in **section 1.4**, the NMDAR is critical in mediating both neuronal protection and neuronal death. Therefore, it is not surprising that the NMDAR has founds to be involved in the pathology of diseases where neuronal loss is observed, including several neurodegenerative diseases and conditions where ischemic brain damage is present. An overarching role of the NMDAR in these conditions appears to be a promotion of neuronal death signalling (rather than a lack of neuroprotective signalling) but such reductionists views should be avoided. Indeed, a long-held hypothesis pertaining to the use of NMDAR antagonists to aid the treatment of stroke was rejected after an increase in mortality was observed in clinical trials (Davis et al. 2000). It is now hypothesized that the lack of efficacy in the trial was because excitotoxicity at the primary injury site is particularly rapid, and consequently, the NMDAR antagonism was too late in preventing neuronal death. On the other hand, it has been proposed that NMDAR antagonism at the secondary site dampened pro-survival signalling thus resulting in the increased mortality. Therefore, when designing a therapeutic strategy aimed at altering the function of the NMDAR, it is imperative to consider the multifaceted nature of NMDAR signalling.

Below is a summary of several pathological conditions where the NMDAR contributes to the diseased state. This inclusion is not intended to be either exhaustive or comprehensive, but rather serves to highlight the far-reaching implications of study basic NMDAR function.

1.6.1 Huntington's Disease

Huntington's disease is a neurodegenerative disorder with a strong genetic component; polyglutamine repeats in the *Huntingtin* gene cause an expansion of the

N terminus of the protein ultimately resulting in a toxic gain of function. The toxicity initiates strongly in the striatum but spreads to to other brain regions as the disease progresses. A mouse model of Huntington's disease shows enhanced NMDA dependent excitotoxicity which is abolished by a GluN2B antagonist (Zeron et al. 2002), This model was later shown to have a higher proportion of extrasynaptic NMDARs (Milnerwood et al. 2010) which has been recapitulated in cultures acutely expressing the mutant *Huntingtin* protein (Puddifoot et al. 2012). Memantine has been shown to delay the progression of Huntington's disease but as the trial was small, it is imperative this is repeated before any definitive conclusions are made (Beister et al. 2004).

1.6.2 Alzheimer's Disease

Unlike Huntington's disease, the pathophysiology of the neurodegenerative Alzheimer's disease (AD) is extremely controversial and is beyond the scope of this thesis. Soluble oligomers of amyloid β (Aβ), a hallmark of the disease, can induce synaptic dysfunction mediated through the NMDAR as measured by a loss of PSD-95 (Roselli et al. 2005) and spine number (Shankar et al. 2007) in mice. Furthermore, Aβ can facilitate NMDAR-dependent LTD (Li et al. 2009) and inhibit LTP (Li et al. 2011). Importantly, recent evidence has managed to link Aβ with Tau and cellular prion proteins (PrP^C), other hallmarks of the diseases, via the NMDAR. Both tau (Ittner et al. 2010) and PrP^C (Um et al. 2012) have been shown to enhance Fyn interacting with the NMDAR; as phosphorylation of Y1472 by Fyn prevents AP-2 mediated endocytosis, this will disrupt regulation of NMDAR surface expression, thus having the ultimate consequence of enhancing Aβ toxicity. Furthermore, PrP^C can modulate the glycine/D-serine affinity of the NMDAR in a Cu^{2+}-dependent manner; Aβ can disrupt this physiological function of PrP^C leading to an excessive and toxic Ca^{2+} influx caused by a dysregulation of desensitization (You et al. 2012).

Memantine was found to be beneficial in treating mild to severe AD (Reisberg et al. 2003) but a re-assessment of three trials, including 431 patients with mild AD, concluded that there is a lack of evidence for the beneficial effects of memantine (Schneider et al. 2011). Furthermore, as previously discussed, memantine has pharmacological effects at 5-HT(3) receptors, nACHRs and dopaminergic (D_2) receptors.

1.6.3 Ischemic brain damage induced by stroke or traumatic brain injury

As discussed earlier in this introduction, ischemic conditions can lead to high levels of glutamate and eventually excitotoxicity. This is because ischemic conditions cause a reduction in cellular ATP levels thus disrupting the function of Na+/K+-ATPase ultimately leading to the collapse of cellular Na^+ gradients. As glutamate transporters are secondary active transporters relying on the Na^+ gradient, glutamate uptake is impaired or under severe instances, can even reverse (Camacho & Massieu 2006). Altogether, this leads to an accumulation of glutamate at synaptic and extrasynaptic sites which leads to overactivation of NMDARs.

1.6.4 Epilepsy and neuropsychiatric disorders

Mutations in G*rin2a* and G*rin2b* can result in intellectual disability, epilepsy and autism (Endele et al. 2010; O'Roak et al. 2012; Talkowski et al. 2012). Such mutations can drastically alter the function of the NMDAR. For example, a patient with early-onset epileptic encephalopathy was found to have a *de novo* missense mutation (L812M) in *grin2a*. This mutation altered agonist potency, Mg^{2+} sensitivity and open probability of the NMDAR (Yuan et al. 2014).

The aetiology of schizophrenia is highly complex yet nevertheless, there is an over-

abundance of evidence which suggests a strong NMDAR hypofunction component. Ketamine is known to induce both the positive and negative symptoms of schizophrenia in humans (Krystal et al. 1994) and administration of ketamine to mice results in elevated motor activity and deficits in social interactions; importantly, genetically reducing NMDAR expression in mice recapitulates the ketamine-induced behaviours (Mohn et al. 1999). Currently, a great deal of research is aimed at treating NMDAR hypofunction by pharmacologically enhancing NMDA function via the glycine binding site (Chang et al. 2014).

Lastly, a recently characterized disease, anti-NMDA-receptor encephalitis, demonstrates that acute perturbation of NMDAR function in adulthood can have profound pathophysiological consequences. Here, an acute autoimmune reaction against GluN1 induces a decrease in the surface density and synaptic localization of the NMDAR (Hughes et al. 2010) which ultimately manifests itself in symptoms inlcuding memory impairment, psychosis and seizures (Dalmau et al. 2008).

1.7 Experimental Hypotheses

It is evident from this introduction that the biological outcome of NMDAR activation is determined by a complicated interrelationship between the concentration of Ca^{2+} influx, NMDAR location (synaptic vs. extrasynaptic) as well as the subtype of the GluN2 subunit. Despite the recognition that NMDAR mediated physiology is multifaceted, tools used to study subunit and location dependent signalling are poorly characterized and in other cases, non-existent. Therefore, the aim of this thesis is to address this issue.

In **chapter 3**, I attempt to resolve conflicting hypotheses regarding how the spatial location of NMDARs determines the ability of NMDARs to couple to excitotoxic signalling. In **section 1.3.1**, I highlighted that Mg^{2+} can inhibit MK-801 binding to the NMDAR but it was currently unknown how Mg^{2+} would effect the dissociation of MK-801. Furthermore, I highlighted in **section 1.4.1** that MK-801 blockade of synNMDARs must be stable in order for selective activation of exNMDARs to occur. Therefore, I questioned what would be the consequence if Mg^{2+} promotes the dissociation of MK-801? Ultimately, this would render blockade of synNMDARs unstable, calling into question the validity of long-term selective exNMDAR activation. Therefore, I re-assessed MK-801 pharmacology in the presence of physiologically concentrations of Mg^{2+} and found MK-801 is not irreversible under constant agonist exposure. The relevance of this finding is that it confines a temporal limit in which selective activation of extrasynaptic NMDARs can occur; I will re-asses previous findings in this new light in the upcoming discussions.

Dissecting subunit-dependent signalling mediated by the two major GluN2 subunits in the forebrain, GluN2A and GluN2B, has been advanced significantly by selective GluN2B antagonism yet a reciprocal GluN2A selective antagonist has been lacking as discussed in **section 1.3.5**. Therefore, in **chapter 4**, I utilized novel GluN2A

antagonists (TCN 201 and TCN 213) to question whether these compounds could detect a developmental upregulation of GluN2A in cortical cultures. Young neurons were highly sensitive to the selective GluN2B antagonist ifenprodil but were insensitive to TCN 201 & TCN 213. However, in older neurons and young neurons overexpressing GluN2A, a reduced sensitivity to ifenprodil and enhanced sensitivity to TCN 201 and TCN 213 was observed. Under certain conditions, young GluN2A transfected neurons show a stronger inhibition by TCN 201 than older cells; I hypothesize this is because young GluN2A transfected cells predominately express diheteromeric GluN2A NMDARs but older cells express both diheteromeric GluN2A and triheteromeric GluN2A-GluN2B NMDARs.

The developmental upregulation of GluN2A detected in **chapter 4** can theoretically occur via transcriptional, translational and post-translational mechanisms as discussed in **section 1.2**. Therefore, in **chapter 5,** I question whether selective post-translational mechanisms at the GluN2B CTD is necessary for the developmental upregulation of GluN2A. To achieve this, cortical cultures where the GluN2A CTD has genetically been replaced with the GluN2B CTD (named GluN2A$^{2B(CTR)}$) were utilized. This has the functional consequence that both GluN2A and GluN2B will be regulated in the same manner via the CTD. There is no significant difference in whole-cell NMDA currents, ifenprodil sensitivity and the proportion of synaptic and extrasynaptic NMDARs when comparing GluN2A$_{(2BCTD)}$ and wild type cultures. Furthermore, GluN2A$_{(2BCTD)}$ cultures showed enhanced NMDA-dependent excitotoxicity but no impairment in the expression of several immediate early genes triggered by synaptic activity. Altogether, it can be concluded that when both GluN2A and GluN2B are subjected to the same post-translational modifications at the CTD, the developmental upregulation of GluN2A still occurs. Consequently, this permits the downstream signalling in GluN2A$^{2B(CTR)}$ cultures to be studied.

Chapter 2
Material and Methods

2.1 Neuron culture and genetic manipulations

2.1.1 Primary culture of cortical neurons derived from rodents

Tissue culture grade 24-well plates (Grenier Bio-One) were incubated for at least two hours at 37°C in poly-D-lysine (molecular weight 30,000 – 70,000) and Laminin (Sigma). Sterile-glass coverslips (VWR) were placed in a well if the neurons were to be used for electrophysiology experiments. Cortical neurons were cultured from embryonic day 21 Sprague Dawley rat pups or from embryonic day 17.5 C57BL/6 mouse pups. Mouse pups were decapitated immediately whereas rat pups were anaesthetized with anintraperitoneal injection of pentobarbital (Ceva Sante Animale, La Ballastiere, France) prior to decapitation; both procedures were in accordance with schedule 1 of the home office guidelines for humane killing of animals. The required number of cortices was promptly removed in dissociation medium at room temperature (81.8mM Na_2SO4, 30 mM K_2SO_4, 5.84 mM $MgCl_2$, 0.252 mM $CaCl_2$, 1 mM HEPES, 20 mM D-glucose, 0.001% Phenol Red) supplemented with 1mM kynurenic acid to block NMDAR mediated excitotoxicity. The cortices were then incubated at 37°C with 2ml of dissociation media supplemented with papain (10 enzymatic units/ml) (Worthington Biochemical Corporation) for 20 minutes and then this process was repeated. From this point forward, all fresh media used were pre-warmed at 37°C. The tissue was then washed twice with dissociation media followed by 2 washes with growth medium (Neurobasal-A medium supplemented with 1% Rat Serum (Harlan SeraLab), B-27 Supplement , 1 mM glutamine and an antibiotic-antimycotic agent (all Invitrogen). After washing, corticies were homogenized by rapid suction/expulsion using a 2 ml disposable plastic pipette in 10 ml of growth medium. This cell suspension was then diluted using Opti-MEM (Invitrogen) supplemented with Glucose (20 mM) and an an antibiotic-antimycotic agent, to obtain a concentration of one cortical hemisphere per 14 ml cell suspension for rat and one cortical hemisphere per 7 ml cell suspension for mouse. This cell suspension was then plated at 0.5ml/well (area

1.9cm^2) and the plates were then placed in a humidified 5% CO2 atmosphere at 37°C for 2 hours. After this plating step, the media was replaced with 1 ml of growth medium (described above). On DIV 4, 1 ml of growth medium containing 9.6 μM cytosine β-Darabinofuranoside hydrochloride (AraC) was added to each well to prevent proliferation of glial cells. To maintain cells, 1ml of conditioned media was removed and replaced with the growth medium described above except the rat serum was absent and 10 mM glucose was supplemented; this maintenance typically occurred on DIV 9, 12 and 14.

2.1.2 Maintenance and preparation GluN2A$^{2B(CTR)}$ cultures

The GluN2A$^{2B(CTR)}$ line was generated by the Komiyama lab (The University of Edinburgh) and details of the creation can be found in (Ryan et al. 2013). For the studies in this thesis, all animals were maintained in house at the Centre for Integrative Physiology. The Ensembl transcripts ID for G*rin2b* described here is: ENSMUST00000053880 and for *Grin2a* is: ENSMUST00000032331. For genotyping of the GluN2A$^{2B(CTR)}$ colony utilizing PCR, the following strategy was implemented as illustrated in **figure 2.1**.

To determine the genotype of mice in the colony, the DNA was extracted from ear notches by boiling at 100°C in 50 mM NaOH (600 μl) for 10 minutes. This was followed by the addition of 60 μl of 1M tris-HCl and protein contamination was minimized by centrifuging at maximum speed for 10 minutes. Each PCR reaction contained: 1 μl of DNA sample, 0.5 μL of 4 primers listed in **figure 2C,** 12 μl HotStarTaq Master Mix (Qiagen) and 10 μl DNAase-free H$_2$O. The PCR conditions were as follows: 5 minutes at 95°C followed by 34 cycles of 94°C for 30 seconds, 55°C for 1 minute and 72°C for 1 minute, followed by an extension step at 72°C for 10 minutes. The PCR products were run on 1.5% agarose gel and visualized using SYBR Safe (Life Technologies) as a DNA stain.

A   Detecting GluN2A²ᴮ⁽ᶜᵀᴿ⁾   Detecting WT GluN2A CTD
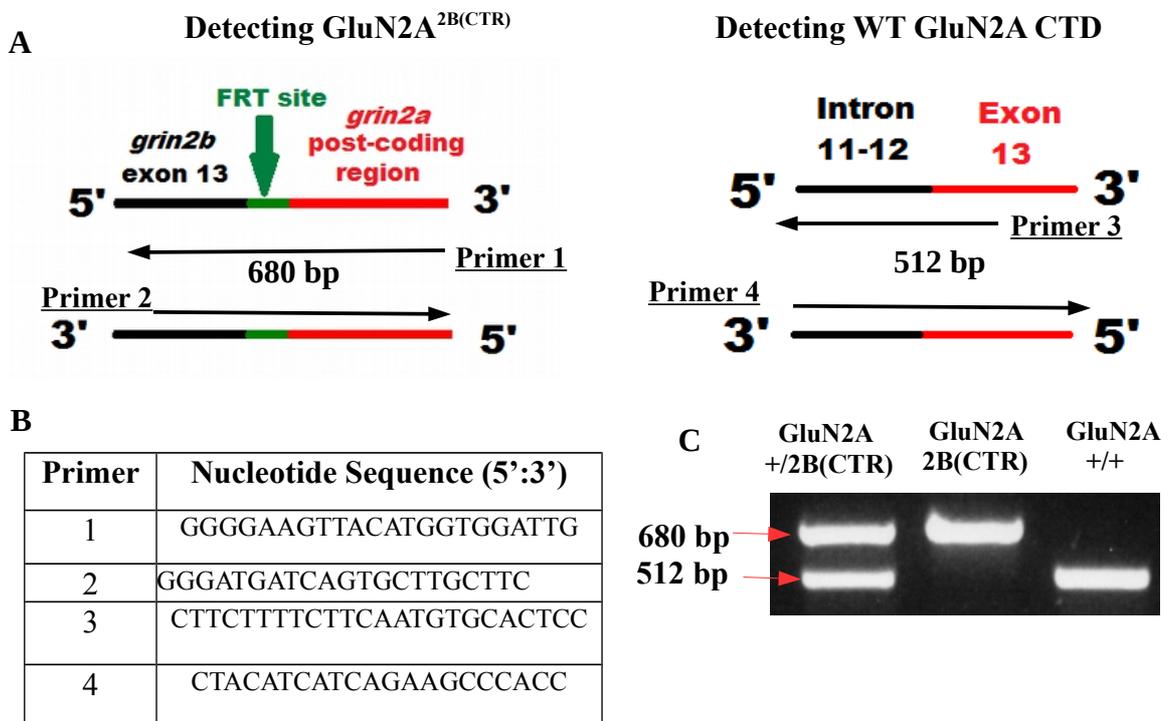
Figure 2.1: Genotyping strategy to detect GluN2A²ᴮ⁽ᶜᵀᴿ⁾ region. **(A)** Primer set 1 and 2 were designed to amplify the G*rin2b* exon coding for the Glun2B CTR inserted into the *Grin2a* gene. Primer set 3 and 4 were designed to amplify the beginning of the exon coding for the GluN2A CTR and the preceding intronic sequence. **(B)** The nucleotide sequence of the primer stated in **(A)**. **(C)** PCR products utilizing mouse genomic DNA from a heterozygous/GluN2A⁺/²ᴮ⁽ᶜᵀᴿ⁾ (left), complete knock-in of GluN2B CTR into GluN2A subunit/GluN2A²ᴮ⁽ᶜᵀᴿ⁾ (middle), and a WT/GluN2A⁺/⁺.

To obtain sister GluN2A⁺/⁺ and GluN2A²ᴮ⁽ᶜᵀᴿ⁾ neuronal cultures, male and female heterozygous GluN2A⁺/²ᴮ⁽ᶜᵀᴿ⁾ mice were mated, and the cortices from individual pups were cultured as described in **section 2.1.1** above. Initially, the pups were genotyped using DNA extracted from the tails in the same manner as the ear notches. However, I found by obtaining a cell-pellet from 0.5ml of the cell suspension and lysing the cells in the same manner as the ear notches, there was sufficient genomic DNA to run the PCR reactions. As this method simplifies the

culture procedure, this method was subsequently adopted.

2.1.3 Transfection of cortical neurons

Neurons were transfected between DIV 5–9 using Lipofectamine 2000 (Invitrogen) according to the manufacturer's suggested protocol. Briefly, pCis-GluN2A (0.4 µg) (Rutter & Stephenson 2000) together with eGFP (0.2 µg) in a volume of 333 µl was added per well of a 24-well plate. After 5 hours this transfection solution was removed and replaced with Neurobasal-A growth medium (2 ml per well). ß-globin was used as a positive control for the transfection procedure in some instances.

Transfection efficiency was approximately 5% with >99% of eGFP-expressing cells being identified as positive for the neuronal nuclear antigen (NeuN), while <1% were positive for glial fibrillary acidic protein (GFAP) (Soriano et al., 2008). Electrophysiological recordings were made from transfected neurons 48 h post transfection; neurons were selected based on having a healthy/non-swollen soma and expression of eGFP extensively in dendrites.

2.2 Electrophysiology

2.2.1 External recording solution: artificial cerebrospinal fluid (aCSF).

Experiments were conducted at room temperature (18–21°C) in an 'external aCSF' solution containing (in mM): NaCl 150, KCl 2.8, HEPES 10, $CaCl_2$ 2, glucose 10, EDTA 0.01; pH to 7.3 with NaOH 3 (320-330 mOsm). Mg^{2+} is omitted from this ACSF to prevent blockade of the NMDAR. Tetrodotoxin (300 nM) was included to block action potential-driven excitatory postsynaptic events when whole-cell NMDA currents were determined. The external solution was applied with a constant gravity fed-flow, at a rate of 3-5 ml/min, and the outflow was generally positioned ~1 cm away from the neuron being patched; this permitted a relatively fast rate of solution exchange as determined by time taken to reach the peak NMDA current (typically

300 ms- 800ms).

2.2.2 Recording electrodes and internal solution

Patch pipettes were made from thick-walled borosilicate glass with dimensions 1.5mm O.D. x 0.86 I.D containing a filament (Harvard Apparatus). Glass was mounted onto a Flaming Brown Micorpipette Puller (Model 97; Sutter instruments) and pulled into a patch electrode to have a final resistance between 4-8MΩ. The recording electrodes were filled with a filtered 'internal' solution that contained (in mM) potassium gluconate 141, NaCl 2.5, HEPES 10, EGTA 11; pH 7.3 with KOH.

2.2.3 Recording Whole cell NMDA currents in voltage clamp

Whole-cell NMDA-evoked currents in cultured neurons were recorded using an Axopatch 200B amplifier (Molecular Devices). Cortical neurons were voltage clamped between -60 mV and -70mV and NMDA currents were evoked by the application of the co-agonists NMDA + glycine in the aCSF described above. Specific details of clamp voltages and concentrations of NMDA/glycine utilized are given in figure legends in subsequent chapters. Access resistances were monitored and, recordings where this changed by >20% or exceeded 30 ΩM were discarded. Holding currents were typically less than -100 pA. Currents were filtered at 2 kHz and digitized at 5 kHz via a BNC-2090A/PCI-6251 DAQ board interface (National Instruments, Austin, TX) and analysed using WinEDR software (Dr John Dempster, University of Strathclyde, Glasgow, UK) for further off-line analysis.

2.2.4 Promoting synaptic activity in current clamp

Whole cell patch clamp recordings were attained in the same manner discussed above. However, 1 mM $MgCl_2$ was included in the aCSF to prevent NMDAR-dependent epileptiform activity and 50 µM bicuculline supplemented to promote

synaptic activity via the inhibition of GABARs. Neurons were allowed to fire action potentials at their resting membrane potential. The liquid junction potential was estimated to be 11 mV using the junction potential calculator (pCLAMP 9) therefore a criteria was set prior to experimentation that the resting membrane potential must be < -50 mV.

2.2.5 Two electrode voltage-clamp of *Xenopus* oocytes expressing NMDARs

Experiments performed by Griffiths N.H., Butters P.A., Edman, S., Samadi, M & Macdonald L.J.

Briefly, two-electrode voltage-clamp (TEVC) recordings were made using a GeneClamp 500 amplifier (Molecular Devices, Sunnyvale, CA) at room temperature (18–21 °C) from oocytes placed in a bath that was perfused with a solution comprising (in mM): NaCl 115, KCl 2.5, HEPES 10, BaCl2 1.8, EDTA 0.01; pH 7.4 with NaOH. Current and voltage electrodes were made from thin-walled borosilicate glass (GC150TF-7.5, Harvard Apparatus, Kent, UK) using a PP-830 electrode puller (Narishige Instruments, Tokyo, Japan) and when filled with 0.3 M KCl possessed resistances of between 1 and 2 MΩ. TEVC recordings were performed at -30 or -40 mV. Currents were filtered at 10 Hz and digitized online at 100 Hz, via a Digidata 1200 A/D interface (Molecular Devices, Union City, CA, USA), using WinEDR 3.1.9 software (Strathclyde Electrophysiology Software, Strathclyde University, UK).

2.3 Determining NMDAR-dependent excitotoxicity

To elicit an excitotoxic insult, neurons were first placed overnight into a minimal defined medium (Papadia et al., 2005) containing 10% MEM (Invitrogen), 90% Salt-Glucose-Glycine (SGG) medium; SGG: 114 mM NaCl, 0.219% NaHCO$_3$, 5.292 mM KCl, 1 mM MgCl$_2$, 2 mM CaCl$_2$, 10 mM HEPES, 1 mM Glycine, 30 mM

Glucose, 0.5 mM sodium pyruvate, 0.1% Phenol Red; osmolarity 325 mosm/l. To induce neuronal death, neurons were exposed to NMDA at various concentrations and times; this is further stipulated in subsequent figure legends where necessary. To terminate NMDAR activation, 10 μM MK-801 was added at the desired time point. Exposure to excitotoxic concentrations of NMDA leads to neurons displaying swollen cell bodies and pyknotic nuclei with small irregular chromatin inclusions. Such characteristics are indicative of necrotic, as opposed to apoptotic, cell death. The cells were fixed 24 hours after exposure to NMDA and the cell death determined by calculating the ratio of DAPI (Vectorlabs) stained pyknotic nuclei as a percentage of the total nuclei. Images were taken using a Leica AF6000 LX imaging system, with a DFC350 FX digital camera.

2.4 Determining changes in mRNA expression upon synaptic activity

2.4.1 Stimulation and harvesting of RNA

DIV 16 neurons were placed overnight in the SGG/10 % MEM media described above. On DIV 17, the neurons were stimulated with 50 μM bicuculline to promote synaptic activity for fours hours. After the stimulation, Total RNA was isolated using High Pure RNA Isolation Kit (Roche) including a DNase-treatment step to degrade genomic DNA. The total RNA was eluted in 50 μl of RNase-free water and stored at -80ºC.

2.4.2 RT-PCR and Quantitative-PCR

cDNA was synthesized from 1-5 μg of total RNA using Transcriptor First Strand cDNA Synthesis Kit (Roche). The reverse transcription reaction was carried out by mixing 7 μl of RNA with 13 μl reverse transcriptase (RT) mix containing Anchored-oligo(dT) primer: random hexamer primer 1:2 (total 3 μl), 4 μl transcriptor reverse

59

transcriptase reaction buffer (5X), 0.5 μl protector RNase inhibitor (40 U/μl), 2 μl deoxynucleotide Mix (1mM each:dATP,dGTP,dTTP, and dCTP), 0.5 μl transcriptor reverse transcriptase (20 U/μl) and 3 μl nuclease free water. At least one sample was prepared with the omission of reverse transcriptase as a positive control. cDNA synthesis reactions were all carried out at 25°C for 10 minutes (for primer annealing), 30 minutes at 55°C (for the reverse-transcription reaction), 5 minutes at 85°C (for enzyme inactivation) and then finally held at 4°C.

This cDNA was then diluted to 6 ng/μl and qPCR was performed in a Mx3000P qPCR System (Stratagene) using FastStart Universal SYBR Green Master Mix (Roche). A qPCR reaction mix, containing 1 μl template cDNA, 7.5 μl SYBR Green master mix ,0.6 μl forward and reverse primers at a final concentration of 200 nM and 5.3 μl nuclease free water was prepared on ice. 15 μl of this reaction mix was pipetted into each well in technical replicates alongside a templatee-free control and a RT-PCR reaction prepared with no reverse transcriptase. The cycling program was 10 min at 95 °C; 40 cycles of30 s at 95 °C, 40 s at 60 °C with detection of fluorescence and 30 s at 72 °C; followed by one cycle of 1 min at 95 °C, 30 s at 55 °C ramping up to 95 °C over 30 s with continuous fluorescence detection. Expression of the gene interest was calculated using the efficiency corrected $2^{(-\Delta\Delta Ct)}$ method (Livak & Schmittgen 2001), normalising to the housekeeping gene GAPDH. The sequence and efficiencies of primers used are shown below.

Gene	Efficiency (%)	Forward Primer (5' to 3')	Reverse Primer (5' to 3')
GAPDH	104	GGGTGTGAACCACGAGAAT	CCTTCCACAATGCCAAAGTT
BDNF	101	AAAGTCCCGGTATCCAAAGG	CTTATGAATCGCCAGCCAAT
FOSB	99	AGGGAGCTGACAGATCGACTT	CTTCGTAGGGGATCTTGCAG
NPAS4	96	AGGGTTTGCTGATGAGTTGC	CCCCTCCACTTCCATCTTC

2.5 Materials

The following drugs were purchased from Tocris (Birstol, UK):(+)/-MK-801 Maleate, ifenprodil hemitartrate, NMDA, tetrodotoxin citrate, bicuculline, and TCN 201. TCN 213 was first initially purchased from Enamine (Kiev, Ukraine) and then subsequently from Tocris. All other components of aCSF and SGG were purchased from Sigma.

2.6 Statistics and curve fitting

All results are presented as mean ± standard error of the mean. Statistical testing largely involved a 2-tailed student *t*-test.(Excel, Microsoft).

To determine the dose-response relationship in an excitotoxicity experiment, the dose-response equation below was fitted using OriginLab for graphing and graphPad Prism for statistics:

$$y = A1 + \frac{A2 - A1}{1 + 10^{(LOGx0 - x)p}}$$

Where:

- A1 = initial Y value
- A2 = final Y value
- p= hill slope
- x0 = EC_{50}

Todetermine whether the dose-response relationships were significantly different between groups, the extra sum of squares F-test was utilized. This fits a global model and subsequently calculates the probability of both groups having the same $logEC_{50}$ by chance.

Chapter 3

Recovery of NMDAR currents from MK-801 blockade is accelerated by Mg^{2+} and the implications for selectively activating exNMDARs

3.1 Introduction

Selective activation of synNMDARs by enhancing phasic synaptic activity is neuroprotective whilst tonic activation of both synNMDARs and exNMDARs leads to excitotoxicity (Giles E. Hardingham & Bading 2010). As discussed in **1.4.1,** by promoting synaptic activity in the presence of the use-dependent antagonist MK-801, it is possible to selectively block synNMDARs and subsequently selectively activate exNMDARs by exogenous application of NMDAR agonists. Such approaches revealed that selective activation of exNMDARs is sufficient to depolarize mitochondria, a critical step in excitotoxicity (Hardingham et al. 2002). This, in part, led to the hypothesis that exNMDARs may preferentially couple to excitotoxicity.

Recently, rather than measuring indirect measurements of excitotoxicity such as mitochondrial depolarization depolarization evoked by exNMDARs, studies have attempted to induce neuronal death itself by selectively activating exNMDARs utilizing MK-801 blockade of synNMDARs (Wroge et al. 2012; Zhou et al. 2013) as elaborated in **section 1.4.1.2.** As the attempted selective activation of exNMDARs failed to induce neuronal death, both studies concluded synNMDARs must be critical in mediating excitotoxicity. As the hypothesis that synNMDARs may be the primary mediator of excitotoxicity is in stark contrast to a wide body of literature (Hardingham & Bading 2010), I decided to investigate this hypothesis further.

It has largely been assumed that MK-801 is an "irreversible" antagonist (reviewed by Parsons & Raymond 2014). Indeed, this must be true for the findings of Wroge et al. and Zhou et al. to be valid.   Neuroprotection from blocking synNMDARs with MK-801 was observed after 2.5 hours of 50 µM glutamate (Wroge et al) and after 24 hours of a 100 µM NMDA exposure (Zhou et al.). However, the original characterization demonstrated the off-rate of MK-801 was use dependent with a time constant for recovery of 92±106min (mean±SD) (Huettner & Bean 1988).

Importantly, the time constant calculated was determined using 30 μM NMDA in steady state conditions; if a higher concentration of NMDA was used then the open probability of the NMDAR would increase ultimately resulting in a decrease in the time constant. Furthermore, the large standard deviation suggests some cells had a faster recovery than others perhaps because of insufficient washout. Nevertheless, it is evident from this very early study that MK-801 is not an irreversible antagonist under constant agonist exposure.

Furthermore, Mg^{2+} can competitively inhibit MK-801 binding (Reynolds & Miller 1988; Huettner & Bean 1988) which is not surprising as they share an overlapping binding site (Kashiwagi 2002). However, the effect of Mg^{2+} on MK-801 dissociation had yet to be established. Therefore, I wished to revisit the issue of MK-801 stability both in the presence and absence of physiological concentrations of Mg^{2+} with a focus on determining the suitability of MK-801 to permit selective exNMDARs activation via the blockade of synNMDARs with MK-801.

I found that high concentrations of agonist (100 μM NMDA) could induce significant recovery from MK-801 blockade in 10 minutes; this recovery could be accelerated by co-applying either 1 mM $MgCl_2$ or 10 μM memantine which also shares an overlapping binding site with both MK-801 and Mg^{2+}. Furthermore, a non-toxic lower agonist dose (15 μM NMDA) could induce significant recovery after 30 minutes in the presence of 1 mM $MgCl_2$. I hypothesized that if low doses of NMDA could induce recovery, then higher doses should result in excitotoxicity. Surprisingly, unlike constant perfusion, I found it is very difficult to remove all MK-801 in a static cell culture well which may explain the lack of unblocking observed by Wroge et al. and Zhou et al. However if washout was thoroughly executed then 2.5 hours of high agonist exposure is sufficient to induce widespread excitotoxicity post blocking all NMDARs with MK-801.

Altogether, it can be concluded that in the presence of both agonist exposure and physiologically relevant concentrations of Mg^{2+}, MK-801 is not an irreversible antagonist. This confines a temporal limit in which selective activation of extrasynaptic NMDARs can occur. These results were published (McKay et al. 2013).

3.2 Results

3.2.1 In the absence of TTX, Mg^{2+}-free conditions result in glutamate spillover to extrasynaptic sites

Previously it has been shown that synNMDARs can be successfully selectively blocked with MK-801 in Mg^{2+}-free conditions but TTX was co-applied in order to silence network activity; spontaneous quantal release of glutamate provides sufficient NMDAR channel opening for MK-801 to block (Puddifoot et al. 2012; Nakayama et al. 2005). Silencing of network activity is critical as lowering Mg^{2+} is well known to induce epileptiform activity due to the relief of the voltage block of NMDAR by Mg^{2+} (Stanton et al. 1987). However, Wroge et al. 2012 attempted to isolate synNMDARs in Mg^{2+}-free conditions supplemented with 50 μM bicuculline but lacking TTX (albeit in lower 1 mM $CaCl_2$ conditions). In our hands, this protocol blocked 98.1±1.1% of all NMDARs as determined by comparing the initial whole-cell NMDA current to that of sister control cells as shown in **Figure 1C** (examples traces in **Figure 1A** and **1B**). **Figure 1D** illustrates the burst firing induced by bicuculline and the epileptic activity than ensues if switched to Mg2+-free ACSF. It is therefore reasonable to conclude that epileptiform activity induced by Mg^{2+}-free conditions results in glutamate spillover to extrasynaptic sites which can be blocked by MK-801. It is possible that the lower density culture used by Wroge *et al.* may not have such drastic epileptiform activity.

Nevertheless, the incremental recovery from MK-801 blockade upon each NMDA application illustrated in **Figure 1B** was of great interest. This observation lead to a review of the literature and the subsequent hypothesis that other channel blockers such as Mg^{2+} and memantine may promote the recovery from MK-801 blockade.
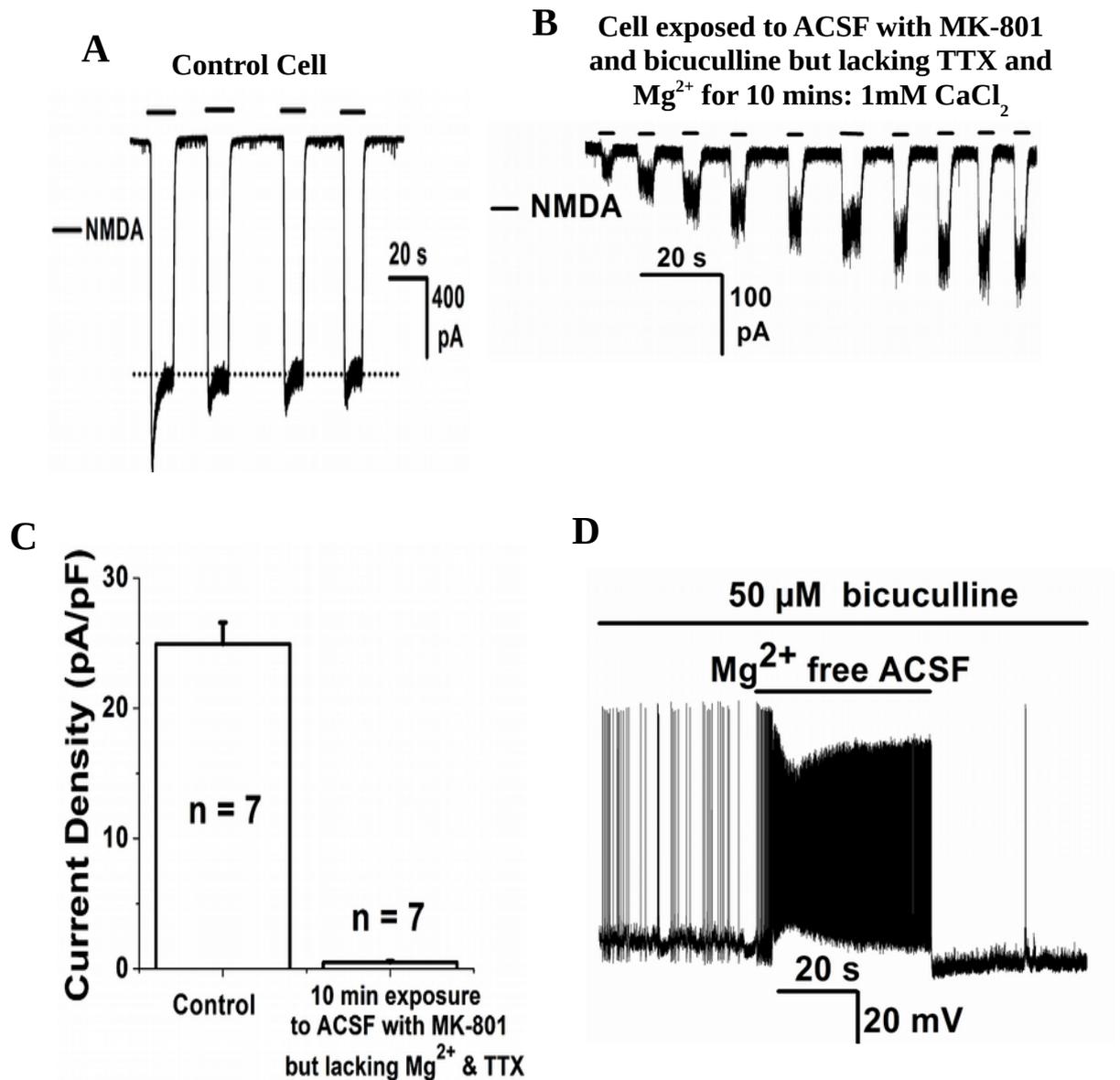
Figure 1:epileptiform activity leads to to glutamate spillover. (A) Untreated cells exposed to NMDA (100 µM) reach a steady state current after 2-3 applications when voltage-clamped at -60mV. **(B)** A cell exposed to ACSF with 10 µM MK-801 and 50 µM bicuculline but lacking TTX and Mg^{2+} for 10 mins has drastically reduced NMDA currents compared to **1A.** Note the incremental increase in NMDA current due to the use-dependent recovery of MK-801 blockade. **(C)** Summary of data: $98.1\pm1.1\%$ reduction in current density of cells treated with MK-801 in the above condition. **(D)** In current clamp, 50 µM bicuculline induces bursts of synaptic activity. If switched to Mg^{2+}-free ACSF, the cell undergoes epileptiform activity.

3.2.2 Antagonism of NMDARs by Mg^{2+} and memantine

Prior to testing the hypothesis that open channel blockers may promote the recovery of MK-801 blockade, I wanted to confirm their antagonism in our hands is consistent with the current literature. Indeed, when a cortical neuron was voltage-clamped at -60mV, the time constant for 1mM $MgCl_2$ block under agonist exposure was < 200 ms and the time constant for the recovery from this blockade < 1s (**Figure 2A**). Furthermore, Mg^{2+} dissociates from the channel pore in the absence of agonist.

On the other hand, 10 µM memantine has a slower on-rate and off-rate than Mg^{2+} (**Figure 2B)** consistent with the literature (Chen & Lipton 1997; Parsons et al. 1995). Nevertheless, unlike MK-801 but similar to Mg^{2+}, memantine can leave the channel pore in the absence of agonist (**Figure 2C**). Of note is the ~90% block by memantine; this is evidence that under high tonic agonist exposure where there is no difference in concentrations at synaptic or extrasynaptic sites, memantine does not discriminate between synaptic and extrasynaptic NMDARs.
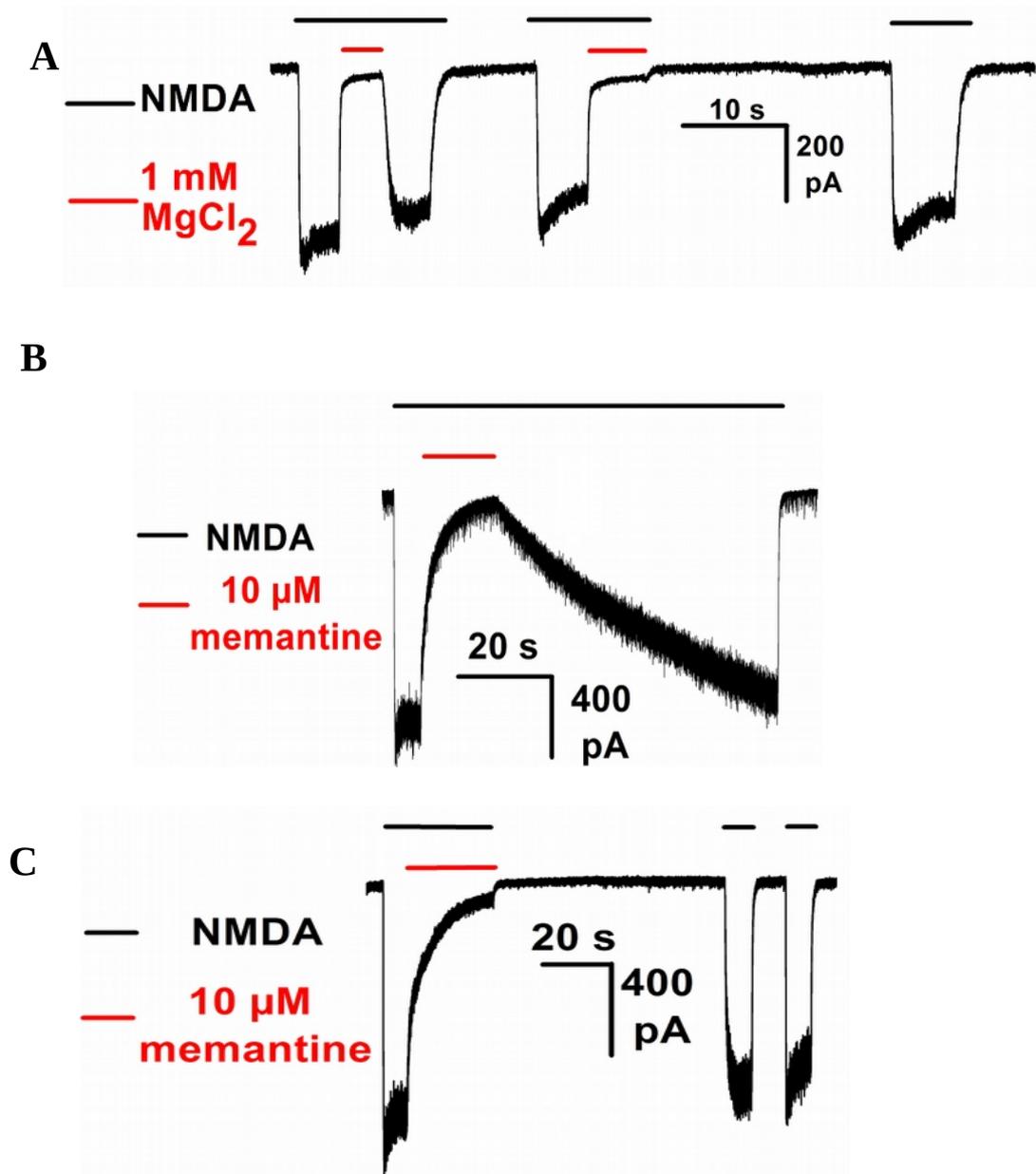
Figure 2: Antagonism of NMDARs by Mg^{2+} and memantine.

(A) When voltage-clamped at -60mV, 1 mM MgCl$_2$ blocks the inward current induced by 100 µM NMDA by ~90%. This blockade can quickly be reversed in the presence and absence of NMDA. **(B)** 10 µM memantine also reduces the inward current induced by 100 µM NMDA by ~90% but both the on-rate and off-rate is considerably slower than Mg^{2+}. **(C)** The recovery from 10 µM memantine blockade also occurs in the absence of agonist exposure.

3.2.3 Mg^{2+} and memantine accelerate the recovery of MK-801 blockade in the presence of agonist

To determine if Mg^{2+} and memantine could accelerate MK-801 leaving the channel pore, I first had to establish a reproducible assay. Firstly, I recorded the inward current induced by 100 μM NMDA with the cortical neurons voltage-clamped at -60mV. Subsequently, I could block all NMDARs by co-applying 100 μM NMDA and 10 μM MK-801. From here, I could perfuse on varying solutions and determine the recovery of MK-801 blockade assayed by repeating the 100 μM NMDA exposure.

As illustrated in **Figure 3A**, ACSF lacking $MgCl_2$ induces very little recovery from the MK-801 blockade but supplementing the ACSF with 100 μM NMDA promotes a significant recovery from the blockade; this is consistent with recovery of MK-801 blockade being use-dependent (Huettner & Bean 1988). Repeating the experiment with ACSF containing 1 mM $MgCl_2$ but with no agonist also provided very little recovery (**Figure 3B**) confirming that Mg^{2+} alone does not promote MK-801 leaving the channel pore which is consistent with previous Ca^{2+} imaging experiments (Yuzaki et al. 1990). However, when ACSF containing 1 mM $MgCl_2$ was supplemented with 100 μM NMDA there was more than twice the recovery from the MK-801 blockade than NMDA alone; NMDA alone provides ~18% recovery whereas 1mM $MgCl_2$ + NMDA provides ~50% recovery. Thus, a combination of the channel in an open activated state, together with Mg^{2+}, promotes recovery of NMDAR currents from MK-801 blockade.

Next I turned my attention to determine if memantine could also promote MK-801 leaving the channel pore. As illustrated in **Figure 2,** memantine has slower off-rate kinetics than Mg^{2+} so I had to modify the protocol. Here, during the MK-801 unblocking phase, I perfused 10 μM memantine + 100 μM NMDA for 9 minutes followed by 1 minute of 100 μM NMDA alone to permit the washout of memantine.
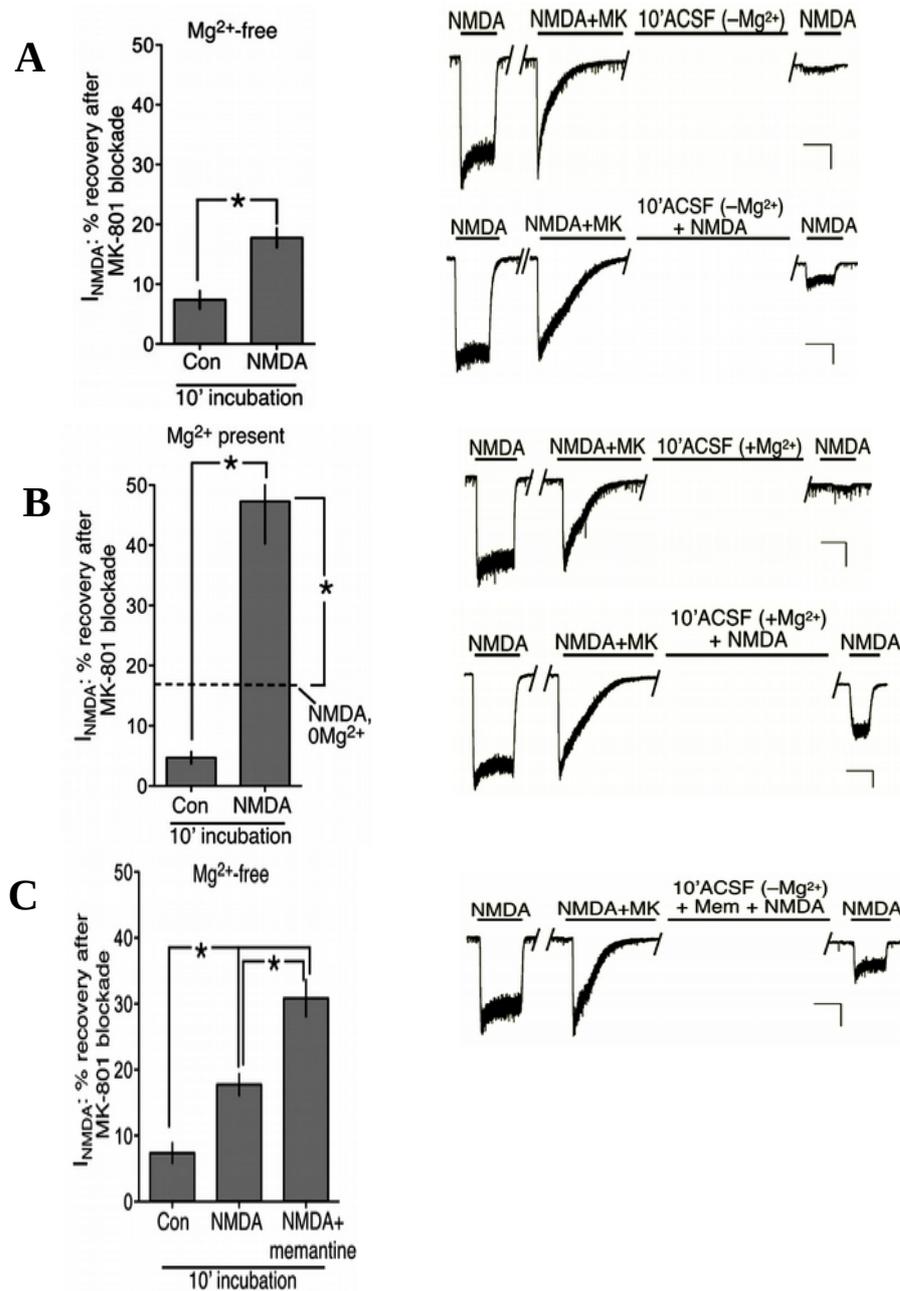
Figure 3: Mg²⁺ and memantine accelerate the recovery of MK-801 blockade in the presence of agonist. Cells voltage-clamped at -60mV, NMDA used at 100 μM, *p < 0.05, Student unpaired t-test and scale bar = 5s (x-axis), 200 pA (y-axis) throughout all.
(A) whole-cell NMDA currents were recorded followed by blocking all NMDARs by co-applying NMDA and 10 μM MK-801 (NMDA + MK). Neurons were then continuously perfused for 10 min in ACSF±NMDA (zero Mg²⁺), after which whole-cell currents were once again recorded and expressed as a % of the original current. (n =8 Con, n =9 NMDA) **(B)** Same protocol as **A** except during 10 min recovery period, ACSF contains 1mM MgCl₂.. Dotted line shows the NMDA-induced unblocking level in the absence of Mg²⁺. (n=7 Con, n = 8 NMDA). **(C)** Same protocol as **(A)** except 10 min recovery with NMDA had first 9 mins supplemented with 10 μM memantine (Mem) followed by 1 min with NMDA alone. (n = 7 Con, n = 8 NMDA, n = 10 NMDA + memantine).

As with Mg^{2+}, memantine also significantly increases the recovery from MK-801 blockade.

Therefore, I propose a model whereby MK-801 cannot leave the channel pore unless the NMDAR is in the open state induced by agonist binding. Once in the open state, there is a finite chance MK-801 will rebind rather than leave the pore entirely; Mg^{2+} and memantine can promote MK-801 leaving the channel pore by interfering with MK-801 rebinding to the channel pore.

The effect of Mg^{2+} promoting MK-801 leaving the channel pore can be visualized in real time by studying the effect of repeated applications of NMDA. In **figure 3A** I recapitulate the finding that Mg^{2+} alone does not promote the recovery from MK-801 blockade. In **figure 3B**, post MK-801 blockade, 9 x 10s pulses of 100 μM NMDA in ACSF lacking Mg^{2+} induces an incremental increase in recovery from MK-801 blockade. However, when the 9 x 10s pulses of 100 μM NMDA is repeated in ACSF containing 1 mM $MgCl_2$ there is no longer a *visual* incremental increase in recovery. As the neurons are voltage-clamped at -60mV, this is to be anticipated because as MK-801 leaves the channel, it is substituted by Mg^{2+} binding to the channel pore and blocking the NMDAR. Only when the neuron is switched to ACSF lacking Mg^{2+} and 100 μM NMDA re-applied is the extent of MK-801 unblocking revealed ; co-applying NMDA + Mg^{2+} induces nearly twice (29%) the recovery of MK-801 blockade compared to NMDA alone (16%). This supports the evidence that Mg^{2+} promotes MK-801 leaving the channel pore.
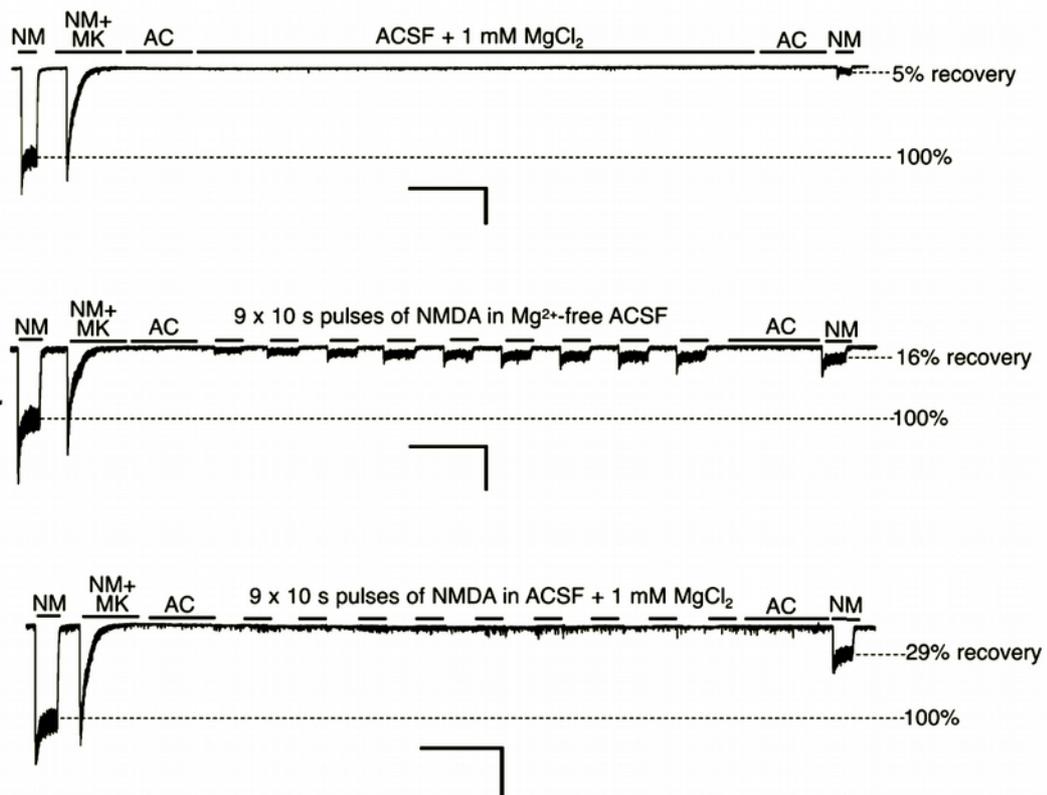
Figure 4: Illustration of the influence of repeated applications of NMDA Mg²⁺ on recovery from MK-801 blockade. Cells voltage-clamped at -60 mV, NMDA (NM) used at 100 µM, MK-801 (MK) used at 10 µM and scale bar = 25s(x-axis), 400 pA (y-axis) throughout all. AC = ACSF

(A) Steady state NMDA current was were determined and all NMDA receptors subsequently blocked by co-applying NMDA + MK-801. Perfusion of ACSF+ 1mM $MgCl_2$ provides little recovery from MK-801 blockade.

(B) Same protocol as **A** except post blockade by MK-801, 9 x 10s pulses of NMDA in ACSF lacking Mg^{2+} results in an incremental recovery of MK-801 blockade.

(C) Same protocol as **B** except 1 mM $MgCl_2$ was co-applied with the 9 x 10s pulses of NMDA. Under these conditions, there is no incremental increase in NMDA currents with each application of NMDA. This is because as MK-801 leaves the channel, it is substituted by Mg^{2+} binding to the channel pore and blocking the NMDAR. When the neuron is switched to ACSF lacking Mg^{2+} and NMDA re-applied the extent of MK-801 unblocking revealed (29%).

3.2.4 Recovery of MK-801 blockade in un-clamped neurons

As the overall aim of this chapter is to determine the suitability of MK-801 to stably block synNMDARs under physiological conditions, it is important to identify caveats in the previous experiments. During the first 10 minutes in the whole-cell configuration of a patch-clamp recording there is a dialysis of intracellular factors, which although unlikely, may effect MK-801 leaving the channel pore. Furthermore, voltage-clamping a neuron by definition is not physiological. Lastly, the above experiments were conducted at room temperature; MK-801 recovery may be greater at the more physiologically relevant 37°C.

To address the above, I wished to determine un-clamped MK-801 recovery in minimal media containing physiologically relevant concentrations of $MgCl_2$ (1mM) at 37°C. To achieve this, all NMDARs were pre-blocked by co-applying 100 μM NMDA + 10 μM MK-801 for 3 mins in the cell culture well. This was followed by thoroughly washing and removing the MK-801 which involved sequentially transferring the coverslip along a row of 5 wells each containing fresh media as illustrated in **Figure 5A**. At this stage, if the neurons were exposed to 100 μM NMDA in the voltage-clamp configuration, virtually no NMDA current was obtained confirming all the NMDARs were blocked **(Figure 5 B + C)**.

From here, the neurons were placed in media containing 15 μM NMDA and 1 mM $MgCl_2$ for either 30 mins or 150 mins (as were untreated control cells). We chose the low 15 μM NMDA dose as it is non-excitotoxic to young rat cortical cultures and I wanted to ensure that the neurons would not die if MK-801 dissociated from a substantial proportion of NMDARs. After 30 mins exposure to 15 μM NMDA, the cells that were pre-blocked with MK-801 had currents that were ~50% of that obtained in sister control cells (**Figure 5A**) and after 150 mins, there was no significant difference between cells that were pre-blocked with MK-801 and control cells (**Figure 5B**). These experiments confirm that even low doses of NMDA,

74

combined with physiologically relevant media containing 1 mM MgCl$_2$, can induce substantial recovery from MK-801 blockade within 30 minutes.

A

All NMDARs blocked by 100 μM NMDA + 10 μM MK-801 for 3 mins

Fresh well → Fresh well → Fresh well → Fresh well → Fresh well

Exposure to 15 μM NMDA for 30 mins or 150 mins in physiological media containing 1 mM $MgCl_2$

B (MK-801 pre-block)

C
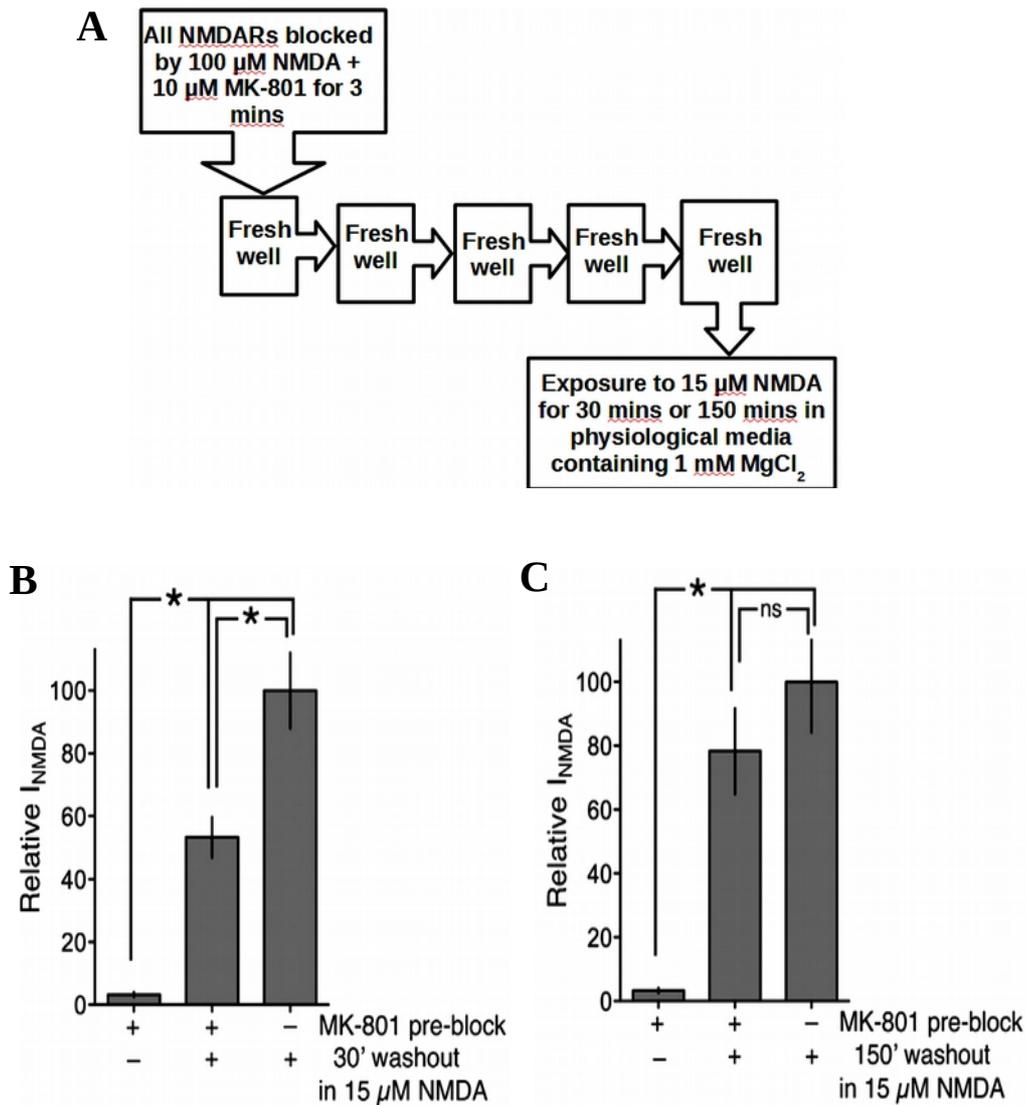
Figure 5: Recovery of MK-801 blockade in un-clamped neurons.
 *$p < 0.05$, Student unpaired t-test (n = 7 in all conditions)
(A) Illustration to demonstrate the blocking of all NMDARs in the culture well (pre-block), the subsequent washing steps to remove all MK-801 and finally, the exposure of the neurons to a non-toxic dose (15 μM) of NMDA for either 30 mins or 150 mins. **(B)** 15 μM NMDA for 30 mins significantly increases recovery of MK-801 blockade. After cells that were pre-blocked with MK-801 and subsequently exposed to 15 μM NMDA, their whole-cell NMDA currents were determined by exposure to 100 μM NMDA as prior. Pre-blocked whole cell currents were normalized to whole-cell NMDA currents of sister control cells. A significant recovery of ~50% was determined. *$p < 0.05$, Student unpaired t-test.
(C) As **(B)** except 15 μM NMDA exposure was for 150 mins. There was no significant difference in whole-cell NMDA currents between cells that were pre-blocked and sister control cells.

76

3.2.5 Agonist-induced recovery from MK-801 blockade can lead to excitotoxic cell death

If 15 μM NMDA can result in ~50% of MK-801 dissociating from the NMDARs within 30 mins, I hypothesized that higher concentration of agonist would provide a faster rate of unblocking and ultimately induce excitotoxic signalling. Furthermore, at this stage, I questioned why Wroge et al. 2012 failed to see very little recovery from MK-801 blockade under hypoxic conditions of 150 mins; the data presented so far in this chapter would predict a substantial MK-801 unblocking under hypoxic conditions.

To this end, I questioned whether the multi-well washout protocol illustrated in **figure 5A** was essential to remove all the MK-801. I specifically designed the protocol to be robust in the removal of MK-801 as it was appreciated that MK-801 is largely used in excess ; MK-801 has an IC_{50} of ~30-50 nM and it is routinely used around 200 times this at 10 μM.

To test this hypothesis, I first blocked all NMDARs by co-applying 100 μM NMDA + 10 μM MK-801 for 10 minutes. One subset of neurons were washed 5 times in a single well with fresh media and then exposed 100 μM NMDA for 150 mins whilst another group had the multi-well wash illustrated in **Figure 4A** followed by the same NMDA exposure as the neurons that underwent the single well wash. The toxicity was terminated by the addition of 10 μM MK-801, the cells were fixed 24 hours later and cell death determined. Only the neurons that received the multi-well had widespread NMDA excitotoxicity **(Figure 6A)**. Two important conclusions were derived from these data. Firstly, even when all NMDARs are blocked, 150 mins of high agonist exposure induces relief of the MK-801 blockade sufficient enough to induce excitotoxicity. Secondly, contaminating MK-801 from incomplete washout is likely to lead to erroneous conclusions.

If it genuinely is difficult to remove all 10 µM of MK-801 by washing a single well, I reasoned that lowering MK-801 concentration would alleviate this problem. However, the concentration would still need to block the majority of NMDARs in addition to blocking NMDA induced excitotoxicity. I determined that lowering MK-801 20-fold to 500 nM and co-applying with 100 µM NMDA for 10 minutes in cell culture media, reduced the whole-cell NMDA currents by 93% when comparing to the whole-cell NMDA currents of sister control cells (**Figure 6B**). Therefore, I concluded 500 nM MK-801 would be suitable to block excitotoxic signalling.

Next, I demonstrated that 100 µM NMDA for either 30 mins or 150 mins causes greater than 80% of the cortical neurons to die (**figure 6C**); the remaining cells are likely to be non-neuronal cells such as astrocytes. 500 nM MK-801 co-applied with 100 µM NMDA for 150 mins blocks this excitotoxicity as predicted. I then demonstrated that pre-blocking the NMDARs with 100 µM NMDA and 500 nM for 10 mins and subsequently then washing the single well 5 times with fresh media does not produce excitotoxicity. If after the pre-block and wash, 100 µM NMDA is applied for 30 mins then little excitotoxicity is observed but if this period is extended to 150 mins then again, I recapitulate greater than 80% of neurons had died 24 hours later.

From this, I conclude that lowering MK-801 20-fold now permits MK-801 to be washed out in a single well. After 30 mins of NMDA exposure post pre-block, even though the recovery from MK-801 may well be complete, there is not sufficient excitotoxic signalling to induce cell death. However, after 150 mins of exposure, there is now adequate excitotoxic signalling that the excitotoxic insult is similar to that if the neurons were not pre-blocked with MK-801 at all. It should be stressed that just because little excitotoxicity occurred at 30 mins does not mean no excitotoxic signalling had occurred; the slow incremental increase in Ca^{2+} influx as the MK-801 leaves NMDARs is in all likelihood, a temporal pattern of Ca^{2+} influx

that will never occur *in vivo*. Measuring any changes in cellular signalling during this period would be difficult to equate to relevant physiology.
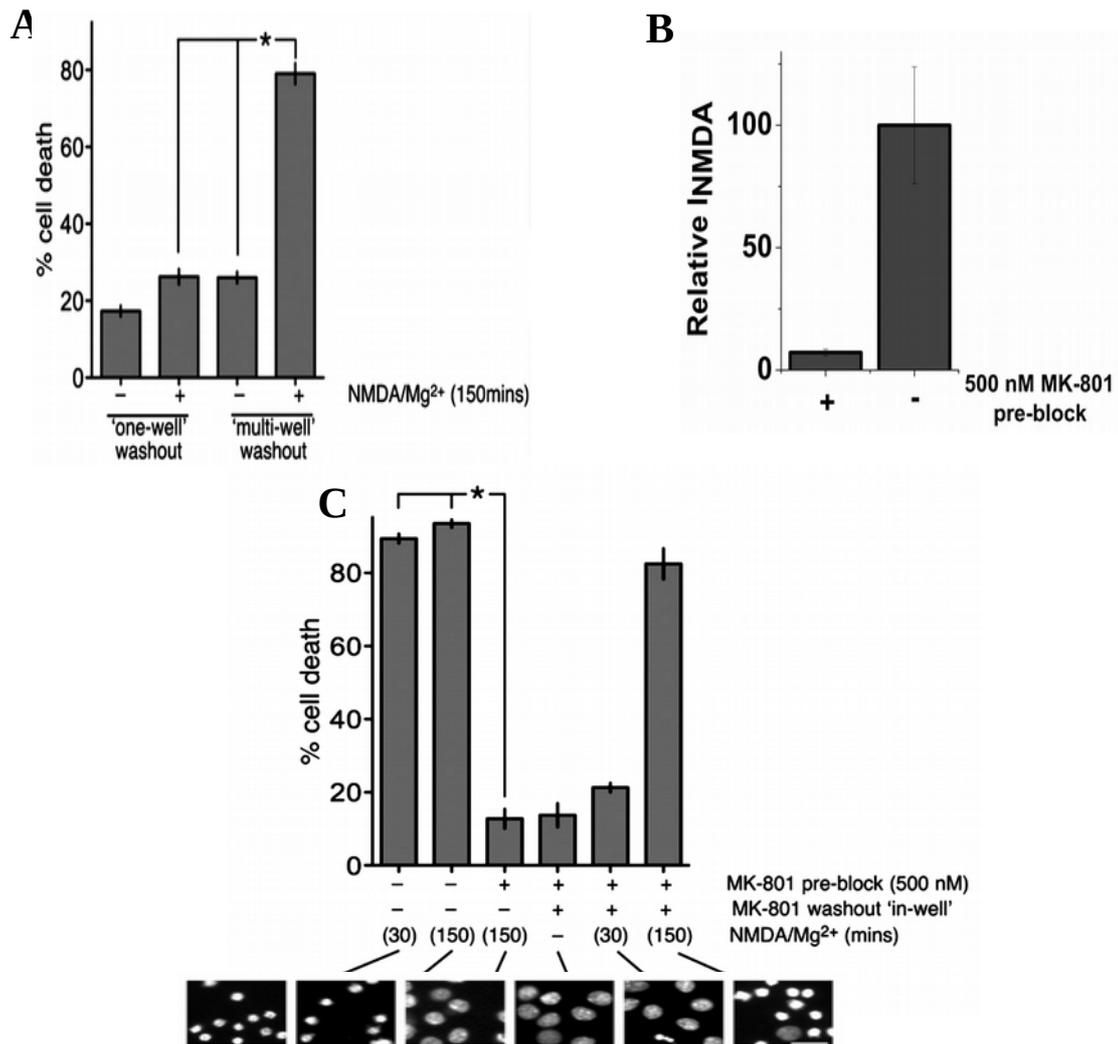
Figure 6: Agonist-induced recovery from MK-801 blockade can lead to excitotoxic cell death. In **A** and **C** each condition, *n* = 3 independent cultures. Each *n* was determined by averaging the cell death in 4 wells or coverslips. *p < 0.05, Student unpaired t-test

(A) Neurons were pre-blocked with 10 μM MK-801 and 100 μM NMDA for 10 mins. Afterwards, one group received a 'one-well' wash which involved washing the single well 5 times with fresh media whereas another group received a 'multi-well' wash as illustrated in **figure 5A.** Afterwards, a subset of each wash group was exposed to 100 μM NMDA for 150 mins. The NMDA insult was terminated by applying 10 μM MK-801. Subsequently,   the cells were fixed 24 hours later and cell death analysed. **(B)** Exposure to 100 μM NMDA and 500 nM MK-801 for 10 mins reduces whole-cell NMDA currents evoked by 100 μM NMDA by 93% when compared to sister control cells. n = 5 for both conditions. **(C)** Exposure to 100 μM NMDA for either 30 mins or 150 mins causes >80% of neurons to die. Co-applying 500 nM MK-801 can block excitotoxicity induced by NMDA for 150 mins. Pre-blocking neurons with 100 μM NMDA + 500 nM for 10 mins does not induce excitotoxicity and neither does subsequently washing the well 5 times with fresh media post pre-block. If after the pre-block + wash, 100 μM NMDA is applied for 30 or 150 mins, only at 150 mins is neuronal death observed. The NMDA insult was terminated by applying 10 μM MK-801. Subsequently,   the cells were fixed 24 hours later and cell death analysed.

3.3 Discussion

3.1 Summary

It can be concluded from this study that in the presence of both continuous agonist exposure and physiologically relevant concentrations of Mg^{2+}, MK-801 is not an irreversible antagonist. This imposes a temporal limit in which selective activation of exNMDARs can occur if experiments are conducted in physiological concentrations of Mg^{2+}. To elaborate, the data presented does negate the selective block of synNMDARs by MK-801 if the observation of exNMDARs occurs over a matter of seconds; the wide spread use of MK-801 to determine the proportion of synaptic vs extrasynaptic NMDARs remains a valuable experimental tool. However, this study clearly demonstrates this approach is not appropriate to investigate specific cellular signalling which occurs over a matter of minutes; this includes investigating downstream signalling of exNMDARs and any potential consequences such as cell death.

It could be argued that utilizing Mg^{2+}-free media to reduce MK-801 dissociation at synNMDARs is an alternate approach to increase the time window in which selective activation of exNMDARs can occur. However, in Mg^{2+}-free media, the Ca^{2+} influx at exNMDARs will be significantly elevated due the Mg^{2+} block of the NMDAR being absent. The same line of reasoning can be projected to synNMDARs that have underwent MK-801 dissociation. Ultimately, conducting experiments in Mg^{2+}-free media will result in an undesirable temporal Ca^{2+} influx, reminiscent of epileptiform activity (as illustrated **in Figure 1D**), which would be difficult to interpret to a pathological condition *in vivo.*

3.2 Do synaptic NMDARs mediate neuronal death?

As discussed in **section 1.4**, selective activation of synNMDARs by enhancing phasic synaptic activity is neuroprotective whilst tonic activation of both synNMDARs and exNMDARs leads to excitotoxicity (Hardingham & Bading 2010). However, this does not prove synNMDARs cannot mediate excitotoxicity as there is a temporal difference between the phasic and tonic activation. Selective block of synNMDARs with MK-801 showed that brief selective activation of exNMDARs was sufficient to depolarize mitochondria suggesting exNMDARs may preferentially couple to excitotoxicity (Hardingham et al. 2002). Again, this does not rule out completely that synNMDARs do not mediate excitotoxicity.

Recently, the MK-801 approach has been extended for a time period which would induce excitotoxicity. This has lead to the hypothesis that synNMDARs alone mediate excitotoxicity (Wroge et al. 2012) in addition to both synNMDARs and exNMDARs mediating excitotoxicity (Zhou et al. 2013). Unfortunately, data in both studies are incompatible with this study. Wroge. et al show that post blocking all NMDARs with MK-801, very little recovery of NMDA currents is observed after 2.5 hours of hypoxic conditions. Although it is difficult to gauge what concentrations of tonic glutamate would be released during hypoxia, it is high enough to induce excitotoxicity, and data in **Figure 5** show that even low non-toxic doses of agonist (15 µM NMDA) for 2.5 hours causes substantial recovery from MK-801 blockade of the NMDAR. Control experiments from Zhou et al are unfortunately even more incompatible. Here, synaptic NMDARs were isolated by co-applying bicuculline and MK-801 for 2 mins. After attempting to wash out the MK-801, 100 µM NMDA was applied for 24 hours and no excitotoxicity was observed. However, the data in **Figure 6** clearly show that when all NMDARs are blocked, only 2.5 hours of 100 µM NMDA is sufficient to remove MK-801 block and induce excitotoxicity. The most rational explanation why this was not observed

after 24 hours is that there is contaminating MK-801 left post washing the cells which protects the neurons from excitotoxicity. Therefore, the conclusions from the above studies must be validated by other experimental approaches that do not implement MK-801 to block synNMDARs.

It should be stressed that the technical manner in which these experiments were conducted is not being questioned. Indeed, I show in **Figure 6** that washing the well 5 times to remove MK-801, the standard practice to remove a drug from a well, was clearly ineffective in removing MK-801. Although, the data presented here leads to the advocation of the 'multi-well wash' illustrated in **Figure 5A** as a control experiment when attempting to wash out any drug or lowering of the drug to a more appropriate concentration as illustrated in **Figure 6C**.

As discussed in **section 1.4.1**, memantine is proposed to block synNMDARs over exNMDARs under high tonic glutamate (Xia et al. 2010; Okamoto et al. 2009) but this conclusion is largely erroneous. This conclusion is derived from evidence that memantine does not block synNMDARs under synaptic activation whereas if exNMDARs are isolated using the MK-801 approach, memantine significantly blocks exNMDARs under high tonic activation. However, as illustrated in **Figure 2**, if both synNMDARs and exNMDARs are activated under tonic activation, 10 µM memantine blocks the current by ~90%. Therefore, memantine would only preferentially block exNMDARs if synaptic activity was preserved at the synapse whilst simultaneously there was high tonic glutamate at extrasynaptic sites. As studies often do not recapitulate this environment, neuroprotection from memantine should not be used as indication that only exNMDARs are mediating excitotoxicity.

Clearly another approach is needed to dissect out spatially distinct populations of NMDARs. One such approach involves using enzymes which degrade the NMDAR co-agonists glycine and D-serine. It has been demonstrated that under physiological

conditions, degrading D-serine effects the activation of synNMDARs whereas degrading glycine effects the activation of exNMDARs (Papouin et al. 2012b). Only degrading D-serine was neuroprotective against NMDA excitotoxicity in a mature hippocampal slice so it was therefore concluded that synNMDARs mediate excitotoxicity. Whereas this may indeed be the case, further control experiments are needed. It is possible that under pathological conditions such as tonic glutamate exposure, the physiological regulation of D-serine at the synapse is lost and it spills to extrasynaptic sites; this must be proven to not occur before it is concluded that synNMDARs mediate excitotoxicity.

Glutamate uncaging has the major advantage of removing the temporal difference in activation of synNMDARs and exNMDARs which has been heavily discussed. Glutamate uncaging (1Hz, 60 secs) at only 7 dendritic spines can activate ERK sufficiently to detect CREB phosphorylation of ser133 (Zhai et al. 2013). This clearly demonstrates that even small synaptic Ca^{2+} transients have the potential to be neuroprotective. Using the same uncaging protocol, it would be interesting to determine the effects of glutamate uncaging at exNMDARs on CREB phosphorylation to determine if an opposing effect was observed.

Altogether, it can be concluded that it is relatively difficult to selectively activate exNMDARs and synNMDARs under the same temporal profile. Whereas there is overwhelming evidence the that phasic activation of synNMDARs mediates neuroprotective signalling, further research will be needed to determine the specific roles synNMDARs and exNMDARs under high tonic glutamate.

Chapter 4

Pharmacological monitoring of the developmental switch in the subtype of the GluN2 NMDA receptor subunit

4.1 Introduction

As a consequence of diheteromeric GluN2A and GluN2B NMDARs having unique biophysical properties and divergent CTD regions, it has long been proposed that much of the complex physiology mediated by NMDARs arises from the two diheteromeric populations coupling to unique signalling cascades (Shipton & Paulsen 2014). However, this hypothesis has been challenged in recent years with evidence that a prominent triheteromeric GluN2A-GluN2B population exists in hippocampal neurons in culture (Tovar et al. 2013) and *in vitro* slices (Gray et al. 2011; Rauner & Kohr 2011).

Nevertheless, selective antagonism of diheteromeric GluN2A and Glun2B containing NMDARs has been utilized extensively to determine subunit-dependent signalling by the NMDAR. Selective antagonism of GluN2B containing NMDARs using ifenprodil has successfully been utilized to study the developmental decrease in the contribution of GluN2B to NMDAR currents (**section 1.2**), excitotoxicity and neuronal protection (**section 1.4**) and finally synaptic plasticity (**section 1.5**).

On the other hand, NVP-AAM077 has been used to selectively block GluN2A containing NMDARs with variable success. As discussed further in **section 1.3**, it is now accepted that low concentrations of NVP-AAM077 (30 nM – 50 nM) can be utilized to selectively antagonise GluN2A NMDAR-mediated EPSCs (Tovar et al. 2013) and GluN2A NMDARs activated under steady-state agonist exposure (Frizelle et al. 2006) with minimal antagonism at GluN2B NMDARs. However, studies have implemented higher concentrations (400 nM) of NVP-AAM077 which antagonizes both GluN2A and GluN2B NMDARs (see for example (Liu et al. 2004; Liu et al. 2007). Accordingly, the use of NVP-AAM007 has led to contradictory hypotheses regarding subunit-dependent signalling mediated by GluN2A and GluN2B.

Therefore it was a great interest when two compounds, subsequently named TCN 213 and TCN 201, were identified by a Ca^{2+} imaging screen that had the pharmacological properties of a GluN2A specific antagonist (Bettini et al. 2010). At concentrations at the limit of their solubility, both TCN 213 and TCN 201 demonstrate no antagonism at GluN2B NMDARs and their potency at GluN2A NMDARs is dependent on the concentration of the co-agonist glycine/D-serine present at the NMDAR as determined by fellow colleagues. The selectivity and mechanism of action of TCN 201 was further clarified by Hansen et al. (2012). TCN 201 also shows no antagonism at GluN2C/GluN2D NMDARs and binds to an allosteric site at a dimer interface between the GluN1 and GluN2A agonist binding domains; here TCN 201 can modulate the agonist affinity of the GluN1 subunit for glycine/D-serine.

As direct pharmacological monitoring of the developmental upregulation of GluN2A has been hampered by the poor selectivity of NVP-AAM077, the pharmacological characterization of these novel GluN2A-specific antagonists provides a unique opportunity to determine the developmental upregulation of GluN2A using a combined electrophysiological and pharmacological approach. It was hypothesized that these compounds would have a low potency in immature cultures where a high proportion of NMDARs are diheteromeric Glu2NB as determined by the high ifenprodil sensitivity. However, it was predicted that upon maturation of cultures and a subsequent fall in ifenprodil sensitivity, this would be juxtaposed with an increase in sensitivity to TN 213 and TCN 201.

Consequently, data in this chapter demonstrates that young neurons are highly sensitive to the selective GluN2B antagonist ifenprodil but are insensitive to TCN 201 & TCN 213 at 3 μM glycine. However, in mature neurons and young neurons overexpressing GluN2A, a reduced sensitivity to ifenprodil and enhanced sensitivity

to TCN 201 and TCN 213 is observed. When glycine was increased 10-fold to 30 µM, GluN2A transfected neurons show a stronger inhibition by TCN 201 than mature cells. It is proposed that this observation is a result of GluN2A transfected cells predominately expressing diheteromeric GluN2A NMDARs whereas mature cells express both diheteromeric GluN2A and triheteromeric GluN2A-GluN2B NMDARs. For this hypothesis to be properly assessed, the potency of TCN 201 at triheteromeric NMDARs must be further clarified. I also discuss the usefulness of these compounds to antagonize GluN2A specific signalling under physiological conditions.

These results were partly published (McKay et al. 2012; Edman et al. 2012).

4.2 Results

4.2.1 Non-endogenous pharmacological characterization of TCN 213 and TCN 201 utilizing *Xenopus* oocytes

All pharmacological characterization of TCN 201 and TCN 213 in *Xenopus* oocytes **was** conducted by fellow colleagues as stipulated in **chapter 2**. TCN 213 was first to be pharmacologically assessed, both non-endogenously in oocytes and endogenously in cortical cultures, solely on the basis it was the first compound to become commercially available. Nevertheless, once TCN 201 became commercially available, it was demonstrated that TCN 201 was more potent than TCN 213 as illustrated in **Figure 1**. This is consistent with the original study where TCN 201 (pIC_{50} = 6.8) was found to be more potent than TCN 213 (pIC_{50} = 5.8) (Bettini et al. 2010). Therefore, it was essential that I further pharmacologically assessed TCN 201 antagonism in cortical cultures as the enhanced potency favours it over TCN 213 for pharmacological studies (Hansen et al. 2012; Hansen et al. 2014) and studying downstream signalling of the NMDAR (Costa et al. 2012; Shin et al. 2012; Hargus & Thayer 2013).
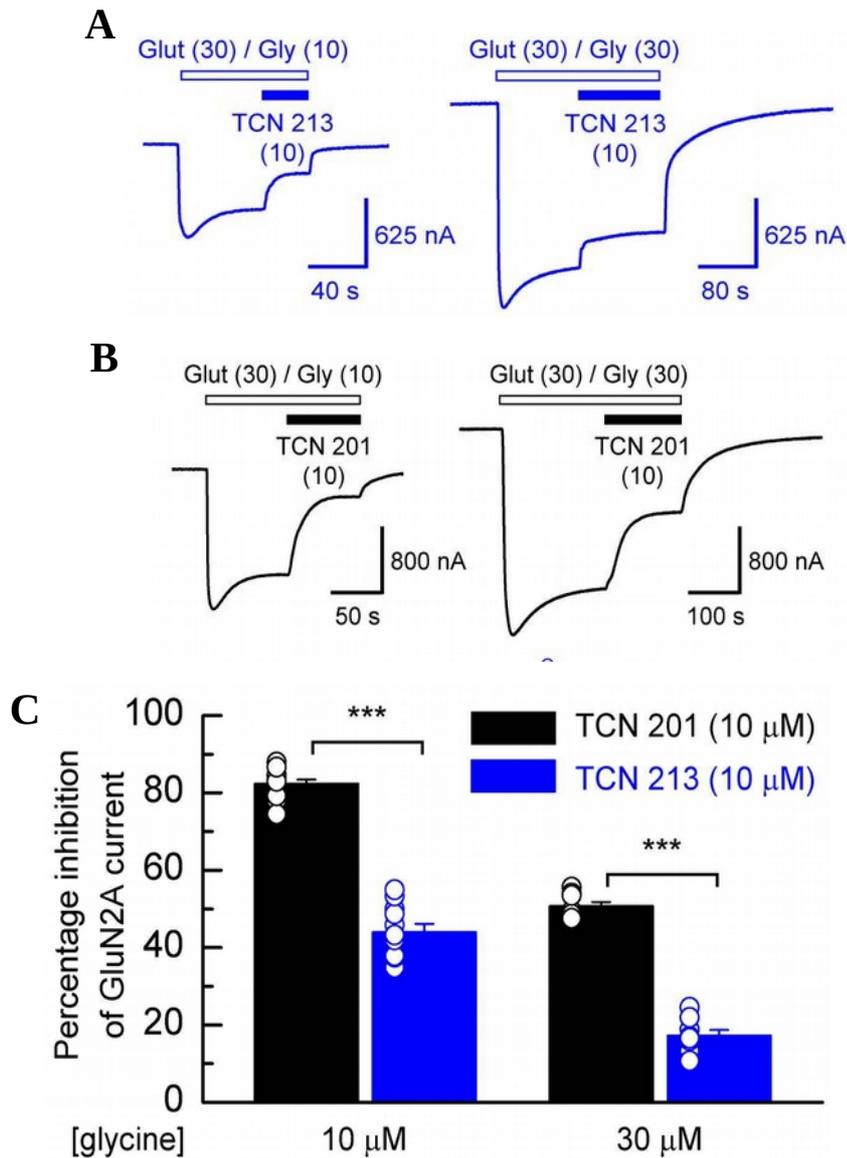
Figure 1: Pharmacological analysis of TCN 213 and TCN 201 antagonism at GluN1/GluN2A NMDARs expressed non-endogenously. *Experiments performed by S. Edman.* **(A)**Two-electrode voltage clamp recordings in oocytes expressing GluN1/GluN2A NMDAR. Cells clamped at -40 mV. Application of glutamate and either 10 μM glycine (left) or 30 µM glycine (right) permits steady state current to be reached.10 µM TCN 213 antagonizes this steady state current in a glycine dependent manner. **(B)** Same conditions as **A** except 10 µM TCN 201 was utilized to antagonize steady state current. This antagonism was again dependent on the concentration of glycine. Note that the potency of TCN 201 is greater than TCN 213 in **(A)**. **(C)** Summary of data. Both the potency of TCN 201 and TCN 213 are dependent on the concentration of glycine but TCN 201 is more potent than TCN 213 at both 10 µM and 30 µM glycine. TCN 201 (10 µM, n = 12; 30 µM, n = 8) and TCN 213 (10 µM, n = 11; 30 µM, n = 9). *P <0.05 (student t-test)

4.2.2 TCN 213 does not block NMDA currents in young rat cortical cultures

It has been previously demonstrated that rat cortical cultures utilized in this study predominately express diheteromeric GluN2B NMDARs between DIV 7 to DIV 11 as demonstrated by ~75% block of whole-cell NMDA currents by 3 µM ifenprodil (M-A Martel et al. 2009). As ifenprodil blocks a pure diheteromeric population by ~80% and a triheteromeric GluN2A-GluN2B by ~30%, the population must be predominately diheteromeric GluN2B. Therefore, this developmental time point could be used to confirm, in accordance with the heterologous *Xenopus* oocyte data, that TCN 213 does not block diheteromeric GluN2B NMDARs endogenously expressed.

To determine this, rat cortical neurons between DIV 7 – 9 were voltage-clamped at -70mV and whole-cell NMDA currents were evoked by 50 µM NMDA and 1.5 µM glycine. Under these conditions, TCN 213 blocked a pure diheteromeric GluN2B population by <5% and a pure GluN2A population by ~75% when heterologously expressed (**Figure 2**). As predicted, TCN 213 failed to block whole-cell NMDA currents under these conditions but 3 µM ifenprodil reduced the steady state current by 72±2% in excellent agreement with (Martel et al. 2009). It can therefore be concluded that TCN 213 fails to block endogenous diheteromeric GluN2B NMDARs as predicted from data in the heterologous system.

This was viewed as a proof of principle experiment and therefore, once TCN 201 subsequently became available, the experiment was not repeated. From here, I wished to focus on TCN 213 and TCN 201 antagonism at NMDARs expressing GluN2A NMDARs either by over-expression or endogenous developmental up-regulation.
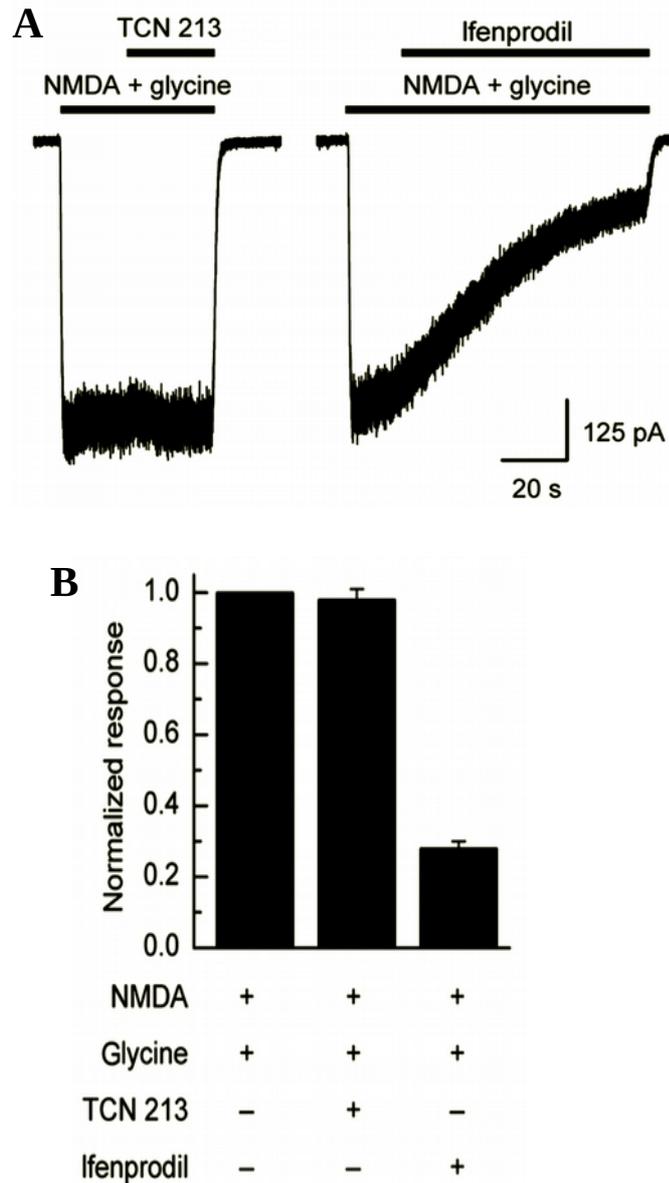
Figure 2: TCN 213 shows no antagonism of NMDARs expressed in young (DIV 7-9) cortical cultures under conditions which would block a pure diheteromeric GluN2A population by 75%.

(A) A rat cortical neuron was voltage-clamped at -70mV and whole-cell NMDA current was evoked by 50 μM NMDA and 1.5 μM glycine. 10 μM TCN 213 fails to antagonize this steady state current. Once the steady state current was re-achieved, 3 μM ifenprodil blocks by ~75%. **(B)** Summary of data. n = 12. TCN 213 fails to demonstrate antagonism at the developmental time point DIV 7-11 suggesting little diheteromeric GluN2A NMDARs. The 72±2% ifenprodil block is consistent with a predominately GluN2B diheteromeric population.

4.2.3 TCN 213 can detect a developmental switch in NMDAR subunits

Developmentally upregulated GluN2A subunits can be incorporated into diheteromeric GluN2A NMDARs or triheteromeric GluN2A-GluN2B NMDARs as discussed in **sections 1.1** and **1.2**. It is now appreciated that triheteromeric NMDARs are largely expressed in mature hippocampal cultures (Tovar et al. 2013) and at the time, I appreciated this possibility in our cortical culture system. It was hypothesized there could potentially be a lack of TCN 213 antagonism in mature cultures due to the presence of triheteromeric NMDARs; as the pharmacological profile of TCN 213 at triheteromeric NMDARs was unknown, it was possible the potency of TCN 213 at diheteromeric and triheteromeric NMDARs was substantially different.

Consequently, two positive controls were established. Firstly, as there is a negative correlation between ifenprodil sensitivity and GluN2A expression (see section 1.2), measuring ifenprodil sensitivity prior to TCN 213 application gives an indirect measurement of GluN2A expression. Secondly, by overexpressing GluN2A, it was hypothesized this would induce a bias towards expression of diheteromeric GluN2A NMDARs rather than triheteromeric NMDARs. This would permit the comparison of ifenprodil and TCN 213 sensitivities of GluN2A transfected cells with that of mature neurons.

DIV 7 -10 neurons that were transfected with globin (as a positive control for the transfection procedure) demonstrated similar average ifenprodil block (70±3%) to untransfected cells (see **Figure 2**, 72±2%). However, in DIV 7-10 neurons than were transfected with GluN2A, the ifenprodil block drastically decreased to an average of 37±5% (compare **Figures 3A & 3B**). This indirectly confirms that GluN2A subunits are expressed at the neuronal membrane as the proportion of diheteromeric GluN2B NMDARs has decreased. In mature neurons (DIV 14-18) the

average ifenprodil block (48±4%), similar to GluN2A transfected neurons, was lower than young neurons thus indicating an endogenous upregulation of GluN2A had occurred (compare **Figures 3A & 3C**).

Once the NMDA steady-state current was re-established in the presence of ifenprodil, 30 µM TCN 213 was applied to all three groups and the current blocked was normalized to the NMDA current pre-ifenprodil (**Figures 3A,3B & 3C**). The data revealed a highly correlated (negative) relationship ($R^2 = 0.87$) between ifenprodil block and TCN 213 block; the cells with the lowest ifenprodil block, GluN2A transfected and mature neurons, showed the highest sensitivity to TCN 213 whereas globin transfected cells had the highest ifenprodil but reciprocally, the lowest TCN 213 block.

Therefore, it can be concluded that TCN 213 successfully detects a developmental upregulation of GluN2A as rat cortical cultures mature under the above conditions. Although a reduction in ifenprodil sensitivity has correlated well with an increase in GluN2A mRNA, protein expression and a change in EPSC decay kinetics (discussed further in section 1.2), this is the first demonstration that a fall in ifenprodil sensitivity during development also correlates with an increase in the sensitivity of a GluN2A antagonist that shows no antagonism at GluN2B NMDARs.
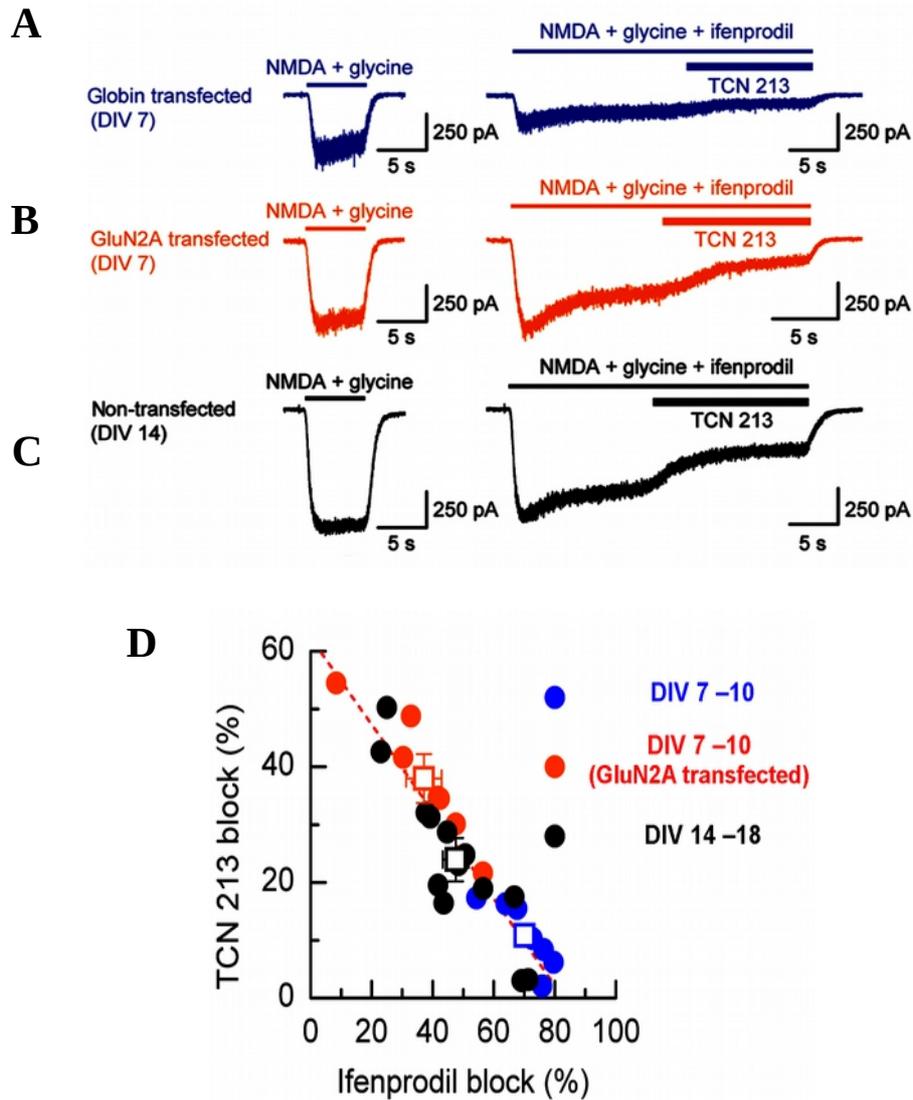
Figure 3: TCN 213 can detect a developmental switch in NMDAR subunits.
All cells voltage-clamped at -70 mV. whole-cell NMDA currents evoked by 50 µM NMDA + 3 µM glycine. Ifenprodil used at 3 µM and TCN 213 used at 30µM. % TCN 213 block normalized to pre-ifenprodil NMDA current.
(A) A DIV 7 globin transfected neuron illustrating a high (70%) blockade of the whole-cell NMDA current by ifenprodil. The remaining current is antagonized little by TCN 213 (11%).
(B) A DIV 7 GluN2A transfected neuron demonstrates a lower ifenprodil block (30%). Remaining ifenprodil insensitive current is sensitive to TCN 213 (42% block).
(C) Mature DIV 14 neuron also shows low ifenprodil block (23%) but high TCN 213 block (43%).
(D) Plot correlating the % ifenprodil block of each cell with the % TCN 213. There is a strong negative correlation ($R^2 = 0.87$) between the ifenprodil block and the TCN 213 block. n = 7 for globin & GluN2A transfected. n = 13 for DIV 14-18

95

4.2.4 TCN 201 can detect a developmental switch in NMDAR subunits

The previous experiment was repeated replacing 30 µM TCN 213 with 10 µM TCN 201 and using the same agonist exposure (50 µM NMDA + 3 µM glycine). However, in this instance, I did not transfect the young (DIV 7-10) control cells with globin as it was previously determined this not change the ifenprodil sensitivity.

As with TCN 213, there was a highly correlated (negative) relationship ($R^2 = 0.91$) between ifenprodil block and TCN 201 block **(Figure 4)**. Therefore, an identical conclusion was reached in that under these conditions, TCN 201 can detect a developmental upregulation of GluN2A.

It is now established that under the above conditions, diheteromeric NMDARs are blocked by 91% and triheteromeric NMDARs blocked by 72% (Hansen et al. 2014). Importantly, the ~20% reduction in TCN 201 potency at triheteromeric NMDARs is not great enough to exclude the possibility of a prominent triheteromeric population contributing to the correlated relationship observed.
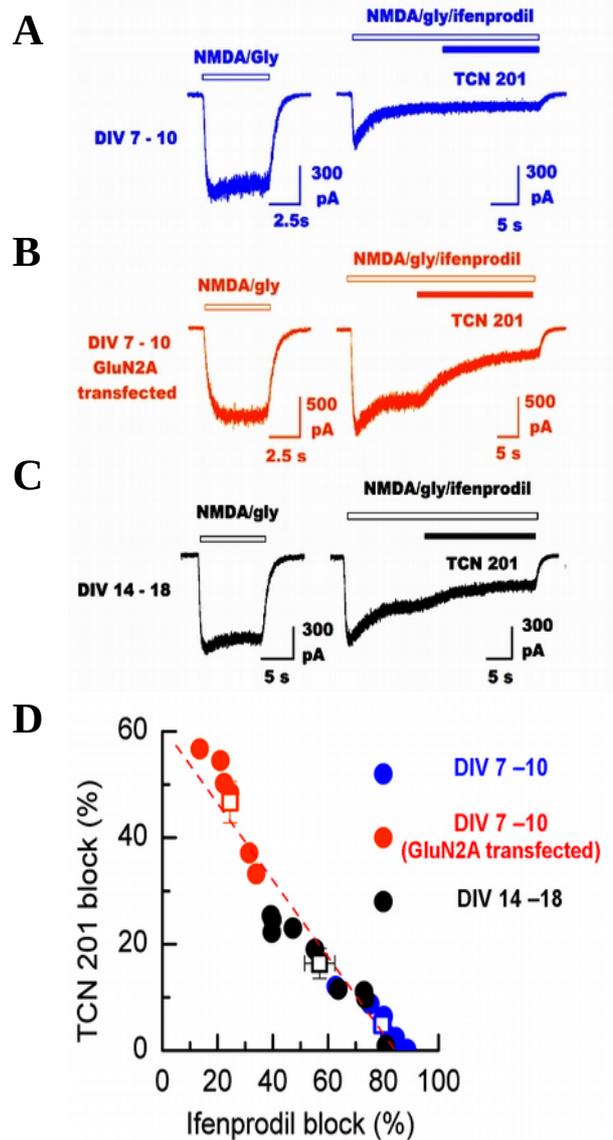
Figure 4: TCN 201 can detect a developmental switch in NMDAR subunits at 3 µM glycine. All cells voltage-clamped at -70 mV. whole-cell NMDA currents evoked by 50 µM NMDA + 3 µM glycine. Ifenprodil used at 3 µM and TCN 201 used at 10 µM. % TCN 201 block normalized to pre-ifenprodil NMDA current.

(A) A DIV 7 neuron illustrating a high (82%) blockade of the whole-cell NMDA current by ifenprodil. The remaining current is antagonized little by TCN 201 (4%). **(B)** A GluN2A transfected neuron demonstrates a lower ifenprodil block (14%). Remaining ifenprodil insensitive current is sensitive to TCN 201 (57% block). **(C)** Mature DIV 14 neuron also shows low ifenprodil block (39%) but high TCN 213 block (25%). **(D)** Plot correlating the % ifenprodil block of each cell with the % TCN 201. There is a strong negative correlation ($R^2 = 0.91$) between the ifenprodil block and the TCN 201 block. n = 7 for DIV 7 – 10 untransfected, n = 6 GluN2A transfected. n = 9 for DIV 14-18

4.2.5 At a higher glycine concentration, TCN 201 potency is different at GluN2A transfected and mature neurons

The previous experiments demonstrated TCN 213 and TCN 201 could detect a developmental upregulation of GluN2A when 3 µM glycine was used as a co-agonist. However, as the EC_{50} for glycine at GluN2A NMDARs is 1.31 µM and 0.72 at GluN2B NMDARs (P. E. Chen et al. 2008) at 3 µM glycine, there is still a bias towards the activation of GluN2B NMDARs. Therefore, I wished to repeat the experiment with a 10-fold increase in glycine concentration.

However, at 30 µM glycine, it was soon apparent that TCN 201 antagonism was not consistent between mature neurons. Mature DIV 17 neurons were recorded on the same day (**Figure 5A & B**), and despite having similar ifenprodil sensitivities (A = 40%, B=42%) the % TCN 201 block was ~3 times greater in the neuron illustrated in **Figure 5B**. There was also a difference between mature and GluN2A transfected cells. Again, recorded on the same day, a mature DIV 21 (**Figure 5C**) and a DIV 7 GluN2A transfected neuron(**Figure 5D**) have similar ifenprodil blocks (25% and 24% respectively) but the GluN2A transfected cell had ~3 times the TCN 201 block.

A summary of the data is illustrated in **Figure 5E**. There was a negative correlation ($R^2 = 0.63$) between ifenprodil bock and TCN 201 block but this relationship was less strong than at 3 µM glycine ($R^2 = 0.91$). However, it is obvious from the data that all the GluN2A transfected cells have a low ifenprodil block and a relatively consistent TCN 201 block whereas there is a wider spread of TCN 201 antagonism in mature cells that have a low ifenprodil block. It was hypothesized the wider spread in TCN 201 block in mature neurons was because at a higher concentration of glycine, TCN 201 antagonizes triheteromeric NMDARs to a lesser extent than diheteromeric NMDARs; I predicted the GluN2A transfection promotes the formation of diheteromeric GluN2A NMDARs and hence a relatively consistent TCN 201 block. Nevertheless, a more qualitative analysis is needed to test the

A

NMDA + Glycine | NMDA + Glycine + Ifenprodil

TCN 201

10 s

1 nA

B

NMDA + Glycine | NMDA + Glycine + Ifenprodil

TCN 201

10 s

1 nA

Both recorded on the same day:

DIV 17

C

NMDA + Glycine | NMDA + Glycine + Ifenprodil

TCN 201

20 s

0.4 nA

D

NMDA + Glycine | NMDA + Glycine + Ifenprodil

TCN 201

20 s

0.5 nA

Both recorded on the same day:

Left: DIV 21

Right: DIV 7 GluN2A transfected

E

TCN 201 Block (%)

$R^2 = 0.63$

DIV 14-18

DIV 7 - 10 (GluN2A transfected)

Ifenprodil Block (%)

99

Figure 5: TCN 201 antagonism at higher 30 µM glycine

All cells voltage-clamped at -70 mV. whole-cell NMDA currents evoked by 100 µM NMDA + 30 µM glycine. Ifenprodil used at 3 µM and TCN 201 used at 10µM.. % TCN 201 block normalized to pre-ifenprodil NMDA current.

(A + B) Illustration of two mature DIV 17 recorded on the same day. Although both neurons have similar ifenprodil sensitivities (A = 40%, B=42%) the neuron illustrated in B has a greater TCN 201 block (20%) compared to than in neuron B (6%).

(C + D) Illustration of a DIV 21 mature neuron (C) and a DIV 7 neuron transfected with GluN2A (D) recorded on the same. Although both neurons have similar ifenprodil sensitivities (C = 25%, D=24%) the GluN2A transfected neuron has a greater TCN 201 block (34%) compared to the mature DIV 21 neuron (12%).

(E) Plot correlating the % ifenprodil block of each cell with the % TCN 201. There is a negative correlation (R^2 = 0.63) between the ifenprodil block and the TCN 201 block. n = 13 for GluN2A transfected. n = 17 for DIV 14+.

…...

hypothesis that GluN2A transfected and mature neurons are differentially antagonized by TCN 201.

4.2.6 Modelling approaches indicate presence of triheteromeric NMDARs in mature neurons

There is a need to qualitatively test the hypothesis that at 30 µM glycine, the TCN 201 block at GluN2A transfected cells is consistent with a diheteromeric GluN2A population whereas mature cells demonstrate a wider range of TCN 201 antagonism due to a prominent triheteromeric population.

By assuming a complete diheteromeric GluN2A and GluN2B population, it is possible to determine the relationship between the ifenprodil block and the TCN 201 block of the ifenprodil insensitive current. This model would therefore permit the comparison of an expected TCN 201 block for a diheteromeric GluN2A population with that of the actual recorded value; a close fit with this model would suggest the neuron expresses a large diheteromeric GluN2A population whereas the greater the deviation from the model, the more likely a triheteromeric GluN2A-GluN2B populations exists.

The prediction was created by determining the linear relationship between the GluN2A and GluN2B fractions with their respective % TCN 201 and % ifenprodil blocks (**Figure 6A**). The predicted % TCN 201 block of the whole-cell NMDA current can be derived from the linear equations and then subsequently, the % TCN 201 block of the ifenprodil insensitive current (**Figure 6B**). Both predictions are of course dependent on the maximal TCN 201 block for a complete GluN2A population expressed non endogenously; at 30 µM glycine, the maximal TCN 201 block was determined to be 50% (Edman et al. 2012). Under these conditions, the relationship between the % ifenprodil block and the % TCN 201 block of the ifenprodil insensitive current is illustrated in **Figure 6C**.

A
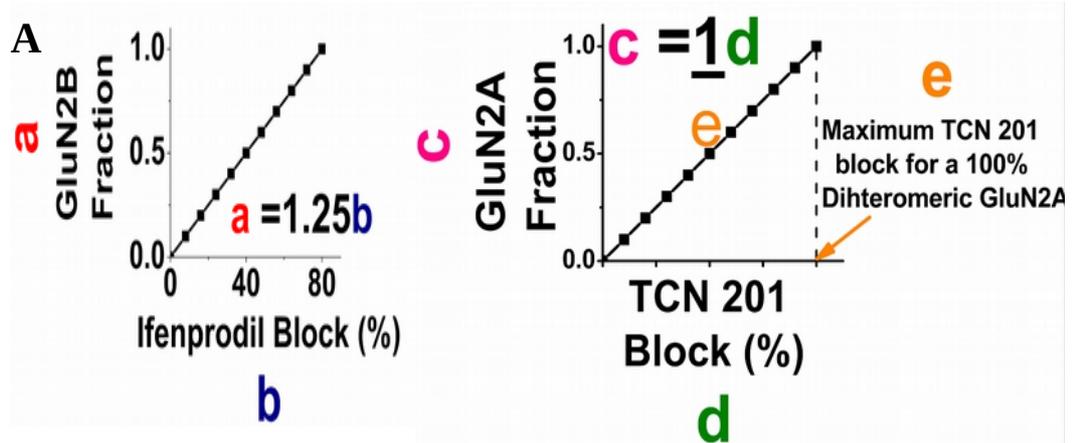
B • For % TCN 201 block of total current :
  • $a + c = 1$
  • $1.25\ b + (\frac{1}{e}\ d) = 1$
  • $d = e\ (1.25\ b)$

• For % TCN Block of ifenprodil insensitive current

$$\frac{d}{1 - b}$$

C
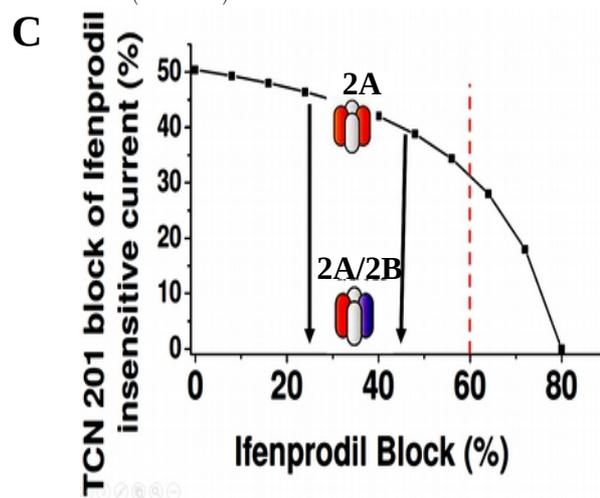
Figure 6: **Predicting % TCN 201 block under assumption that only diheteromeric GluN2A and GluN2B NMDARs are expressed. (A)** The linear relationship between the GluN2A and GluN2B fractions with their respective % TCN 201 and % ifenprodil blocks.
(B) The predicted % TCN 201 block of the whole-cell NMDA current can be derived from the linear equations (left) and then subsequently, the % TCN 201 block of the ifenprodil insensitive current can be determined (right)
(C) The relationship between the % ifenprodil block and % TCN 201 block of ifenprodil insensitive current. At 30 µM glycine, the maximal TCN 201 block of a pure GluN2A diheteromeric population expressed non-endogenously is 50%.
Only cells with <60% ifenprodil block were included for further analysis.

To determine how well each individual neuron fits the diheteromeric prediction, the recorded TCN 201 block was normalized to the diheteromeric predicted block. An analysis of the average normalized value reveals the GluN2A transfected cells fit this model extremely well (0.95±5) whereas the mature neurons to a significantly less extent (0.39±9) (**Figure 7A**). This confirms the hypothesis that GluN2A transfected and mature neurons are differentially antagonized by 10 μM TCN 201 at 30 μM glycine as a consequence of GluN2A transfected neurons expressing a higher proportion of diheteromeric GluN2A NMDARs. Nevertheless, it is evident from the spread of data that some mature neurons exhibit a TCN 201 antagonism that is consistent with a prominent diheteromeric GluN2A population. It is therefore proposed that mature neurons can express a wide complement of diheteromeric and triheteromeric NMDARs.

Finally, it is important to reiterate a caveat of the current approach. Approximately 30% of any triheteromeric GluN2A-GluN2B NMDAR current had already been pre-blocked by ifenprodil prior to antagonism by TCN 201. This does not change the conclusions derived from the data as both GluN2A transfected and mature neurons were treated identically. Nevertheless, it does suggest that where reduced TCN 201 antagonism was observed, it is likely this is an underestimation as 30% of triheteromeric NMDARs had been pre-blocked by ifenprodil.
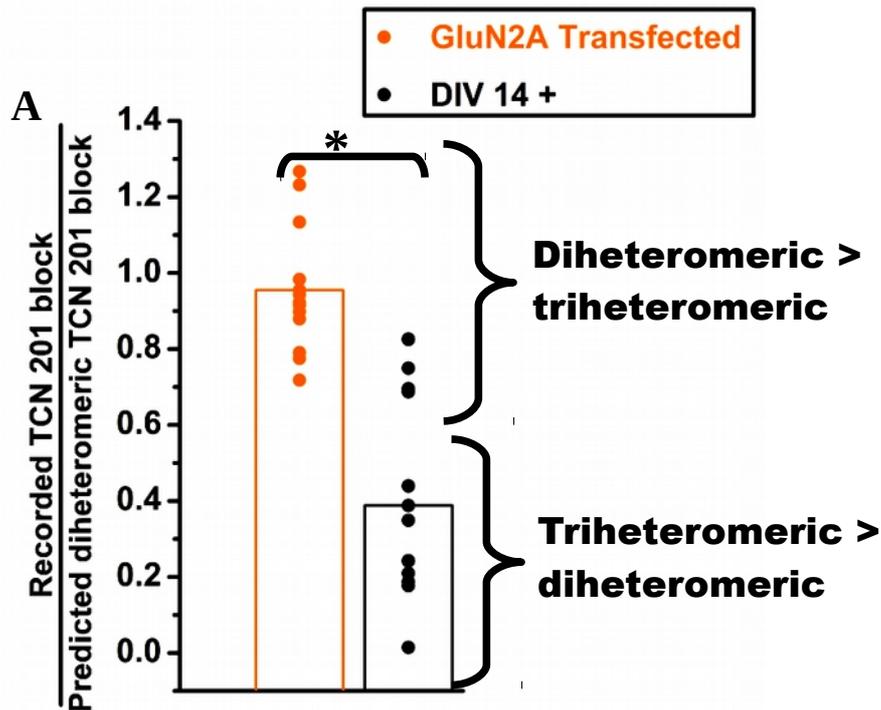
Figure 7: **Modelling 10 µM TCN 201 at 30 µM glycine antagonism with predicted diheteromeric block.**
*p < 0.05, Student unpaired t-test
 n = 13 for GluN2A transfected. n = 15 for DIV 14+

(A) The TCN 201 block of the ifenprodil insensitive current was calculated for each cell in **figure 4E** under the condition the ifenprodil block <60% (2 DIV 14+ cells were excluded).   Concurrently, under the assumption that only diheteromeric GluN2A and GluN2B NMDARs are expressed, the predicted TCN 201 block the ifenprodil insensitive current was calculated using the cell's ifenprodil block. Normalizing the recorded block with the predicted block determines to what extent GluN2A diheteromeric NMDARs are expressed. A significant difference between GluN2A transfected (0.95±5) and mature DIV 14+ (0.39±9) was observed. Due to the greater deviation in data recorded for DIV 14+ neurons, it is proposed that a wide complement of diheteromeric and triheteromeric NMDARs can be expressed.

4.3 Discussion

4.3.1 Summary

It can therefore be concluded that at 3 µM glycine, 30 µM TCN 213 and 10 µM TCN 201 can detect a developmental upregulation of GluN2A during the maturation of cortical cultures. The highly correlated negative relationship between ifenprodil sensitivity and TCN 201/213 sensitivity in low glycine suggests that either triheteromeric NMDARs are not expressed to a great extent or TCN 201 and TCN 213 have similar potencies at diheteromeric and triheteromeric NMDARs under these conditions. Regarding TCN 201, it is now established that triheteromeric NMDARs only have a 20% reduction in antagonism compared to diheteromeric at 3 µM glycine; it is likely such as small difference in potency would still permit a highly correlated relationship between GluN2B antagonism and GluN2A antagonism regardless if triheteromeric or diheteromeric NMDARs are expressed.

Moreover, increasing the glycine concentration 10-fold to 30 µM caused the correlated negative relationship between ifenprodil and TCN 201 sensitivity to decrease. By modelling the data on a predicted TCN 201 block of a pure diheteromeric population, it was revealed that the loss of correlation was due to a lack of diheteromeric GluN2A NMDARs in mature DIV 14+ neurons; this conclusion could be reached as transfecting GluN2A permits a TCN 201 antagonism in excellent accordance with a diheteromeric population. It is assumed the lack of diheteromeric GluN2A in mature neurons is due to a prominent triheteromeric population.

However, for this conclusion to be reached it is imperative that the difference in TCN 201 potency between diheteromeric and triheteromeric NMDARs at 30 µM glycine is far greater than the ~20% observed at 3 µM. The determination of this is essential for a full and comprehensive interpretation of the data. Nevertheless, a

proposed model from the data presented is summarized in **Figure 8**. Determining the robustness of this model is essential for understanding NMDAR mediated signalling as if correct, it would expand the small but growing body of evidence that suggests triheteromeric NMDARs may be the prominent subtype expressed at hippocampal synapses in culture (Tovar et al. 2013) and hippocampal *in vitro* slices(Gray et al. 2011; Rauner & Kohr 2011). This has yet to be demonstrated in the cortical culture system used here.
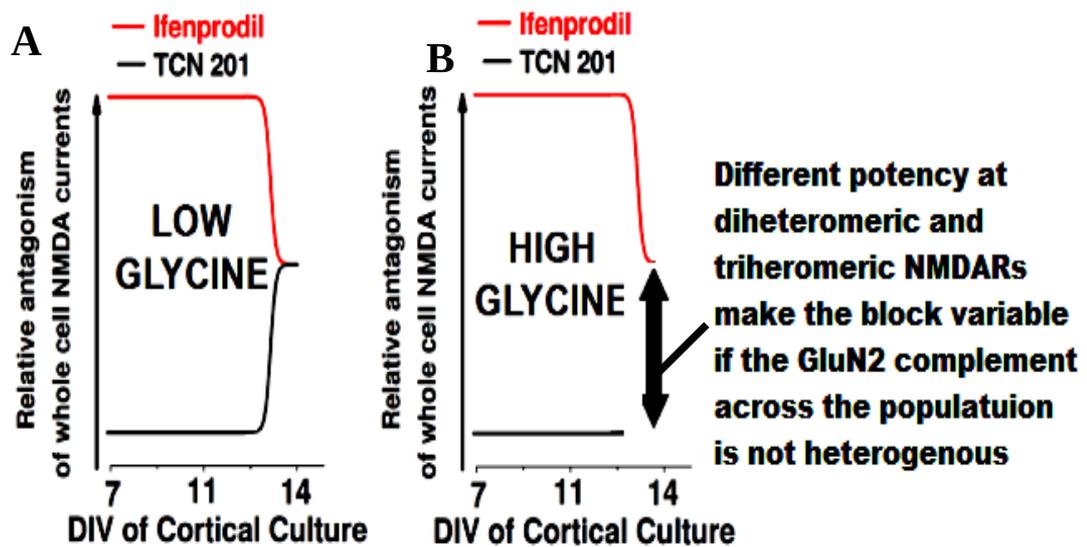
Figure 8: **Proposed developmental changes in GluN2A and GluN2NB antagonism by TCN 201 during cortical culture development**.

(A) At low glycine concentrations, TCN 201 blocks whole-cell NMDA currents in a consistent manner which is dependent on the ifenprodil block of the cell; the TCN 201 blockade is consistent due to a high TCN 201 potency at both diheteromeric and triheteromeric NMDARs.
(B) At higher glycine concentrations the TCN 201 antagonism is dependent on the ifenprodil block of the cell and also the relative proportion of diheteromeric and triheteromeric expressed; it is assumed there is a greater difference in TCN 201 potency at diheteromeric and triheteromeric NMDARs at higher glycine.

4.3.2 The relevance of the cortical culture system in detecting developmental changes in GluN2 subunits

The network activity in culture system utilized in this study is artificially created; this suggests specific electrical input is not required for the developmental upregulation of GluN2A. Furthermore, chronic silencing of network activity in hippocampal slice cultures induces synaptic scaling, via both AMPARs and NMDARs, without altering the subunit composition of NMDARs (Arendt et al. 2013). Nevertheless, as discussed further in **section 1.2.2**, young hippocampal neurons subjected to an LTP protocol can have a rapid upregulation of GluN2A at the synapse in minutes (Bellone & Nicoll 2007; Matta et al. 2011) and visual experience has been shown the increase the expression of the GluN2A subunit in the visual cortex (Quinlan et al. 1999). Altogether, it is feasible that there is a cell-autonomous upregulation of GluN2A which can be modified by synaptic plasticity upon specific patterns of electrical activity.

4.3.3 Utilizing TCN 201 to antagonize GluN2A-dependent signalling

As previously discussed, the use of NVP-AAM077 to study GluN2 dependent signalling in neuroprotection, excitotoxicity and synaptic plasticity has led to the generation of type I errors. That is, NVP-AAM077 was used at a concentration which was intended to selectively block GluN2A but in fact, blocked a substantial proportion of both GluN2A and GluN2B leading to contradictory results regarding subunit dependent signalling. On the other hand, as TCN 201 is an allosteric modulator specifically at the GluN2A subunit, this has functional consequence that the compound shows no antagonism at the other three GluN2 subunits. This completely removes the possibility of type I errors and is undoubtedly the major advantage of TCN 201.

However, the major drawback of TCN 201 for blocking NMDARs signalling is the dependency of glycine/D-serine present at synaptic and extrasynaptic sites.

Commercially available media, such Neurobasal-A and DMEM, have 400 µM glycine present and TCN 201 would give no antagonism of NMDAR currents under these glycine concentrations. Nevertheless, several studies have utilized TCN 201 *in vitro* using such media (Costa et al. 2012; Shin et al. 2012; Hargus & Thayer 2013). Whereas neuronal and glial cells will take-up and metabolize glycine thus lowering the glycine concentration, to what rate this occurs is not clear. Even if glycine and D-serine free media was utilized, both astrocytes and neurons will release and take-up the co-agonist and the manner in which this occurs is multifactorial; the cell density of the culture and the neuron:astrocyte ratio would need to be considered. Lastly, any perturbation of the system such as inducing excitotoxicity, would have to be checked that it does not cause a rapid release of glycine/D-serine. Altogether, it is evident that the use of TCN 201 to investigate NMDAR signalling unfortunately suffers from the opposite problem of NVP-AAM077; potential antagonism of GluN2A NMDARs by TCN 201 can be masked by high concentrations of glycine/D-serine leading to potential type II errors.

Another caveat is that TCN 201 has limited solubility in salt solutions such as ACSF and therefore this may limit the use of TCN 201 to study NMDARs *in vivo*. Nevertheless, a recent study successfully utilized TCN 201 and ifenprodil separately to reduce drug seeking behaviour (Gipson et al. 2013). Of note, ifenprodil was administered systemically whereas TCN 201 was micro-injected into the nucleus accumbens core; it was not stated whether the micro-injection was a prerequisite due to the poor solubility of TCN 201. Regardless, it is encouraging that alterations in behaviours can be induced by selective antagonism of NMDARs containing the GluN2A subunit.

4.3.4 Concluding Remarks

The data presented in this chapter is noteworthy as it is the first pharmacological demonstration of a developmental change in the expression of GluN2 subunits using antagonists that are entirely specific for GluN2A and GluN2B. Further research into the pharmacological profile of TCN 201 at triheteromeric NMDARs will be imperative in interpreting TCN 201 antagonism of endogenously expressed NMDARs. Meticulous measurement of glycine and D-serine at synaptic and extrasynaptic sites is needed to determine the potency of TCN 201 antagonism; this is the major limitation of utilizing TCN 201 to dissect GluN2A-dependent NMDAR signalling.

The pharmacological demonstration of the developmental upregulation of GluN2A presented here strengthened the rationale of utilizing cortical cultures derived from knock-in mice whereby the CTD of GluN2A had been replaced with that of GluN2B. The consequence of this genetic alteration in the developmental expression of GluN2A and also in it's role in excitotoxicity/neuroprotection is the focus of the next chapter.

Chapter 5

The role of the GluN2 C-termini in the expression of GluN2 subtypes, excitotoxicity and neuroprotection

5.1 Introduction

It was demonstrated in **chapter 4** the cortical culture system is a useful tool to study the molecular underpinnings of the developmental switch in GluN2 subunits.

One such mechanism involves Ca^{2+} influx through GluN2B containing NMDARs starting a negative feedback loop which ultimately promotes the upregulation of GluN2A containing NMDARs indirectly by dampening the expression of GluN2B-NMDARs at the membrane as illustrated in **Figure 1**.

Ca^{2+} influx activates CaMKII which promotes CaMKII binding to the GluNB CTD
↓
CaMKII binding to the GluN2B CTD promotes the phosphorylation of the GluN2B CTD at S1480 by CK2
↓
Phosphorylation of S1480 promotes the endocytosis of GluN2B containing NMDARs thus favouring GluN2A-containing NMDARs exprressed at the membrane
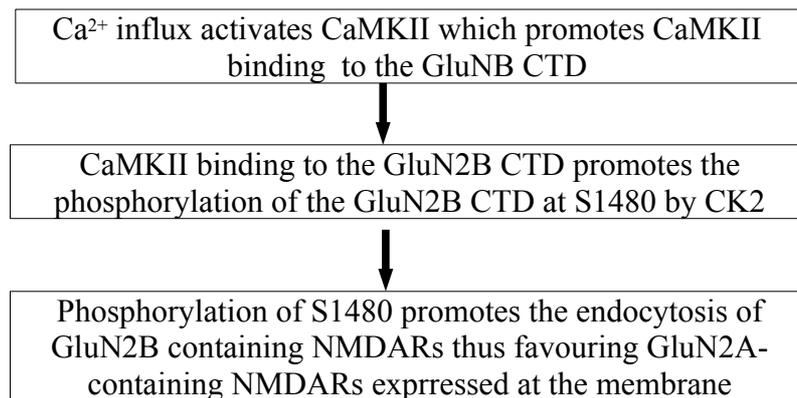
Figure 1: Ca^{2+} influx through GluN2B-NMDARs can initiate a negative feedback loop which limits GluN2B expression at the membrane.

In greater detail, Ca^{2+} influx activates CaMKII where it binds to the GluNB CTD in the region 1290-1309 (Strack et al. 2000) and can subsequently promote the phosphorylation of ser1480 by CK2 (Chung et al. 2004). Subsequently, CK2 phosphorylates the C-terminus of GluN2B at S1480 thus disrupting the interaction of GluN2B CTD with MAGUK proteins which ultimately leads to the NMDAR being endocytosed at extrasynaptic sites (Sanz-Clemente et al. 2010; Sanz-Clemente et al. 2013). The endocytosis is itself regulated by SAP-102 which can promote the retrieval of GluN2B from the membrane via its N-terminus binding to the GluN2B CTD (Chen et al. 2012). Secondly, the GluN2B CTD is trafficked through recycling endosomes whereas the GluN2A is sorted into late endosomes destined for degradation in non-neuronal cells (Tang et al. 2010). Lastly, there is strong evidence

that PSD-95 is necessary for the selective forward trafficking of GluN2A containing NMDARs to the synapse (Elias et al. 2008). However, although the interaction of PSD-95 with the PDZ domain of the GluN2A subunit is the most studied, it has yet to be proven that the forward trafficking is dependent on the GluN2A CTD.

However the use of protein overexpression, which can result in off-target or non-specific protein interactions, was utilized extensively in the above studies. To circumvent this issue, an elegant genetic knock-in approach whereby the C-terminal of GluN2A was replaced with that of GluN2B (named GluN2A$^{2B(CTR)}$) and reciprocally, the GluN2B CTD with that of GluN2A (named GluN2B$^{2A(CTR)}$) was implemented(Ryan et al. 2013). This genetic alteration in the GluN2A$^{2B(CTR)}$ mouse line would prevent the selective CK2-dependent endocytosis of GluN2B-NMDARs as GluN2A$^{2B(CTR)}$ neurons would also be subjected to CK2 phosphorylation at S1480. Consequently, in GluN2A$^{2B(CTR)}$ neurons, both GluN2A and GluN2B will be undergo CTD regulated endocytosis at the same rate; if selective endocytosis of GluN2B via the CTD is essential for the upregulation of GluN2A at the neuronal membrane then this developmental upregulation will be disrupted in GluN2A$^{2B(CTR)}$ neurons.

I wished to test the above hypothesis utilizing the GluN2A$^{2B(CTR}$ mouse and the cortical culture system utilized in **chapter 4**; a developmental loss of ifenprodil potency, rather than a developmental gain of TCN 201 potency, was decided as the assay to determine the upregulation of GluN2A as ifenprodil sensitivity does not depend on the concentration of the co-agonist glycine/D-serine. If the hypothesis was correct, and there was an impedence in the upregulation of GluN2A, then there would a reduced loss of ifenprodil sensitivity during cortical culture maturation. In this case, no further experiments were planned as there would be two distinct populations of NMDARs in the WT and GluN2A$^{2B(CTR)}$ neurons. However, if the hypothesis was incorrect, then it would be possible to determine if the GluN2A$^{2B(CTR}$ neurons had altered responses to excitotoxic insults or the induction of immediate

early genes by synaptic activity as summarized in **Figure 2**.
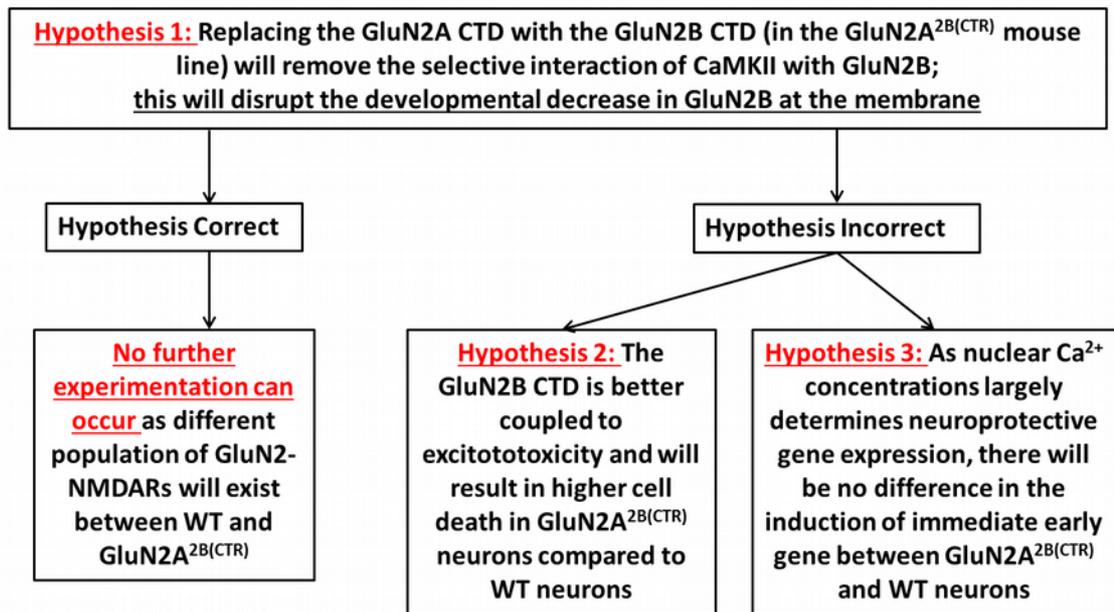
Figure 2: The plan and development of experimental hypotheses in **chapter 5**.

As discussed in **sect ion 1.4.3**, it has previously been demonstrated that the reciprcoal CTD switch from this study, GluN2B$^{2A(CTR)}$ neurons, are less vulnerable to NMDA-dependent excitotoxicity both *in vitro* and *in vivo;* this confirms the GluN2B CTD preferentially couples to excitotoxic signalling (Martel et al. 2012). Interestingly, the reduction in excitotoxicity afforded by replacing GluN2B CTD with the GluN2A CTD could be overridden by higher Ca^{2+} influx. This suggests that at extremely high intracellular Ca^{2+} concentrations, NMDARs signalling dependent on the GluN2 CTD may be irrelevant to the biological outcome of an excitotoxic insult possibly because of the direct disruption of mitochondrial health by Ca^{2}.

Furthermore, transfection of GluN2A$^{2B(CTR)}$ in young DIV 9-10 neurons induced a greater vulnerability to excitotoxicity than neurons transfected with WT GluN2A (Martel et al. 2012). The enhanced excitotoxicity in over-expressing GluN2A$^{2B(CTR)}$ neurons is in excellent accordance with the overwhelming evidence of decreased excitotoxicity in the reciprocal neurons derived from the GluN2B$^{2A(CTR)}$ mouse line.

Altogether, it is logical to hypothesize the converse, an increrase in excitotoxicity, is would be present in GluN2A$^{2B(CTR)}$ neurons.

As discussed further in **section 1.4.2**, CREB is a master transcriptional regulator of neuroprotective genes and itself is regulated via phosphorylation by nuclear Ca^{2+}-activated CaM kinases; chelating Ca^{2+} specifically in the nucleus blocks CREB mediated transcription of neuroprotective genes (Hardingham et al. 1997). At a developmental time point where diheteromeric GluN2B NMDARs are dominant, synaptic activity can result in the activation of CREB and provide neuroprotection which is maintained as GluN2A is developmentally upregulated (Martel et al. 2009a; Hardingham & Bading 2010). Moreover, although disrupting the PDZ ligand domain on the GluN2B CTD with TAT-NR2B9c reduces excitotoxicity, it does not impair the induction of the CREB target genes by synaptic activity (Martel et al. 2009b); this suggests the PDZ domain of the GluN2B CTD is not necessary for NMDAR activity to modify the phosphorylation of CREB. Furthermore, Ca^{2+} influx through L-type Ca^{2+} channels via depolarization (Weick et al. 2003) or agonist activation utilizing the agonist FPL 64176 (Rajadhyaksha et al. 1999) can also result in CREB activation. Although Ca^{2+} can activate CREB via slower and indirect mechanisms such as via ERK, it is evident that nuclear Ca^{2+} concentrations itself is the main determinant in the transcription of neuroprotective genes (Bading 2013). Furthermore, nuclear CaM kinases activated by Ca^{2+} can also promote the transcription of other neuroprotective transcription factors such as NPAS4 (Qiu et al. 2013).

In disagreement with the above, It has been reported that GluN2A containing NMDARs exclusively mediate neuroprotective signalling in mature neurons regardless of their membrane location (Liu et al. 2007) and that GluN2A and GluN2B differentially regulate the induction of the CREB target gene brain-derived neurotrophic factor (BDNF) upon synaptic activity (Chen et al. 2007). However,

both these studies utilized a concentration of NVP-AAM077 which blocks both GluN2A and GluN2B NMDARs, with the intention of selectively blocking GluN2A thus making the data difficult to interpret.

It is imperative that the molecular underpinnings of neuroprotection are understood in order that they are minimally antagonized by therapeutic strategies aimed at blocking excitotoxic signalling. Therefore, I wished to test the hypothesis that there will be no difference in the induction of immediate early genes by synaptic activity between WT and GluN2A$^{2B(CTR)}$ neurons; the reasoning being is that nucelar Ca^{2+} concentration, rather than GluN2-dependent signalling, determines the transcription of neuroprotective genes.

To summarize the findings from the study, the whole-cell NMDA currents and ifenprodil sensitivities of GluN2A$^{2B(CTR)}$ cultures were not significantly different from WT cultures indicating a developmental upregulation of GluN2A had occurred. Furthermore, the proportion of NMDARs at synaptic and extrasynaptic sites was not altered in GluN2A$^{2B(CTR)}$ cultures and a loss of GluN2B at both synaptic and extrasynaptic sites could be detected in both WT and GluN2A$^{2B(CTR)}$ cultures. As it was established that replacing the CTD of GluN2A with GluN2B induced no impairment in the expression of NMDARs, it was then subsequently possible to determine if there were any deficits in excitotoxic and neuroprotective signalling. GluN2A$^{2B(CTR)}$ cultures were more vulnerable to NMDA-dependent excitotoxicity in an agonist-dependent manner but showed no impairment in the expression of several immediate early genes triggered by synaptic activity.

Altogether, it can be concluded that when both GluN2A and GluN2B are subjected to regulation by CK2 and other specific post-translational modifications at the GluN2B CTD, the developmental upregulation of GluN2A still occurs indicating that CTD-subtype specific interactions are not required contrary to current models.

Consequently, this permits the downstream signalling in GluN2A$^{2B(CTR)}$ cultures to be studied.

5.2 Results

5.2.1 whole-cell NMDA currents and ifenprodil sensitivities are unchanged in mature GluN2A$^{2B(CTR)}$ cultures

As the data in **chapter 4** demonstrated a developmental upregulation of GluN2A between DIV 7 and DIV 14 in rat cortical cultures, sister WT and GluN2A$^{2B(CTR)}$ cultures were prepared and maintained in parallel for a minimum of 15 days to permit the endogenous upregulation of GluN2A to occur.

Although the NMDA current density alone is a valuable tool to determine the proportion of NMDARs expressed in young neurons, where mainly diheteromeric GluN2B NMDARs are expressed (see Puddifoot et al. 2012 for an example), it is difficult to do the same in mature cultures as the upregulation of GluN2A into triheteromeric and diheteromeric NMDARs will introduce NMDARs with different biophysical properties. Nevertheless, NMDA currents were evoked under saturating agonist exposure (150 μM NMDA + 100 μM glycine) to determine the NMDAR current density of each neuron and there was no significant difference between WT and GluN2A$^{2B(CTR)}$ cultures (**Figure 3A**).

A more valuable measurement to determine the developmental upregulation of GluN2A in GluN2A$^{2B(CTR)}$ neurons is by the measurement of the ifenprodil sensitivity of the whole-cell NMDA current. Similar to the rat cortical cultures in **chapter 4**, both WT and GluN2A$^{2B(CTR)}$ cultures contained neurons with a wide range of ifenprodil sensitivities as can be observed in **Figure 3B.** Nevertheless**,** as young DIV 7-10 neurons consistently have ifenprodil block of around ~75% indicative of a predominately diheteromeric GluN2B population, the wide spread of ifenprodil sensitivities in both WT and GluN2A$^{2B(CTR)}$ cultures demonstrate many neurons have incorporated GluN2A containing NMDARs into the neuronal membrane.

Importantly, there was no significant difference between WT and GluN2A$^{2B(CTR)}$ cultures confirming the developmental incorporation of GluN2A-NMDARs is not impeded by replacing the GluN2A CTD with that of GluN2B.
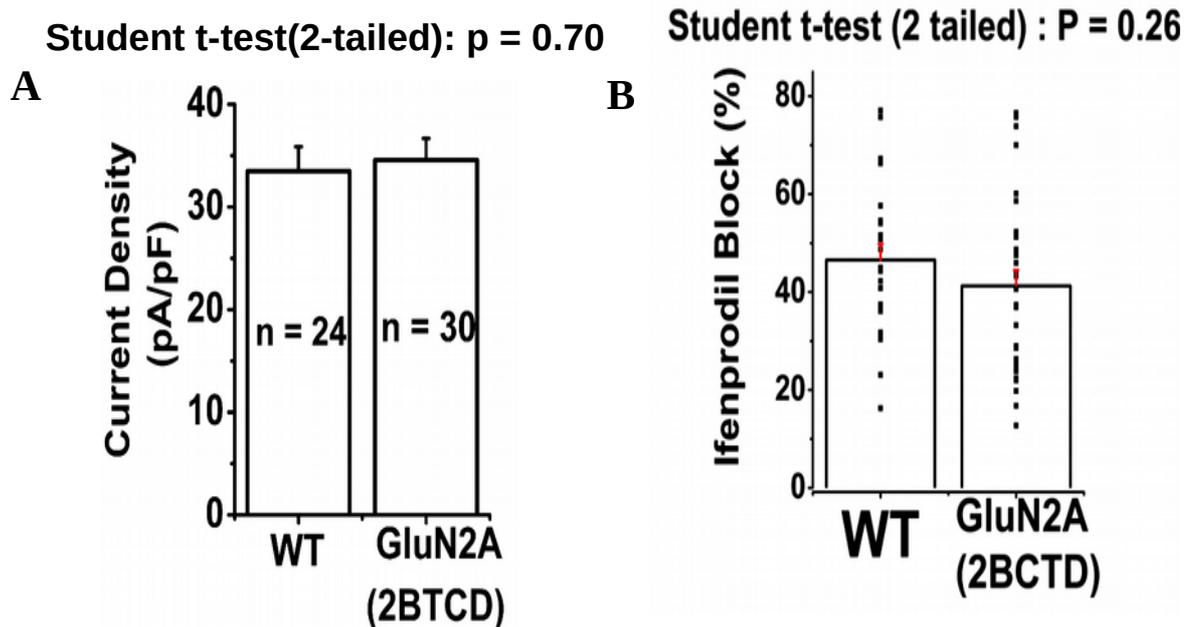
Figure 3: **Replacing the CTD of GluN2A with GluN2B does not affect the whole-cell NMDA currents or ifenprodil sensitivity of mature neurons.**

All cells recorded between DIV15-16 and were voltage-clamped at -60 mV. Recordings only made if it was possible to record sister WT and GluN2A$^{2B(CTR)}$ cells on the same day.

(A) whole-cell NMDA currents in sister WT and GluN2A$^{2B(CTR)}$ were evoked under saturating agonist exposure(150 µM NMDA + 100 µM glycine) and the current measured normalized to the cell's capacitance to give the NMDA current density. There was no significant difference between WT and GluN2A$^{2B(CTR)}$ neurons.

(B) In the same neurons as **A**, the whole-cell NMDA current was antagonized by 3 µM ifenprodil and the ifenprodil block (%) of each neuron was determined. There was no significant difference between WT and WT and GluN2A$^{2B(CTR)}$ neurons.

119

5.2.2 The proportion and subunit composition of NMDARs at synaptic and extrasynaptic sites are unchanged in mature GluN2A²ᴮ⁽ᶜᵀᴿ⁾ cultures

The developmental upregulation of GluN2A occurs during a period of intense synaptogenesis and spinogenesis and in juxtaposition, NMDARs switch from existing as predominately extrasynaptic to synaptic (discussed further **in section 1.2.3**). Therefore, it has largely been hypothesised that the two developmental changes are correlated and an increase in the content of synaptic NMDARs is a consequence of the upregulation of GluN2A. Ultimately, this has led to a dogma that asserts that GluN2A-NMDARs are specifically expressed at the synapse whereas GluN2B-NMDARs are expressed extrasynaptically (see Lau & Zukin 2007 for an excellent review). However, this has been challenged in recent years by the observation there is a developmental loss of ifenprodil sensitivities at extrasynaptic NMDARs (Thomas et al. 2006; M-A Martel et al. 2009).

Truncation of the GluN2 CTD has been proposed to impair synaptic but not extrasynaptic targetting of NMDARs (Steigerwald et al. 2000). However, this conclusion was largely obtained utilizing electrophysiology, and it is now recognized truncation of the GluN2 CTD alters the channel kinetics of the NMDAR(Maki et al. 2012; Punnakkal et al. 2012). Furthermore, the definition of extrasynaptic NMDARs in this study were defined as those activated by fast application of glutamate in nucleated whole-soma patches of CA1 pyramidal neurons which is an approach not adopted in subsequent studies. On the other hand, over-expression of C-terminally truncated GluN2A in NR2A$^{-/-}$ neurons permits GluN2A to be expressed at the synapse suggesting the GluN2A CTD is not essential for localization at the synapse ; improper localization due to over-expression is of course a caveat of this approach (Thomas et al. 2006).

Therefore as the role of the GluN2A CTD in synaptic targeting to membrane

locations is unclear, I wished to test the hypothesis that replacing the GluN2A CTD with that of GluN2B would not disrupt the synaptic targetting of NMDARs (GluN2A$^{2B(CTR)}$ NMDARs). As the ifenprodil sensitivity of all NMDARs expressed on a neuron (synNMDARS + exNMDARs) varies greatly between neurons in both WT and GluN2A$^{2B(CTR)}$ cultures (**Figure 3B**), if one were to only measure ifenprodil sensitivity at exNMDARs then a similar high sample size would be required to be confident in any statistical measurements between the WT and GluN2A$^{2B(CTR)}$ being robust. A more elegant approach is to correlate the ifenprodil sensitivity of the whole neuron (synNMDARs + exNMDARs) with that of the ifenprodil sensitivity at exNMDARs alone. This would require the experimental paradigm illustrated in **Figure 4.**

| Determine the % antagonism of the whole cell NMDA current by 3 µM ifenprodil in ACSF containing 0-Mg^{2+}/ 300 nM TTX |

➤ **300 nM TTX must washout**

| Promote phasic activity in ACSF containing 1mM MgCl$_2$/50 µM Bicuculline/ 10 µM MK-801 |

➤ **3 µM ifenprodil must washout out**

| Determine the % antagonism of the extrasynaptic NMDA current by 3 µM ifenprodil in ACSF containing 0-Mg^{2+}/ 300 nM TTX |
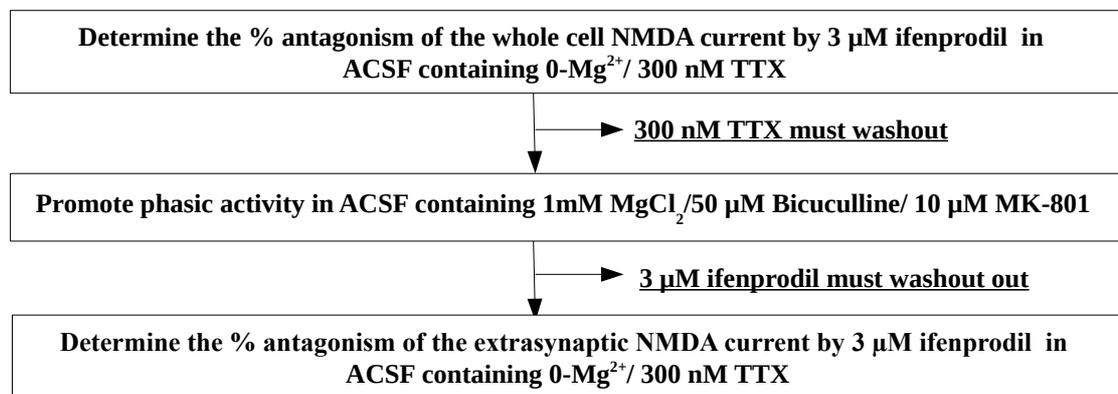
<u>**Figure 4:**</u> **Proposed experimental paradigm for measuring ifenprodil sensitivity of the whole-cell NMDA current then subsequently at exNMDARs only.**

However, after the measurement of the ifenprodil sensitivity of the whole-cell NMDA current, TTX must washout in order that phasic activity permits MK-801 to block synNMDARs in a time period of around 5 minutes. Furthermore, after 3 µM ifenprodil has antagonized the whole-cell NMDA current, it must be completely washed out in order to selectively measure ifenprodil sensitivity at exNMDARs.

Therefore, I utilized WT cultures at a developmental time point (DIV 7), where only

diheteromeric GluN2B NMDAR are expressed, to test the pharmacological wash-out profiles of TTX and ifenprodil are suitable for the proposed above experiment. To achieve this, the ifenprodil sensitivity of a neuron was determined in Mg^{2+}-free ACSF with TTX present in the voltage-clamp configuration. Subsequently, the neuron was then switched to a reciprocal Mg^{2+}-containing but lacking TTX ACSF and allowed to fire at the cell's resting membrane potential in the current-clamp configuration. During the first 2 minutes of the "wash" period, all the neurons recorded fired bursts of action potentials indicating TTX had successfully washed out (**Figure 5B shows an illustrative burst firing**). After the first action potential, the wash period was extended for a further 5 minutes, and the ifenprodil block of the NMDA current was re-determined under identical conditions and was found not to be significantly different from the initial ifenprodil block (**Figure 5A**). It can therefore be concluded that measuring ifenprodil sensitivity of the whole-cell NMDA current (synNMDARs + exNMDARs) and then subsequently at exNMDARs alone is a feasible pharmacological approach. This data also demonstrates that at DIV 7, there is very little rundown of NMDA currents (<10%) during the wash period.

Nevertheless, run down of NMDA currents may be greater in more mature neurons. To test this, WT neurons derived from CD1 mice, were cultured to DIV 16-18. For each cell, the whole cell NMDA current was determined followed by the wash period described above, either in the absence or presence of 10 μM MK-801. In the absence of MK-801 during the wash period, there was a 7% decrease in whole cell NMDA currents attributed to run down. However, when MK-801 was included in the wash period to block synNMDARs, a 62% reduction in whole cell NMDA currents was observed (data not shown). This illustrates that run down of NMDA currents contributes approximately 11% the overall synaptic blockade by MK-801.

A

B
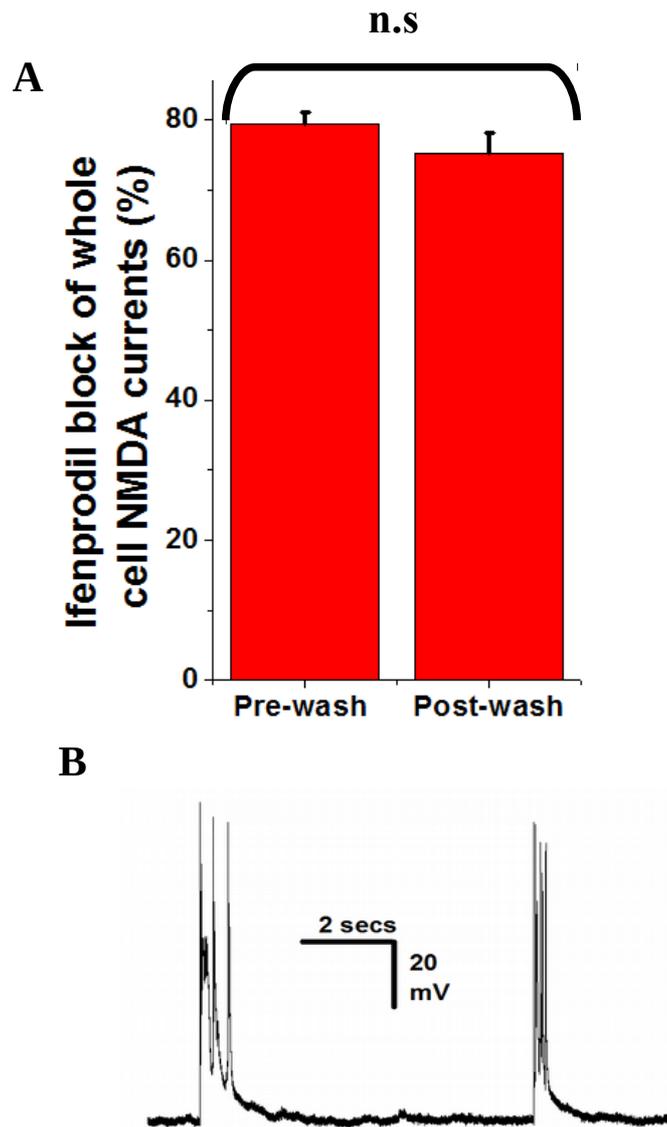
Figure 5: Determining the wash-out profile of ifenprodil and TTX.
(A) All neurons were recorded on DIV 7 and voltage-clamped at -60mV. In the presence of 300 nM TTX and 0-Mg^{2+}, whole-cell NMDA current was evoked (by 150 μM NMDA + 100 μM glycine) and then subsequently blocked by 3 μM ifenprodil. The neurons were then switched to an ACSF containing 1 mM $MgCl_2$ but lacking TTX in the current-clamp configuration for a 5 minute "wash" period thus permitting the firing of action potentials. Finally, the whole-cell NMDA current was re-determined in the voltage-clamp configuration which was then subsequently blocked by ifenprodil. The ifenprodil block pre and post "wash" period was 80±2% and 75±3% respectively confirming the ifenprodil block was removed during this time. $P > 0.05$ paired student test (2-tailed). n = 6 neurons.
(B) During the wash period, neurons robustly fire bursts of action potentials indicating TTX block had successfully been removed.

123

I then turned my attention to utilizing this pharmacological approach, with the inclusion of 10 µM MK-801 during the phasic activity to block synNMDARs, in mature WT and GluN2A$^{2B(CTR)}$ cultures as illustrated in **Figure 6A**. In both WT and GluN2A$^{2B(CTR)}$ cultures, 10 µM MK-801 blocked ~80% of the whole-cell NMDA currents during phasic activation indicating that the ratio of synaptic:extrasynaptic in mature neurons is approximately 4:1. Importantly, there was no significant difference between the two cultures (**Figure 6B**). Furthermore, there was a clear positive correlation between the ifenprodil sensitivity of the whole-cell (synNMDARs + exNMDARs) with exNMDARs alone in both cultures **(Figure 6C)** indicating GluN2A containing NMDARs are present at extrasynaptic sites. By determining the ratio of ifenprodil sensitivity of extrasynaptic:whole-cell for each neuron, the average values for WT (1.22±0.05) and GluN2A$^{2B(CTR)}$ (1.13±0.03) reveal that there is a small but preferential loss of GluN2B at synNMDARs yet there was no significant between WT and GluN2A$^{2B(CTR)}$ cultures (**Figure 6D**).

Altogether, it can be concluded that replacing the GluN2A CTD does not alter synaptic targetting of the NMDAR to synaptic and extrasynaptic sites. This has the important consequence that any activation of the NMDAR will result in similar spatial Ca^{2+} influx in both WT and GluN2A$^{2B(CTR)}$ cultures thus permitting the study of downstream signalling.
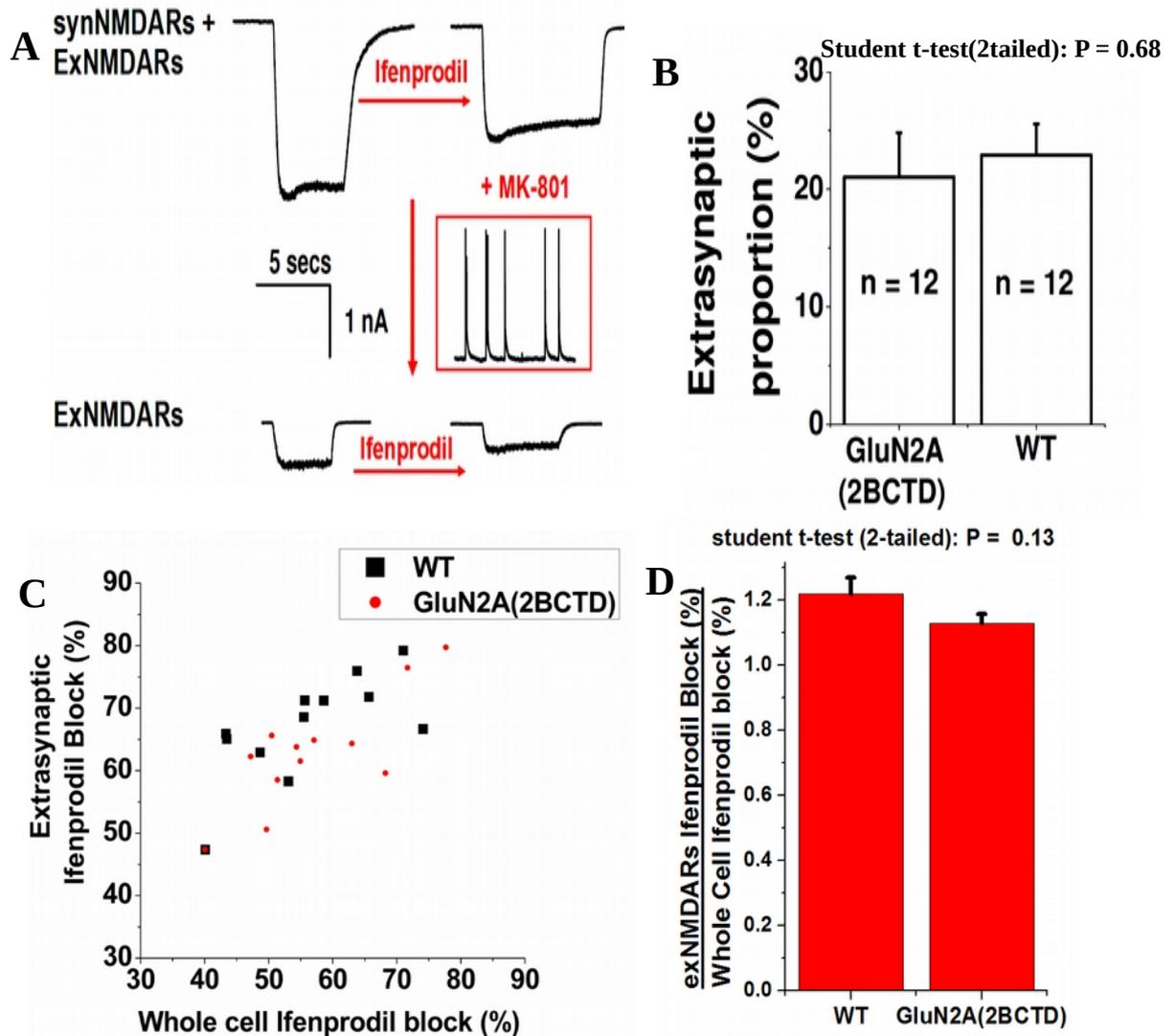
Figure 6: **The proportion and subunit composition of NMDARs at synaptic and extrasynaptic sites are unchanged in mature GluN2A[2B(CTR)] cultures**

All cells voltage-clamped at -60mV and recorded between DIV 15-17. NMDA currents were evoked by 150 µM NMDA + 100 µM glycine. Ifenprodil used at 3 µM and MK-801 at 10 µM.

(A) The whole-cell ifenprodil sensitivity of a WT DIV 15 neuron was determined in 0-Mg^{2+} ACSF. The neuron was then switch to an ACSF with 1 mM MgCl$_2$ + 10µM MK-801 + 50 µM bicuculline and allowed to fire phasically in the current-clamp configuration. After 5 minutes, the neuron was switched back to the voltage-clamp configuration and the ifenprodil sensitivity at exNMDARs was now determined.

(B) There was no significant difference in the extrasynaptic portion of WT (23±3%) and GluN2A[2B(CTR)] (21±4%) neurons. *n* = 12 for both WT and GluN2A[2B(CTR)]

(C) Correlation of the whole-cell ifenprodil block and the ifenprodil block at exNMDARs only for both WT and GluN2A[2B(CTR)]neurons.

(D) The ifenprodil block at exNMDARs only was normalized to the ifenprodil block of the whole-cell ifenprodil block. The average values for WT (1.22±0.05) and GluN2A[2B(CTR)](1.13±0.03) reveal that there was a small but preferential loss of GluN2B at synNMDARs yet there was no significant between WT and GluN2A[2B(CTR)] cultures.

5.2.3 GluN2A$^{2B(CTR)}$ cultures are more vulnerable to NMDAR-dependent excitotoxicity

As the GluN2A$^{2B(CTR)}$ cultures have no deficits in the expression of endogenous NMDARs, they can be utilized to test the hypothesis that these neurons are more vulnerable to excitotoxicity. By determining the dose-response relationship between NMDA concentration and cell death, it was revealed that GluN2A$^{2B(CTR)}$ neurons had enhanced vulnerability to NMDA excitotoxicity as determined by a significant difference (P = 0.034) in the calculated logEC$_{50}$ values (GluN2A$^{2B(CTR)}$ = 12.0, WT = 17.7)(**Figure 7A & 7B**).

As an aside, although 15 µM NMDA was quoted as non-toxic in **chapter 3**, this was utilizing young rat cortical cultures rather than mature mouse cortical cultures used here; mouse neurons are more vulnerable to excitotoxicity and maturation also increases vulnerability to excitotoxicity.

It can therefore be concluded, that in agreement with the over-expression studies, replacing the GluN2A CTD with GluN2B renders neurons more vulnerable to NMDAR dependent excitotoxicity. Furthermore, in the same light as the reciprocal GluN2B$^{2A(CTR)}$ study, this data demonstrates that the role of the GluN2 CTD in determining excitotoxicity is lost at high Ca^{2+} influx thus strengthening the concept that the role of the GluN2 CTD in governing excitotoxicity is highly complex.
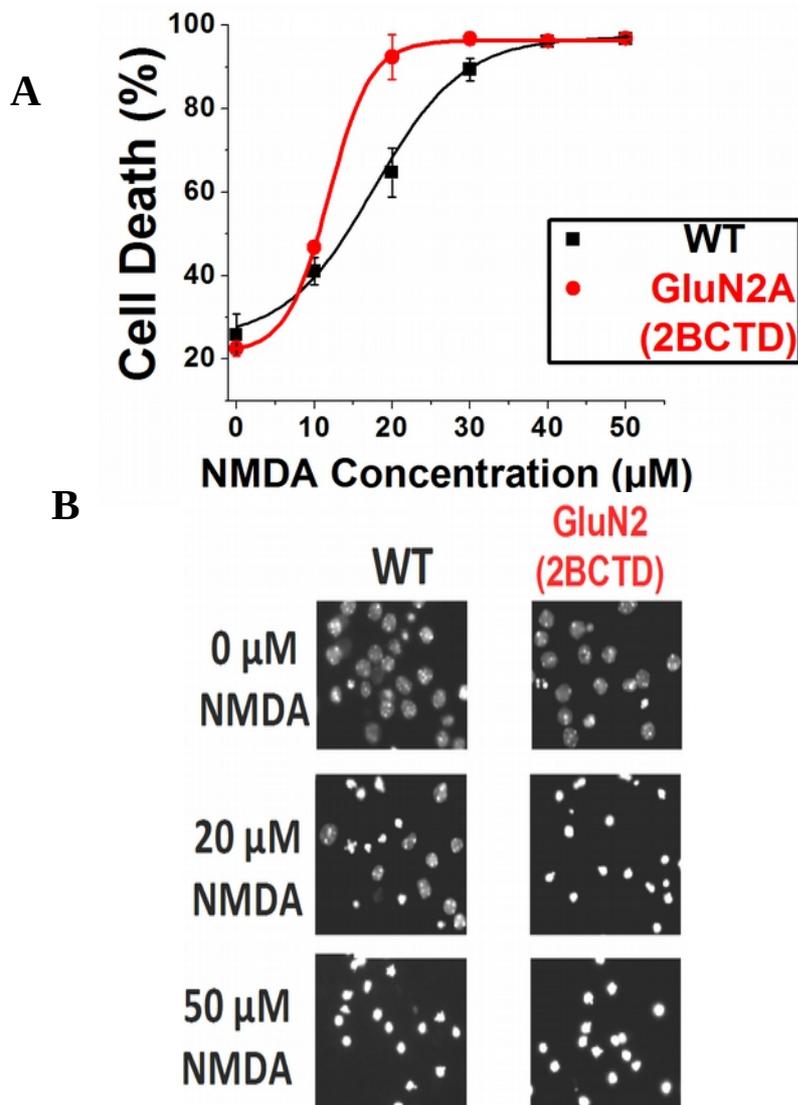
Figure 7:GluN2A[2B(CTR)] cultures are more vulnerable to NMDA-dependent excitotoxicity

(A) The dose-response relationship between NMDA concentration and cell death utilizing an increment of 10 µM NMDA was determined for DIV 17 sister WT and GluN2A(2BTC) cultures. The 1 hour NMDA exposure was terminated with 10 µM MK-801, the cells fixed 24 hours later and the cell death subsequently determined. The averaged data was fitted using the dose-response equation (see methods for elaboration). A significant difference (P = 0.034) in the calculated $logEC_{50}$ values (GluN2A[2B(CTR)] = 12.0 µM, WT = 17.7 µM). was observed using an extra sum of squares F-test. WT R^2 = 0.96, GluN2A[2B(CTR)] R^2 = 0.99. n = 3 independent cultures. Each n was determined by averaging the cell death in 2 wells.

(B) Example DAPI images. Both WT and GluN2A[2B(CTR)] neurons have similar basal death at DIV 17 but GluN2A[2B(CTR)] cultures have >90% neuronal death after a 1 hour exposure to 20 µM NMDA whereas WT neurons have ~65% neuronal death. This difference is lost at higher (50 µM) NMDA.

127

5.2.4 The induction of several immediate early genes by synaptic activity is not impaired in GluN2A$^{2B(CTR)}$ neurons

An increase in synaptic activity was achieved by inhibiting GABA$_A$ receptors in DIV 17 cultures for 4 hours, utilizing 50 µM bicuculline, juxtaposed with a control untreated group and a control group with 50 µM bicuculline pre-treated with 10 µM MK-801 to block NMDARs. After the 4 hours stimulation, the RNA from both WT and GluN2A$^{2B(CTR)}$ neurons was harvested in parallel and subsequently converted to cDNA. Subsequently, qRT-PCR was utilized to determine the mRNA expression of a neuroprotective CREB regulated gene (BDNF), a neuroprotective CREB-independent gene (NPAS4) and FOSB (as it is rapidly upregulated upon nuclear Ca^{2+}) (**Figures 8A/B/C**). It is evident that promoting synaptic activity with bicuculline increases the transcription of all three genes in an NMDAR-dependent manner as the upregulation was readily blocked by MK-801. However, there was no significant difference in the expression of all 3 genes after 4 hours of enhanced synaptic activity between WT and GluN2A$^{2B(CTR)}$ cultures.

It can therefore be concluded that that replacing the GluN2A CTD with that of GluN2B does not impede the transcription of the CREB target gene BDNF nor the CREB-independent gene NPAS4 both of which are neuroprotective. This is consistent with the evidence that it is the temporal and spatial profile of nuclear Ca^{2+} that largely determines the transcription of neuroprotective genes and is inconsistent with reports that GluN2A-NMDARs exclusively mediate neuroprotection.
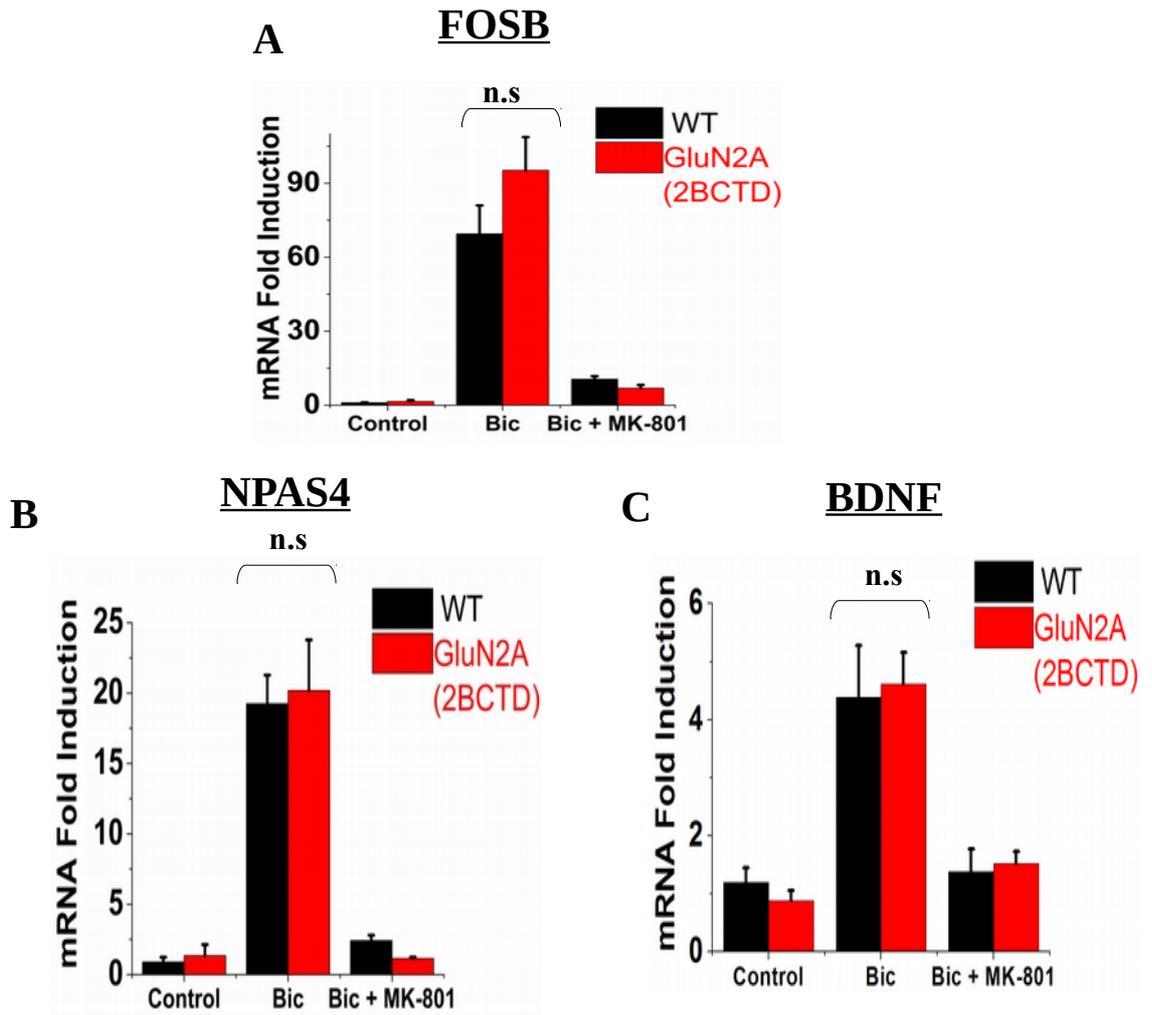
Figure 8: **The induction of several immediate early genes by synaptic activity is not impaired in GluN2A[2B(CTR)] neurons**

(A-C) Using the qRT-PCR method, the mRNA expression of FOSB **(A)**, NPAS4 **(B)** and BDNF **(C)** were measured in the following conditions for 4 hours at DIV 17: untreated control; 50 µM bicuculline; 50 µM bicuculline + 10 µM MK-801. 50 µM bicuculline increased the transcription of all 3 genes which could be reduced by 10 µM MK-801 confirming the upregulation was NMDAR-dependent. There was no significant difference in the mRNA expression of all three genes after being treated for 4 hours with bicuculline. p > 0.05, student unpaired t-test (2-tailed). n = 4 independent cultures for both WT and GluN2A[2B(CTR)].

5.3 Discussion

5.3.1 Summary

It can therefore be concluded that when both GluN2A and GluN2B are subjected to regulation by CK2 and other specific post-translational modifications at the GluN2B CTD, the developmental upregulation of GluN2A still occurs indicating that CTD-subtype specific interactions are not required contrary to current models. Consequently, this permits the downstream signalling in GluN2A$^{2B(CTR)}$ cultures to be studied as discussed below.

5.3.2 The role of the GluN2 CTD in the developmental upregulation of GluN2A-NMDARs

As previously discussed, it has been proposed that Ca^{2+}-activated CaMKII binds to CK2, independent of its kinase activity, where it promotes CK2 phosphorylation of the GluN2B C-terminus at S1480. This has the functional consequence of disrupting the interaction of of GluN2B with MAGUK proteins ultimately leading to endocytosis at extrasynaptic sites via clathrin-AP-2-mediated endocytosis (Sanz-Clemente et al. 2010; Chen et al. 2012; Sanz-Clemente et al. 2013).The capacity of S1480 phosphorylation to drive endocytosis is almost maximal. This is most elegantly and beautifully demonstrated by the transfection of a phosphomimetic S1480E GluN2B into GluN2A$^{-/-}$/GluN2B$^{-/-}$ hippocampal slice cultures; whereas transfection of WT GluN2B permitted ~90% recovery of EPSC, transfection of S1480E GluN2B strikingly provided no recovery of the EPSC. Even more fascinatingly, the effect of S1480E could be abolished by mutating D1391K and D1392K which disrupts the N-terminal of SAP-102 promoting endocytosis.

However, whereas the use of over-expression and phosphomimetic mutations are excellent in unequivocally demonstrating the existence of a signalling pathway, it does not address the role of the pathway under physiological conditions. This was

firstly addressed by the utilization of the CK2 inhibitor TBB in cortical cultures. It was observed that overnight incubation of DIV 10 cortical cultures with TBB decreased the surface:total ratio of GluN2A protein expression whilst reciprocally increasing that of GluN2B (Sanz-Clemente et al. 2010). However in our hands, DIV 10 neurons predominately express diheteromeric GluN2B NMDARs. Therefore, this is a developmental time point in which GluN2A is minimally expressed; the effect of CK2 inhibition may be lost when other developmental programmes, such as changes in the transcription of *Grin2a* and *Grin2b*, occur naturally at a later developmental time point as used in this study.

Synaptic plasticity requires more rapid changes in synaptic composition thus making post-translational modification of the GluN2B CTD ideal. The LTP induction protocol which induces a rapid upregulation of GluN2A at the synapse is highly excitatory (voltage-clamping CA1 neurons at 0mV whilst stimulating the Schaffer collateral axons at 1Hz for 120 seconds) and therefore the rapid upregulation of GluN2A may function to dampen the insertion of AMPA receptors at the synapse (Gray et al. 2011). It should also be stressed that whilst mGluR5$^{-/-}$ mice have a small but significant deficit in the expression of GluN2A containing NMDARs receptors in CA1 hippocampal neurons, blocking mGluR5 with MTEP in young hippocampal neurons completely abolishes the rapid upregulation of GluN2A induced by the LTP protocol (Matta et al. 2011). Therefore, the LTP protocol may be highly sensitive to post-synaptic Ca^{2+} changes to a degree which is not physiologically relevant; indeed, there is no compensatory mechanism in this system as blocking either NMDARs alone or mGluR5 alone completely abolishes the upregulation of GluN2A. As an aside, the LTP protocol described above was utilized in rat hippocampal slices and if used in mouse hippocampal slices, it fails to induce an upregulation of GluN2A (Matta, et al. 2011); the reason for this is unclear. Nevertheless, it is clear CK2 phosphorylation of the GluN2B CTD is critical in this developmental upregulation of GluN2A upon the induction of the LTP protocol as demonstrated by the

antagonism by the CK2 inhibitor TBB (Sanz-Clemente et al. 2010).

On the other hand it is evident from **chapter 4**, that by increasing *Grin2a* mRNA by transfection, a replacement of GluN2B with that of GluN2A at the neuronal membrane can occur within 48 hours. It is therefore reasonable to assume that a developmental change in GluN2B endocytosis is not an absolute pre-requisite for GluN2A expression at the neuronal membrane. Determined by single-cell RT-PCR, there is a strong correlation between *Grin2a* expression and a fall in ifenprodil sensitivity in cortical cultures (Hoffmann et al. 2002). Furthermore, the temporal pattern of *Grin2a* transcription (Watanabe et al. 1992; Monyer et al. 1994) and GluN2A expression (Sheng et al. 1994; Portera-Cailliau et al. 1996) *in vivo* corresponds excellently with electrophysiological data suggesting incorporation of GluN2A containing NMDARs at the synapse (Kirson & Yaari 1996). Epigenetic silencing of *Grin2b* has been proposed to be essential for the development upregulation of GluN2A (Rodenas-Ruano et al. 2012). Altogether, this suggests a prominent role for the protein expression of GluN2A and GluN2B in determining the upregulation of GluN2A containing NMDARs rather than post-translational modification.

The major advantage of replacing the GluN2A CTD with that of GluN2B in this study is that it permits the evaluation of the CTD without the need for over-expressing proteins of interest nor utilizing pharmacology to acutely perturb homoeostasis. Here, when both GluN2A and GluN2B NMDARs are subjected to the same regulation via the CTD in GluN2A[2B(CTR)] neurons, the developmental upregulation of GluN2A and synaptic targetting of NMDARs is the same as WT neurons. This suggests that selective CK2-dependent regulation of the GluN2B CTD is not required for the developmental upregulation of GluN2A at the neuronal membrane in cortical cultures.

I propose the conflicting results can be explained by the initial observation that GluN2A upregulation can occur in both an artificially created culture system in a time period of days, but also in hippocampal slices in a matter of minutes induced by an LTP protocol. It has largely been assumed that the two mechanisms of GluN2A upregulation are correlated but the evidence for this is lacking. The slow developmental upregulation of GluN2A is likely mediated through transcriptional and translational mechanisms whereas the rapid upregulation of GluN2A induced by LTP protocols requires the faster mechanism of post-translational modifications including that of the GluN2B CTD.

It is also interesting to note that dark rearing rats from birth can result in an increase in the phosphorylation of ser1303 at the GluN2B CTD, juxtaposed with a decrease in the protein expression of GluN2A:GluN2B, which correlates with a delayed upregulation of GluN2A in the visual cortex and retina; even more remarkable, only 6 hours of light can reverse both the delayed expression of GluN2A and the increased phosphorylation of ser1303 (Giannakopoulos et al. 2010). Phosphorylation of ser1303 would prevent CaMKII binding and therefore block CK2 regulated endocytosis of GluN2B NMDARs making this an attractive mechanism to partly explain this form of metaplasticity. Repeating the experiments in GluN2A$^{B(CTR)}$ mice would permit the testing of this hypothesis.

For completeness, it has been reported that blockade of NMDARs and AMPARs has been reported to increase GluN2A expression within hours with no effect on GluN2B expression in culture (von Engelhardt et al. 2009). As TTX could not reproduce this effect, it must be presumed this effect is due to blocking action potential independent miniature release of glutamate at the synapse ("minis") which can tonically suppress local dendritic protein synthesis (Sutton et al. 2006). Nevertheless, this phenomenon has yet to be explored in any great detail.

5.3.3 The role of the GluN2 CTD in excitotoxicity

The data presented here demonstrate GluN2A$^{2B(CTR)}$ cultures are more vulnerable to excitotoxicity in a concentration-dependent manner. This result is in excellent accordance with over-expression of GluN2A$^{2B(CTR)}$ in young DIV 9-10 neurons being more vulnerable to excitotoxicity but also the *in vitro* and *in vivo* data from the reciprocal GluN2B$^{2A(CTR)}$ mouse line having reduced vulnreability to excitotoxicity (Martel et al. 2012). This work could easily be expanded by investigating signalling cascades involved in the GluN2B CTD preferentially coupling to excitotoxicity. Initially, the most obvious candidate would be the previous identified PSD-95-nNOS pathway preferentially coupling to CREB shut-off (Soriano et al. 2008; Martel et al. 2012) but other mechanisms, such as the phosphorylation of the GluN2B CTD by DAPK1 (Tu et al. 2010) could also be investigated.

An interesting and open question is to what extent does one GluN2B CTD in a triheteromeric NMDAR saturate preferential excitotoxic signalling? Unfortunately, this cannot be addressed with the current approach. Nevertheless, coupling the GluN2A$^{2B(CTR)}$ and GluN2B$^{2A(CTR)}$ constructs with the recently developed approach to isolate triheteromeric NMDARs (Hansen et al. 2014) would be a promising strategy to address this question.

The data presented here strengthens the concept that the GluN2B CTD is a valuable target to disrupt in order to uncouple the NMDAR from excitotoxicity. From a clinical perspective, it is promising that disrupting the interaction of the GluN2B CTD and PSD-95, utilizing NA-1/Tat-NR2B9c, has the beneficial effect of not only reducing lesion size but also improving general outcome of non human primates post stroke (Cook et al. 2012). Furthermore, in a phase II clinical trial assessing whether NA-1/Tat-NR2B9c would be beneficial in reducing the pathophysiological outcome post intracranial aneurysm, NA-1/Tat-NR2B9c was found to reduce lesion

size 12-95 hours after infusion (Hill et al. 2012). Further research will be needed to determine the therapeutic potential of NA-1/Tat-NR2B9c in stroke and other neurodegenerative diseases.

5.3.4 The role of the GluN2 CTD in the transcription of neuroprotective genes

Nuclear Ca^{2+} concentrations is a major determinant in the transcription of neuroprotective genes (Hardingham et al. 1997; Zhang et al. 2009; Bading 2013) and neurons that predominantly express diheteromeric GluN2B NMDARs are capable of upregulating neuroprotective genes upon synaptic activity. Therefore, the proposition that GluN2A NMDARs exclusively mediate neuroprotective signalling (Liu et al. 2007) is surprising. As selective Ca^{2+} influx through L-type voltage-operated calcium channels (VOCCs) can also result in the activation of CREB and promote the transcription of neuroprotective genes, it is unlikely subtle differences in the biophysical properties of GluN2A and GluN2B could impart selective neuroprotective signalling to GluN2A. As an aside, it now appears the major source of somatic/nuclear Ca^{2+} during synaptic activity is through VOCCs with Ca^{2+} influx through synNMDARs functioning to amplify this signal (Bengtson et al. 2013). Nevertheless, it is logical that any potential selective neuroprotective signalling is through the GluN2A CTD rather than biophysical properties.

However, the mRNA expression of a neuroprotective CREB regulated gene (BDNF) and a neuroprotective CREB-independent gene (NPAS4) were equally upregulated in WT and GluN2A$^{2B(CTR)}$cultures upon synaptic activity. This suggests the GluN2 CTD subtype is not relevant in the transcriptional upregulation of these genes despite reports that GluN2A and gluN2B differentially regulate BDNF (M. Chen et al. 2008). This discrepancy and that of Liu et. al. are likely explained by the use of a concentration of NVP (400 nM) which blocks both GluN2A and GluN2B NMDARs, with the intention of selectively blocking GluN2A.

Nevertheless, it is feasible that a small subset of genes are differentially regulated by the GluN2A and GluN2B CTD. To address this, the above experiments were designed so that there is sufficient RNA from the control and bicuculline experiments to run an RNA-seq experiment utilizing current Illumina sequencing technology if required in the near future.

5.3.5 Limitations and advantages of experimental approach

To summarize previous points, replacing the Glun2A CTD with that of the GluN2B CTD circumnavigates the need to overexpress proteins of interests which can produce off-target effects. This approach also allows the developmental upregulation of GluN2A to be monitored without pharmacological perturbation of homoeostatic conditions. Also, as previously discussed, the poor selectivity of NVP-AAM077 has led to conflicting evidence regarding the role of GluN2A in NMDAR signalling and the dependency of TCN 201 and TCN 213 on concentration of the co-agonsit glycine/D-serine is a major hindrance on their use for the same purpose (see **chapter 4**); therefore, genetic manipulation of GluN2 subunits are still essential for understanding NMDAR dependent signalling.

On the other hand, it could be argued that replacing the entire GluN2A CTD with GluN2B can lead to off-target effects itself. Therefore, this study would benefit from a greater understanding of the physiological state of the GluN2B CTD incorporated into the GluN2A subunit; this include post-translational modifications of the CTD and identifying its key binding partners.

Additionally, another approach to investigate the role of CAMKII in the regulation of GluN2B-NMDARs surface expression at the membrane is to utilize a knock-in mouse where the CAMKII binding site on the GluN2B CTD is mutated; this avoids the off-target effects of either overexpressing mutated GluN2B subunits (as used

heavily in other studies) or replacing entire CTD as used in this chapter.

Chapter 6

Concluding Statement

The introduction to this thesis clearly identifies that the NMDAR can couple to multiple physiological and pathophysiological signalling cascades. It is evident that this is possible because the biological outcome of NMDAR activation is determined by a complicated interrelationship between the concentration of Ca^{2+} influx, NMDAR location as well as the subtype of the GluN2 subunit. Despite the recognition that NMDAR mediated physiology is multifaceted, tools used to study subunit and location dependent signalling are poorly characterized and in other cases, non-existent. The research reported herein has addressed this issue by establishing the following three key findings:

- Contrary to the current dogma, MK-801 blockade is unstable during tonic agonist exposure in the presence of physiologically relevant concentrations of Mg^{2+}. This confines a temporal limit in which selective activation of exNMDARs can occur.
- Novel GluN2A antagonists, TCN 201 and TCN 213, can detect a developmental upregulation of GluN2A during cortical culture maturation.
- Genetically replacing the GluN2A CTD with GluN2B does not impede the developmental upregulation of GluN2A nor the induction of several immediate genes by synaptic activity. It does, however, render neurons more vulnerable to NMDAR-dependent excitotoxicity.

It is hoped the identification of these findings will impact future studies aimed at elucidating the complex signalling of the NMDAR. Firstly, the data in **chapter 3** demonstrate it is relatively difficult to selectively activate exNMDARs and synNMDARs under the same temporal profile utilizing MK-801; current data acquired using this experimental paradigm must be re-assessed in this new light. On a longer time scale, as there is a great deal of interest in selective signalling downstream of synNMDARs and exNMDARs (Giles E. Hardingham & Bading 2010) another experimental strategy is clearly required to dissect out cellular signalling by spatially distinct populations of NMDARs. Consequently, the use of glutamate or MK-801 uncaging is arguably the most promising avenue currently available. Another potential approach involves involves using enzymes which degrade the NMDAR co-agonists glycine and D-serine; it has been demonstrated that under physiological conditions, degrading D-serine effects the activation of synNMDARs whereas degrading glycine effects the activation of exNMDARs in hippocampal slices (Papouin et al. 2012). This of course would have to be verified to function in every new system utilized and also shown to function under any change to the system such as inducing an excitotoxic insult.

Secondly, the data in **chapter 4** demonstrate novel GluN2A antagonists, TCN 201 and TCN 213, can inhibit endogenously expressed GluN2A containing NMDARs. This is noteworthy as both compounds are the first class of selective GluN2A antagonists. These compounds were utilized to demonstrate a developmental upregulation of GluN2A, which concurrently dilutes the contribution of GluN2B-NMDARs. This observation is in agreement with a noted increase of *grin2a* and GluN2A expression, juxtaposed with a decrease in *grin2b* and GluN2B expression, during forebrain development. Moreover, this study also advocates that further determination of TCN 201 potency at triheteromeric GluN2A-GluN2B NMDARs would be invaluable in the interpretation of not only the data presented herein but also future studies. However, the potency of these compounds is determined by the

concentration of glycine/D-serine acting as a co-agonist at the NMDAR. Therefore, it absolutely paramount that any future studies utilizing these compounds ensure that the glycine/D-serine concentrations at synaptic and extrasynaptic sites is determined in order that an expected antagonism is gauged. To date, *in vitro* studies (Costa et al. 2012; Shin et al. 2012; Hargus & Thayer 2013) utilizing TCN 201 have failed to demonstrate direct antagonism of TCN 201 in the system used yet correlate a lack of TCN 201 modifying a biological effect with GluN2A containing NMDARs not being involved in the signalling cascade observed. Consequently, it is extremely difficult to interpret the data from these studies; it is hoped this is remedied in future studies in order that complex subunit-dependent signalling by NMDARs signalling is elucidated correctly.

Lastly, data in **chapter 5** reveal that selective post-translational modification of the GluN2B CTD is not an absolute pre-requisite for the developmental upregulation of GluN2A to occur in a cortical culture system. This was was concluded by the replacement of the GluN2A CTD with that of GluN2B in order that all GluN2 subunits were subjected to the same post-translational modifications; it was observed developmental upregulation of GluN2A was not impeded. However, this study does not exclude the possibility that the post-translational modification of the GluN2B CTD may be critical for other forms of GluN2A upregulation including that induced by synaptic plasticity. Furthermore, it was revealed that replacing the GluN2A CTD with GluN2B rendered neurons more vulnerable to NMDAR-dependent excitotoxicity thus strengthening the concept that the GluN2B CTD is a valuable target to disrupt in order to uncouple the NMDAR from excitotoxicity. Future research into the usefulness of disrupting the interaction of the GluN2B CTD and PSD-95, utilizing NA-1/Tat-NR2B9c, may yield an important therapeutic strategy in treating stroke and neurodegenerative diseases. Moreover, the observation that the induction of neuroprotective immediate early genes by synaptic activity were not impaired in GluN2A$^{2B(CTR)}$ neurons supports the hypothesis that

nuclear Ca^{2+} may be the main determinant in the transcription of neuroprotective genes. This further supports the use of NA-1/Tat-NR2B9c as a neuroprotective agent as disrupting the GluN2B CTD may minimally effect neuronal survival signalling as previously shown by Martel et al., 2009.

An overarching theme maintained throughout this thesis is that carefully designed and complex tools are needed to study the NMDAR. The need for such elegant experimental approaches arises from the composite structure of the NMDAR juxtaposed with the intricate signalling cascades the receptor can couple to. Future research will undoubtedly develop new and exciting avenues to explore the role of this fascinating receptor in mediating essential physiological and pathophysiological functions in the nervous system.

References

Aarts, M., Liu, Y., Liu, L., Besshoh, S., Arundine, M., Gurd, J.W., Wang, Y.-T., Salter, M.W., Tymianski, M., 2002. Treatment of ischemic brain damage by perturbing NMDA receptor- PSD-95 protein interactions. Science (New York, N.Y.) 298, 846–50. doi:10.1126/science.1072873

Abraham, W.C., 2008. Metaplasticity: tuning synapses and networks for plasticity. Nature reviews. Neuroscience 9, 387. doi:10.1038/nrn2356

Al-Hallaq, R.A., Conrads, T.P., Veenstra, T.D., Wenthold, R.J., 2007. NMDA di-heteromeric receptor populations and associated proteins in rat hippocampus. The Journal of neuroscience : the official journal of the Society for Neuroscience 27, 8334–43. doi:10.1523/JNEUROSCI.2155-07.2007

Anggono, V., Huganir, R.L., 2012. Regulation of AMPA receptor trafficking and synaptic plasticity. Current opinion in neurobiology 22, 461–9. doi:10.1016/j.conb.2011.12.006

Aracava, Y., Pereira, E.F.R., Maelicke, A., Albuquerque, E.X., 2005. Memantine blocks alpha7* nicotinic acetylcholine receptors more potently than n-methyl-D-aspartate receptors in rat hippocampal neurons. The Journal of pharmacology and experimental therapeutics 312, 1195–205. doi:10.1124/jpet.104.077172

Arendt, K.L., Sarti, F., Chen, L., 2013. Chronic inactivation of a neural circuit enhances LTP by inducing silent synapse formation. The Journal of neuroscience : the official journal of the Society for Neuroscience 33, 2087–96. doi:10.1523/JNEUROSCI.3880-12.2013

Auberson, Y.P., Allgeier, H., Bischoff, S., Lingenhoehl, K., Moretti, R., Schmutz, M., 2002. 5-Phosphonomethylquinoxalinediones as competitive NMDA receptor antagonists with a preference for the human 1A/2A, rather than 1A/2B receptor composition. Bioorganic & medicinal chemistry letters 12, 1099–102.

Babiec, W.E., Guglietta, R., Jami, S.A., Morishita, W., Malenka, R.C., O'Dell, T.J., 2014. Ionotropic NMDA Receptor Signaling Is Required for the Induction of Long-Term Depression in the Mouse Hippocampal CA1 Region. Journal of Neuroscience 34, 5285–5290. doi:10.1523/JNEUROSCI.5419-13.2014

Bading, H., 2013. Nuclear calcium signalling in the regulation of brain function. Nature reviews. Neuroscience 14, 593–608. doi:10.1038/nrn3531

Bading, H., Ginty, D.D., Greenberg, M.E., 1993. Regulation of gene expression in hippocampal neurons by distinct calcium signaling pathways. Science (New York, N.Y.) 260, 181–6.

Balasuriya, D., Goetze, T.A., Barrera, N.P., Stewart, A.P., Suzuki, Y., Edwardson, J.M., 2013. α-Amino-3-hydroxy-5-methyl-4-isoxazole propionic acid (AMPA)

and N-methyl-D-aspartate (NMDA) receptors adopt different subunit arrangements. The Journal of biological chemistry 288, 21987–98. doi:10.1074/jbc.M113.469205

Bannerman, D.M., Niewoehner, B., Lyon, L., Romberg, C., Schmitt, W.B., Taylor, A., Sanderson, D.J., Cottam, J., Sprengel, R., Seeburg, P.H., Köhr, G., Rawlins, J.N.P., 2008. NMDA receptor subunit NR2A is required for rapidly acquired spatial working memory but not incremental spatial reference memory. The Journal of neuroscience : the official journal of the Society for Neuroscience 28, 3623–30. doi:10.1523/JNEUROSCI.3639-07.2008

Beister, A., Kraus, P., Kuhn, W., Dose, M., Weindl, A., Gerlach, M., 2004. The N-methyl-D-aspartate antagonist memantine retards progression of Huntington's disease. Journal of neural transmission. Supplementum 117–22.

Bellone, C., Nicoll, R.A., 2007. Rapid bidirectional switching of synaptic NMDA receptors. Neuron 55, 779–85. doi:10.1016/j.neuron.2007.07.035

Bengtson, C.P., Kaiser, M., Obermayer, J., Bading, H., 2013. Calcium responses to synaptically activated bursts of action potentials and their synapse-independent replay in cultured networks of hippocampal neurons. Biochimica et biophysica acta 1833, 1672–9. doi:10.1016/j.bbamcr.2013.01.022

Berberich, S., Punnakkal, P., Jensen, V., Pawlak, V., Seeburg, P.H., Hvalby, Ø., Köhr, G., 2005. Lack of NMDA receptor subtype selectivity for hippocampal long-term potentiation. The Journal of neuroscience : the official journal of the Society for Neuroscience 25, 6907–10. doi:10.1523/JNEUROSCI.1905-05.2005

Bettini, E., Sava, A., Griffante, C., Carignani, C., Buson, A., Capelli, A.M., Negri, M., Andreetta, F., Senar-Sancho, S.A., Guiral, L., Cardullo, F., 2010. Identification and characterization of novel NMDA receptor antagonists selective for NR2A- over NR2B-containing receptors. The Journal of pharmacology and experimental therapeutics 335, 636–44. doi:10.1124/jpet.110.172544

Boyer, C., Schikorski, T., Stevens, C.F., 1998. Comparison of hippocampal dendritic spines in culture and in brain. The Journal of neuroscience : the official journal of the Society for Neuroscience 18, 5294–300.

Bradley, J., Carter, S.R., Rao, V.R., Wang, J., Finkbeiner, S., 2006. Splice variants of the NR1 subunit differentially induce NMDA receptor-dependent gene expression. The Journal of neuroscience : the official journal of the Society for Neuroscience 26, 1065–76. doi:10.1523/JNEUROSCI.3347-05.2006

Braithwaite, S.P., Adkisson, M., Leung, J., Nava, A., Masterson, B., Urfer, R., Oksenberg, D., Nikolich, K., 2006. Regulation of NMDA receptor trafficking and function by striatal-enriched tyrosine phosphatase (STEP). The European

journal of neuroscience 23, 2847–56. doi:10.1111/j.1460-9568.2006.04837.x

Briggs, C.A., McKenna, D.G., 1996. Effect of MK-801 at the human alpha 7 nicotinic acetylcholine receptor. Neuropharmacology 35, 407–14.

Buisson, B., Bertrand, D., 1998. Open-channel blockers at the human alpha4beta2 neuronal nicotinic acetylcholine receptor. Molecular pharmacology 53, 555–63.

Calabrese, B., Wilson, M.S., Halpain, S., 2006. Development and regulation of dendritic spine synapses. Physiology (Bethesda, Md.) 21, 38–47. doi:10.1152/physiol.00042.2005

Camacho, A., Massieu, L., 2006. Role of glutamate transporters in the clearance and release of glutamate during ischemia and its relation to neuronal death. Archives of medical research 37, 11–8. doi:10.1016/j.arcmed.2005.05.014

Carmigoto, G., Vicini, S., 1992. Activity-dependent decrease in NMDA receptor responses during development of the visual cortex. Science (New York, N.Y.) 258, 1007–11.

Cerne, R., Rusin, K.I., Randić, M., 1993. Enhancement of the N-methyl-D-aspartate response in spinal dorsal horn neurons by cAMP-dependent protein kinase. Neuroscience letters 161, 124–8.

Chang, H.-J., Lane, H.-Y., Tsai, G.E., 2014. NMDA Pathology and Treatment of Schizophrenia. Current pharmaceutical design.

Chen, B.-S., Gray, J.A., Sanz-Clemente, A., Wei, Z., Thomas, E. V, Nicoll, R.A., Roche, K.W., 2012. SAP102 mediates synaptic clearance of NMDA receptors. Cell reports 2, 1120–8. doi:10.1016/j.celrep.2012.09.024

Chen, H.S., Lipton, S.A., 1997. Mechanism of memantine block of NMDA-activated channels in rat retinal ganglion cells: uncompetitive antagonism. The Journal of physiology 499 (Pt 1, 27–46.

Chen, H.S., Pellegrini, J.W., Aggarwal, S.K., Lei, S.Z., Warach, S., Jensen, F.E., Lipton, S.A., 1992. Open-channel block of N-methyl-D-aspartate (NMDA) responses by memantine: therapeutic advantage against NMDA receptor-mediated neurotoxicity. The Journal of neuroscience : the official journal of the Society for Neuroscience 12, 4427–36.

Chen, M., Lu, T.-J., Chen, X.-J., Zhou, Y., Chen, Q., Feng, X.-Y., Xu, L., Duan, W.-H., Xiong, Z.-Q., 2008. Differential roles of NMDA receptor subtypes in ischemic neuronal cell death and ischemic tolerance. Stroke; a journal of cerebral circulation 39, 3042–8. doi:10.1161/STROKEAHA.108.521898

Chen, P.E., Geballe, M.T., Katz, E., Erreger, K., Livesey, M.R., O'Toole, K.K., Le, P., Lee, C.J., Snyder, J.P., Traynelis, S.F., Wyllie, D.J.A., 2008. Modulation of glycine potency in rat recombinant NMDA receptors containing chimeric NR2A/2D subunits expressed in Xenopus laevis oocytes. The Journal of

physiology 586, 227–45. doi:10.1113/jphysiol.2007.143172

Chen, Q., He, S., Hu, X.-L., Yu, J., Zhou, Y., Zheng, J., Zhang, S., Zhang, C., Duan, W.-H., Xiong, Z.-Q., 2007. Differential roles of NR2A- and NR2B-containing NMDA receptors in activity-dependent brain-derived neurotrophic factor gene regulation and limbic epileptogenesis. The Journal of neuroscience : the official journal of the Society for Neuroscience 27, 542–52. doi:10.1523/JNEUROSCI.3607-06.2007

Chen, W.S., Bear, M.F., 2007. Activity-dependent regulation of NR2B translation contributes to metaplasticity in mouse visual cortex. Neuropharmacology 52, 200–14. doi:10.1016/j.neuropharm.2006.07.003

Cho, K.K.A., Khibnik, L., Philpot, B.D., Bear, M.F., 2009. The ratio of NR2A/B NMDA receptor subunits determines the qualities of ocular dominance plasticity in visual cortex. Proceedings of the National Academy of Sciences of the United States of America 106, 5377–82. doi:10.1073/pnas.0808104106

Choi, D.W., 1987. Ionic dependence of glutamate neurotoxicity. The Journal of neuroscience : the official journal of the Society for Neuroscience 7, 369–79.

Choi, D.W., Koh, J.Y., Peters, S., 1988. Pharmacology of glutamate neurotoxicity in cortical cell culture: attenuation by NMDA antagonists. The Journal of neuroscience : the official journal of the Society for Neuroscience 8, 185–96.

Choi, D.W., Maulucci-Gedde, M., Kriegstein, A.R., 1987. Glutamate neurotoxicity in cortical cell culture. The Journal of neuroscience : the official journal of the Society for Neuroscience 7, 357–68.

Chung, H.J., Huang, Y.H., Lau, L.-F., Huganir, R.L., 2004. Regulation of the NMDA receptor complex and trafficking by activity-dependent phosphorylation of the NR2B subunit PDZ ligand. The Journal of neuroscience : the official journal of the Society for Neuroscience 24, 10248–59. doi:10.1523/JNEUROSCI.0546-04.2004

Clarke, P.B., Reuben, M., 1995. Inhibition by dizocilpine (MK-801) of striatal dopamine release induced by MPTP and MPP+: possible action at the dopamine transporter. British journal of pharmacology 114, 315–22.

Cook, D.J., Teves, L., Tymianski, M., 2012. Treatment of stroke with a PSD-95 inhibitor in the gyrencephalic primate brain. Nature 483, 213–7. doi:10.1038/nature10841

Costa, R.O., Lacor, P.N., Ferreira, I.L., Resende, R., Auberson, Y.P., Klein, W.L., Oliveira, C.R., Rego, A.C., Pereira, C.M.F., 2012. Endoplasmic reticulum stress occurs downstream of GluN2B subunit of N-methyl-d-aspartate receptor in mature hippocampal cultures treated with amyloid-β oligomers. Aging cell 11, 823–33. doi:10.1111/j.1474-9726.2012.00848.x

Cull-Candy, S., Brickley, S., Farrant, M., 2001. NMDA receptor subunits: diversity,

development and disease. Current Opinion in Neurobiology 11, 327–335. doi:10.1016/S0959-4388(00)00215-4

Dalmau, J., Gleichman, A.J., Hughes, E.G., Rossi, J.E., Peng, X., Lai, M., Dessain, S.K., Rosenfeld, M.R., Balice-Gordon, R., Lynch, D.R., 2008. Anti-NMDA-receptor encephalitis: case series and analysis of the effects of antibodies. Lancet neurology 7, 1091–8. doi:10.1016/S1474-4422(08)70224-2

Davis, S.M., Lees, K.R., Albers, G.W., Diener, H.C., Markabi, S., Karlsson, G., Norris, J., 2000. Selfotel in acute ischemic stroke : possible neurotoxic effects of an NMDA antagonist. Stroke; a journal of cerebral circulation 31, 347–54.

Delaney, A.J., Power, J.M., Sah, P., 2012. Ifenprodil reduces excitatory synaptic transmission by blocking presynaptic P/Q type calcium channels. Journal of neurophysiology 107, 1571–5. doi:10.1152/jn.01066.2011

Destexhe, A., Mainen, Z., Sejnowski, T., 1995. Fast kinetic models for simulating AMPA, NMDA, GABA A and GABA B receptors. The Neurobiology of Computation.

Dravid, S.M., Erreger, K., Yuan, H., Nicholson, K., Le, P., Lyuboslavsky, P., Almonte, A., Murray, E., Mosely, C., Barber, J., French, A., Balster, R., Murray, T.F., Traynelis, S.F., 2007. Subunit-specific mechanisms and proton sensitivity of NMDA receptor channel block. The Journal of physiology 581, 107–28. doi:10.1113/jphysiol.2006.124958

Edman, S., McKay, S., Macdonald, L.J., Samadi, M., Livesey, M.R., Hardingham, G.E., Wyllie, D.J.A., 2012. TCN 201 selectively blocks GluN2A-containing NMDARs in a GluN1 co-agonist dependent but non-competitive manner. Neuropharmacology 63, 441–9. doi:10.1016/j.neuropharm.2012.04.027

Elias, G.M., Elias, L.A.B., Apostolides, P.F., Kriegstein, A.R., Nicoll, R.A., 2008. Differential trafficking of AMPA and NMDA receptors by SAP102 and PSD-95 underlies synapse development. Proceedings of the National Academy of Sciences of the United States of America 105, 20953–8. doi:10.1073/pnas.0811025106

Endele, S., Rosenberger, G., Geider, K., Popp, B., Tamer, C., Stefanova, I., Milh, M., Kortüm, F., Fritsch, A., Pientka, F.K., Hellenbroich, Y., Kalscheuer, V.M., Kohlhase, J., Moog, U., Rappold, G., Rauch, A., Ropers, H.-H., von Spiczak, S., Tönnies, H., Villeneuve, N., Villard, L., Zabel, B., Zenker, M., Laube, B., Reis, A., Wieczorek, D., Van Maldergem, L., Kutsche, K., 2010. Mutations in GRIN2A and GRIN2B encoding regulatory subunits of NMDA receptors cause variable neurodevelopmental phenotypes. Nature genetics 42, 1021–6. doi:10.1038/ng.677

Feng, B., Tse, H.W., Skifter, D.A., Morley, R., Jane, D.E., Monaghan, D.T., 2004. Structure-activity analysis of a novel NR2C/NR2D-preferring NMDA receptor

antagonist: 1-(phenanthrene-2-carbonyl) piperazine-2,3-dicarboxylic acid. British journal of pharmacology 141, 508–16. doi:10.1038/sj.bjp.0705644

Flint, A.C., Maisch, U.S., Weishaupt, J.H., Kriegstein, A.R., Monyer, H., 1997. NR2A subunit expression shortens NMDA receptor synaptic currents in developing neocortex. The Journal of neuroscience : the official journal of the Society for Neuroscience 17, 2469–76.

Frizelle, P.A., Chen, P.E., Wyllie, D.J.A., 2006. Equilibrium constants for (R)-[(S)-1-(4-bromo-phenyl)-ethylamino]-(2,3-dioxo-1,2,3,4-tetrahydroquinoxalin-5-yl)-methyl]-phosphonic acid (NVP-AAM077) acting at recombinant NR1/NR2A and NR1/NR2B N-methyl-D-aspartate receptors: Implications for studies of sy. Molecular pharmacology 70, 1022–32. doi:10.1124/mol.106.024042

Furukawa, H., 2012. Structure and function of glutamate receptor amino terminal domains. The Journal of physiology 590, 63–72. doi:10.1113/jphysiol.2011.213850

Gabernet, L., Pauly-Evers, M., Schwerdel, C., Lentz, M., Bluethmann, H., Vogt, K., Alberati, D., Mohler, H., Boison, D., 2005. Enhancement of the NMDA receptor function by reduction of glycine transporter-1 expression. Neuroscience letters 373, 79–84. doi:10.1016/j.neulet.2004.09.064

Gambrill, A.C., Barria, A., 2011. NMDA receptor subunit composition controls synaptogenesis and synapse stabilization. Proceedings of the National Academy of Sciences of the United States of America 108, 5855–60. doi:10.1073/pnas.1012676108

Gardoni, F., Bellone, C., Cattabeni, F., Di Luca, M., 2001. Protein kinase C activation modulates alpha-calmodulin kinase II binding to NR2A subunit of N-methyl-D-aspartate receptor complex. The Journal of biological chemistry 276, 7609–13. doi:10.1074/jbc.M009922200

Giannakopoulos, M., Kouvelas, E.D., Mitsacos, A., 2010. Experience-dependent regulation of NMDA receptor subunit composition and phosphorylation in the retina and visual cortex. Investigative ophthalmology & visual science 51, 1817–22. doi:10.1167/iovs.09-4438

Gipson, C.D., Reissner, K.J., Kupchik, Y.M., Smith, A.C.W., Stankeviciute, N., Hensley-Simon, M.E., Kalivas, P.W., 2013. Reinstatement of nicotine seeking is mediated by glutamatergic plasticity. Proceedings of the National Academy of Sciences of the United States of America 110, 9124–9. doi:10.1073/pnas.1220591110

Granger, A.J., Shi, Y., Lu, W., Cerpas, M., Nicoll, R.A., 2013. LTP requires a reserve pool of glutamate receptors independent of subunit type. Nature 493, 495–500. doi:10.1038/nature11775

Gray, J.A., Shi, Y., Usui, H., During, M.J., Sakimura, K., Nicoll, R.A., 2011. Distinct

modes of AMPA receptor suppression at developing synapses by GluN2A and GluN2B: single-cell NMDA receptor subunit deletion in vivo. Neuron 71, 1085–101. doi:10.1016/j.neuron.2011.08.007

Groc, L., Heine, M., Cousins, S.L., Stephenson, F.A., Lounis, B., Cognet, L., Choquet, D., 2006. NMDA receptor surface mobility depends on NR2A-2B subunits. Proceedings of the National Academy of Sciences of the United States of America 103, 18769–74. doi:10.1073/pnas.0605238103

Halt, A.R., Dallapiazza, R.F., Zhou, Y., Stein, I.S., Qian, H., Juntti, S., Wojcik, S., Brose, N., Silva, A.J., Hell, J.W., 2012. CaMKII binding to GluN2B is critical during memory consolidation. The EMBO journal 31, 1203–16. doi:10.1038/emboj.2011.482

Hansen, H.H., Briem, T., Dzietko, M., Sifringer, M., Voss, A., Rzeski, W., Zdzisinska, B., Thor, F., Heumann, R., Stepulak, A., Bittigau, P., Ikonomidou, C., 2004. Mechanisms leading to disseminated apoptosis following NMDA receptor blockade in the developing rat brain. Neurobiology of disease 16, 440–53. doi:10.1016/j.nbd.2004.03.013

Hansen, K.B., Ogden, K.K., Traynelis, S.F., 2012. Subunit-selective allosteric inhibition of glycine binding to NMDA receptors. The Journal of neuroscience : the official journal of the Society for Neuroscience 32, 6197–208. doi:10.1523/JNEUROSCI.5757-11.2012

Hansen, K.B., Ogden, K.K., Yuan, H., Traynelis, S.F., 2014. Distinct Functional and Pharmacological Properties of Triheteromeric GluN1/GluN2A/GluN2B NMDA Receptors. Neuron 81, 1084–96. doi:10.1016/j.neuron.2014.01.035

Hardingham, G.E., Arnold, F.J., Bading, H., 2001a. A calcium microdomain near NMDA receptors: on switch for ERK-dependent synapse-to-nucleus communication. Nature neuroscience 4, 565–6. doi:10.1038/88380

Hardingham, G.E., Arnold, F.J., Bading, H., 2001b. Nuclear calcium signaling controls CREB-mediated gene expression triggered by synaptic activity. Nature neuroscience 4, 261–7. doi:10.1038/85109

Hardingham, G.E., Bading, H., 2010. Synaptic versus extrasynaptic NMDA receptor signalling: implications for neurodegenerative disorders. Nature Reviews Neuroscience 11, 682–696. doi:10.1038/nrn2911

Hardingham, G.E., Chawla, S., Johnson, C.M., Bading, H., 1997. Distinct functions of nuclear and cytoplasmic calcium in the control of gene expression. Nature 385, 260–5. doi:10.1038/385260a0

Hardingham, G.E., Fukunaga, Y., Bading, H., 2002. Extrasynaptic NMDARs oppose synaptic NMDARs by triggering CREB shut-off and cell death pathways. Nature neuroscience 5, 405–14. doi:10.1038/nn835

Hargus, N.J., Thayer, S.A., 2013. Human immunodeficiency virus-1 Tat protein

increases the number of inhibitory synapses between hippocampal neurons in culture. The Journal of neuroscience : the official journal of the Society for Neuroscience 33, 17908–20. doi:10.1523/JNEUROSCI.1312-13.2013

Harms, K.J., Craig, A.M., 2005. Synapse composition and organization following chronic activity blockade in cultured hippocampal neurons. The Journal of comparative neurology 490, 72–84. doi:10.1002/cne.20635

Harris, A.Z., Pettit, D.L., 2007. Extrasynaptic and synaptic NMDA receptors form stable and uniform pools in rat hippocampal slices. The Journal of physiology 584, 509–19. doi:10.1113/jphysiol.2007.137679

Hatton, C.J., Paoletti, P., 2005. Modulation of triheteromeric NMDA receptors by N-terminal domain ligands. Neuron 46, 261–74. doi:10.1016/j.neuron.2005.03.005

Hayashi, T., Thomas, G.M., Huganir, R.L., 2009. Dual palmitoylation of NR2 subunits regulates NMDA receptor trafficking. Neuron 64, 213–26. doi:10.1016/j.neuron.2009.08.017

Henson, M.A., Larsen, R.S., Lawson, S.N., Pérez-Otaño, I., Nakanishi, N., Lipton, S.A., Philpot, B.D., 2012. Genetic deletion of NR3A accelerates glutamatergic synapse maturation. PloS one 7, e42327. doi:10.1371/journal.pone.0042327

Hill, M.D., Martin, R.H., Mikulis, D., Wong, J.H., Silver, F.L., Terbrugge, K.G., Milot, G., Clark, W.M., Macdonald, R.L., Kelly, M.E., Boulton, M., Fleetwood, I., McDougall, C., Gunnarsson, T., Chow, M., Lum, C., Dodd, R., Poublanc, J., Krings, T., Demchuk, A.M., Goyal, M., Anderson, R., Bishop, J., Garman, D., Tymianski, M., 2012. Safety and efficacy of NA-1 in patients with iatrogenic stroke after endovascular aneurysm repair (ENACT): a phase 2, randomised, double-blind, placebo-controlled trial. Lancet neurology 11, 942–50. doi:10.1016/S1474-4422(12)70225-9

Hoffmann, H., Gremme, T., Hatt, H., Gottmann, K., 2002. Synaptic Activity-Dependent Developmental Regulation of NMDA Receptor Subunit Expression in Cultured Neocortical Neurons. Journal of Neurochemistry 75, 1590–1599. doi:10.1046/j.1471-4159.2000.0751590.x

Horak, M., Wenthold, R.J., 2009. Different roles of C-terminal cassettes in the trafficking of full-length NR1 subunits to the cell surface. The Journal of biological chemistry 284, 9683–91. doi:10.1074/jbc.M807050200

Huettner, J.E., Bean, B.P., 1988. Block of N-methyl-D-aspartate-activated current by the anticonvulsant MK-801: selective binding to open channels. Proceedings of the National Academy of Sciences of the United States of America 85, 1307–11.

Hughes, E.G., Peng, X., Gleichman, A.J., Lai, M., Zhou, L., Tsou, R., Parsons, T.D., Lynch, D.R., Dalmau, J., Balice-Gordon, R.J., 2010. Cellular and synaptic

mechanisms of anti-NMDA receptor encephalitis. The Journal of neuroscience : the official journal of the Society for Neuroscience 30, 5866–75. doi:10.1523/JNEUROSCI.0167-10.2010

Ikonomidou, C., Bosch, F., Miksa, M., Bittigau, P., Vöckler, J., Dikranian, K., Tenkova, T.I., Stefovska, V., Turski, L., Olney, J.W., 1999. Blockade of NMDA receptors and apoptotic neurodegeneration in the developing brain. Science (New York, N.Y.) 283, 70–4.

Ilyin, V., Whittemore, E., Guastella, J., Weber, E., Woodward, R., 1996. Subtype-selective inhibition of N-methyl-D-aspartate receptors by haloperidol. Mol. Pharmacol. 50, 1541–1550.

Iravani, M.M., Muscat, R., Kruk, Z.L., 1999. MK-801 interaction with the 5-HT transporter: a real-time study in brain slices using fast cyclic voltammetry. Synapse (New York, N.Y.) 32, 212–24. doi:10.1002/(SICI)1098-2396(19990601)32:3<212::AID-SYN7>3.0.CO;2-M

Ittner, L.M., Ke, Y.D., Delerue, F., Bi, M., Gladbach, A., van Eersel, J., Wölfing, H., Chieng, B.C., Christie, M.J., Napier, I.A., Eckert, A., Staufenbiel, M., Hardeman, E., Götz, J., 2010. Dendritic function of tau mediates amyloid-beta toxicity in Alzheimer's disease mouse models. Cell 142, 387–97. doi:10.1016/j.cell.2010.06.036

Karakas, E., Simorowski, N., Furukawa, H., 2011. Subunit arrangement and phenylethanolamine binding in GluN1/GluN2B NMDA receptors. Nature 475, 249–53. doi:10.1038/nature10180

Kashiwagi, K., Masuko, T., Nguyen, C.D., Kuno, T., Tanaka, I., Igarashi, K., Williams, K., 2002. Channel blockers acting at N-methyl-D-aspartate receptors: differential effects of mutations in the vestibule and ion channel pore. Molecular pharmacology 61, 533–45.

Kessels, H.W., Malinow, R., 2009. Synaptic AMPA receptor plasticity and behavior. Neuron 61, 340–50. doi:10.1016/j.neuron.2009.01.015

Kessels, H.W., Nabavi, S., Malinow, R., 2013. Metabotropic NMDA receptor function is required for β-amyloid-induced synaptic depression. Proceedings of the National Academy of Sciences of the United States of America 110, 4033–8. doi:10.1073/pnas.1219605110

Kew, J.N., Richards, J.G., Mutel, V., Kemp, J.A., 1998. Developmental changes in NMDA receptor glycine affinity and ifenprodil sensitivity reveal three distinct populations of NMDA receptors in individual rat cortical neurons. The Journal of neuroscience : the official journal of the Society for Neuroscience 18, 1935–43.

Kirson, E.D., Yaari, Y., 1996. Synaptic NMDA receptors in developing mouse hippocampal neurones: functional properties and sensitivity to ifenprodil. The

Journal of physiology 497 (Pt 2, 437–55.

Kossel, A.H., Williams, C. V, Schweizer, M., Kater, S.B., 1997. Afferent innervation influences the development of dendritic branches and spines via both activity-dependent and non-activity-dependent mechanisms. The Journal of neuroscience : the official journal of the Society for Neuroscience 17, 6314–24.

Kotermanski, S.E., Johnson, J.W., 2009. Mg2+ imparts NMDA receptor subtype selectivity to the Alzheimer's drug memantine. The Journal of neuroscience : the official journal of the Society for Neuroscience 29, 2774–9. doi:10.1523/JNEUROSCI.3703-08.2009

Krystal, J.H., Karper, L.P., Seibyl, J.P., Freeman, G.K., Delaney, R., Bremner, J.D., Heninger, G.R., Bowers, M.B., Charney, D.S., 1994. Subanesthetic effects of the noncompetitive NMDA antagonist, ketamine, in humans. Psychotomimetic, perceptual, cognitive, and neuroendocrine responses. Archives of general psychiatry 51, 199–214.

Lakhan, S.E., Caro, M., Hadzimichalis, N., 2013. NMDA Receptor Activity in Neuropsychiatric Disorders. Frontiers in psychiatry 4, 52. doi:10.3389/fpsyt.2013.00052

Larsen, R.S., Corlew, R.J., Henson, M.A., Roberts, A.C., Mishina, M., Watanabe, M., Lipton, S.A., Nakanishi, N., Pérez-Otaño, I., Weinberg, R.J., Philpot, B.D., 2011. NR3A-containing NMDARs promote neurotransmitter release and spike timing-dependent plasticity. Nature neuroscience 14, 338–44. doi:10.1038/nn.2750

Lau, C.G., Zukin, R.S., 2007. NMDA receptor trafficking in synaptic plasticity and neuropsychiatric disorders. Nature reviews. Neuroscience 8, 413–26. doi:10.1038/nrn2153

Lee, C.-H., Lü, W., Michel, J.C., Goehring, A., Du, J., Song, X., Gouaux, E., 2014. NMDA receptor structures reveal subunit arrangement and pore architecture. Nature. doi:10.1038/nature13548

Li, S., Hong, S., Shepardson, N.E., Walsh, D.M., Shankar, G.M., Selkoe, D., 2009. Soluble oligomers of amyloid Beta protein facilitate hippocampal long-term depression by disrupting neuronal glutamate uptake. Neuron 62, 788–801. doi:10.1016/j.neuron.2009.05.012

Li, S., Jin, M., Koeglsperger, T., Shepardson, N.E., Shankar, G.M., Selkoe, D.J., 2011. Soluble Aβ oligomers inhibit long-term potentiation through a mechanism involving excessive activation of extrasynaptic NR2B-containing NMDA receptors. The Journal of neuroscience : the official journal of the Society for Neuroscience 31, 6627–38. doi:10.1523/JNEUROSCI.0203-11.2011

Li, Z., Okamoto, K.-I., Hayashi, Y., Sheng, M., 2004. The importance of dendritic

mitochondria in the morphogenesis and plasticity of spines and synapses. Cell 119, 873–87. doi:10.1016/j.cell.2004.11.003

Liao, G.Y., Wagner, D.A., Hsu, M.H., Leonard, J.P., 2001. Evidence for direct protein kinase-C mediated modulation of N-methyl-D-aspartate receptor current. Molecular pharmacology 59, 960–4.

Lipton, S.A., 2006. Paradigm shift in neuroprotection by NMDA receptor blockade: memantine and beyond. Nature reviews. Drug discovery 5, 160–70. doi:10.1038/nrd1958

Liu, L., Wong, T.P., Pozza, M.F., Lingenhoehl, K., Wang, Y., Sheng, M., Auberson, Y.P., Wang, Y.T., 2004. Role of NMDA receptor subtypes in governing the direction of hippocampal synaptic plasticity. Science (New York, N.Y.) 304, 1021–4. doi:10.1126/science.1096615

Liu, Y., Wong, T.P., Aarts, M., Rooyakkers, A., Liu, L., Lai, T.W., Wu, D.C., Lu, J., Tymianski, M., Craig, A.M., Wang, Y.T., 2007. NMDA receptor subunits have differential roles in mediating excitotoxic neuronal death both in vitro and in vivo. The Journal of neuroscience : the official journal of the Society for Neuroscience 27, 2846–57. doi:10.1523/JNEUROSCI.0116-07.2007

Livak, K.J., Schmittgen, T.D., 2001. Analysis of relative gene expression data using real-time quantitative PCR and the 2(-Delta Delta C(T)) Method. Methods (San Diego, Calif.) 25, 402–8. doi:10.1006/meth.2001.1262

Low, C.-M., Lyuboslavsky, P., French, A., Le, P., Wyatte, K., Thiel, W.H., Marchan, E.M., Igarashi, K., Kashiwagi, K., Gernert, K., Williams, K., Traynelis, S.F., Zheng, F., 2003. Molecular determinants of proton-sensitive N-methyl-D-aspartate receptor gating. Molecular pharmacology 63, 1212–22. doi:10.1124/mol.63.6.1212

Low, C.M., Zheng, F., Lyuboslavsky, P., Traynelis, S.F., 2000. Molecular determinants of coordinated proton and zinc inhibition of N-methyl-D-aspartate NR1/NR2A receptors. Proceedings of the National Academy of Sciences of the United States of America 97, 11062–7. doi:10.1073/pnas.180307497

Lu, W., Bushong, E.A., Shih, T.P., Ellisman, M.H., Nicoll, R.A., 2013. The cell-autonomous role of excitatory synaptic transmission in the regulation of neuronal structure and function. Neuron 78, 433–9. doi:10.1016/j.neuron.2013.02.030

Lucas, D.R., Newhouse, J.P., 1957. The toxic effect of sodium L-glutamate on the inner layers of the retina. A.M.A. archives of ophthalmology 58, 193–201.

Luo, J., Wang, Y., Yasuda, R.P., Dunah, A.W., Wolfe, B.B., 1997. The majority of N-methyl-D-aspartate receptor complexes in adult rat cerebral cortex contain at least three different subunits (NR1/NR2A/NR2B). Molecular pharmacology 51, 79–86.

152

Maki, B.A., Aman, T.K., Amico-Ruvio, S.A., Kussius, C.L., Popescu, G.K., 2012. C-terminal domains of N-methyl-D-aspartic acid receptor modulate unitary channel conductance and gating. The Journal of biological chemistry 287, 36071–80. doi:10.1074/jbc.M112.390013

Malenka, R.C., Bear, M.F., 2004. LTP and LTD: an embarrassment of riches. Neuron 44, 5–21. doi:10.1016/j.neuron.2004.09.012

Martel, M.-A., Ryan, T.J., Bell, K.F.S., Fowler, J.H., McMahon, A., Al-Mubarak, B., Komiyama, N.H., Horsburgh, K., Kind, P.C., Grant, S.G.N., Wyllie, D.J.A., Hardingham, G.E., 2012. The subtype of GluN2 C-terminal domain determines the response to excitotoxic insults. Neuron 74, 543–56. doi:10.1016/j.neuron.2012.03.021

Martel, M.-A., Soriano, F.X., Baxter, P., Rickman, C., Duncan, R., Wyllie, D.J.A., Hardingham, G.E., 2009. Inhibiting pro-death NMDA receptor signaling dependent on the NR2 PDZ ligand may not affect synaptic function or synaptic NMDA receptor signaling to gene expression. Channels 3, 12–15. doi:10.4161/chan.3.1.7864

Martel, M.-A., Wyllie, D.J.A., Hardingham, G.E., 2009. In developing hippocampal neurons, NR2B-containing N-methyl-D-aspartate receptors (NMDARs) can mediate signaling to neuronal survival and synaptic potentiation, as well as neuronal death. Neuroscience 158, 334–43. doi:10.1016/j.neuroscience.2008.01.080

Matsui, T., Sekiguchi, M., Hashimoto, A., Tomita, U., Nishikawa, T., Wada, K., 1995. Functional comparison of D-serine and glycine in rodents: the effect on cloned NMDA receptors and the extracellular concentration. Journal of neurochemistry 65, 454–8.

Matta, J.A., Ashby, M.C., Sanz-Clemente, A., Roche, K.W., Isaac, J.T.R., 2011. mGluR5 and NMDA receptors drive the experience- and activity-dependent NMDA receptor NR2B to NR2A subunit switch. Neuron 70, 339–51. doi:10.1016/j.neuron.2011.02.045

McKay, S., Bengtson, C.P., Bading, H., Wyllie, D.J.A., Hardingham, G.E., 2013. Recovery of NMDA receptor currents from MK-801 blockade is accelerated by Mg2+ and memantine under conditions of agonist exposure. Neuropharmacology. doi:10.1016/j.neuropharm.2013.01.024

McKay, S., Griffiths, N.H., Butters, P.A., Thubron, E.B., Hardingham, G.E., Wyllie, D.J.A., 2012. Direct pharmacological monitoring of the developmental switch in NMDA receptor subunit composition using TCN 213, a GluN2A-selective, glycine-dependent antagonist. British journal of pharmacology 166, 924–37. doi:10.1111/j.1476-5381.2011.01748.x

Milnerwood, A.J., Gladding, C.M., Pouladi, M.A., Kaufman, A.M., Hines, R.M.,

Boyd, J.D., Ko, R.W.Y., Vasuta, O.C., Graham, R.K., Hayden, M.R., Murphy, T.H., Raymond, L.A., 2010. Early increase in extrasynaptic NMDA receptor signaling and expression contributes to phenotype onset in Huntington's disease mice. Neuron 65, 178–90. doi:10.1016/j.neuron.2010.01.008

Mohn, A.R., Gainetdinov, R.R., Caron, M.G., Koller, B.H., 1999. Mice with reduced NMDA receptor expression display behaviors related to schizophrenia. Cell 98, 427–36.

Monyer, H., Burnashev, N., Laurie, D.J., Sakmann, B., Seeburg, P.H., 1994. Developmental and regional expression in the rat brain and functional properties of four NMDA receptors. Neuron 12, 529–40.

Moody, T.D., Watabe, A.M., Indersmitten, T., Komiyama, N.H., Grant, S.G.N., O'Dell, T.J., 2011. Beta-adrenergic receptor activation rescues theta frequency stimulation-induced LTP deficits in mice expressing C-terminally truncated NMDA receptor GluN2A subunits. Learning & memory (Cold Spring Harbor, N.Y.) 18, 118–27. doi:10.1101/lm.2045311

Morris, R.G., Anderson, E., Lynch, G.S., Baudry, M., 1986. Selective impairment of learning and blockade of long-term potentiation by an N-methyl-D-aspartate receptor antagonist, AP5. Nature 319, 774–6. doi:10.1038/319774a0

Nabavi, S., Kessels, H.W., Alfonso, S., Aow, J., Fox, R., Malinow, R., 2013. Metabotropic NMDA receptor function is required for NMDA receptor-dependent long-term depression. Proceedings of the National Academy of Sciences of the United States of America 110, 4027–32. doi:10.1073/pnas.1219454110

Nakayama, K., Kiyosue, K., Taguchi, T., 2005. Diminished neuronal activity increases neuron-neuron connectivity underlying silent synapse formation and the rapid conversion of silent to functional synapses. The Journal of neuroscience : the official journal of the Society for Neuroscience 25, 4040–51. doi:10.1523/JNEUROSCI.4115-04.2005

Neyton, J., Paoletti, P., 2006. Relating NMDA receptor function to receptor subunit composition: limitations of the pharmacological approach. The Journal of neuroscience : the official journal of the Society for Neuroscience 26, 1331–3. doi:10.1523/JNEUROSCI.5242-05.2006

Nicoll, R.A., Roche, K.W., 2013. Long-term potentiation: peeling the onion. Neuropharmacology 74, 18–22. doi:10.1016/j.neuropharm.2013.02.010

O'Roak, B.J., Vives, L., Girirajan, S., Karakoc, E., Krumm, N., Coe, B.P., Levy, R., Ko, A., Lee, C., Smith, J.D., Turner, E.H., Stanaway, I.B., Vernot, B., Malig, M., Baker, C., Reilly, B., Akey, J.M., Borenstein, E., Rieder, M.J., Nickerson, D.A., Bernier, R., Shendure, J., Eichler, E.E., 2012. Sporadic autism exomes reveal a highly interconnected protein network of de novo mutations. Nature

485, 246–50. doi:10.1038/nature10989

Okamoto, S., Pouladi, M.A., Talantova, M., Yao, D., Xia, P., Ehrnhoefer, D.E., Zaidi, R., Clemente, A., Kaul, M., Graham, R.K., Zhang, D., Vincent Chen, H.-S., Tong, G., Hayden, M.R., Lipton, S.A., 2009. Balance between synaptic versus extrasynaptic NMDA receptor activity influences inclusions and neurotoxicity of mutant huntingtin. Nature medicine 15, 1407–13. doi:10.1038/nm.2056

Olney, J., Labruyere, J., Price, M., 1989. Pathological changes induced in cerebrocortical neurons by phencyclidine and related drugs. Science 244, 1360–1362. doi:10.1126/science.2660263

Olney, J.W., Price, M.T., Fuller, T.A., Labruyere, J., Samson, L., Carpenter, M., Mahan, K., 1986. The anti-excitotoxic effects of certain anesthetics, analgesics and sedative-hypnotics. Neuroscience letters 68, 29–34.

Olsten, M.E.K., Litchfield, D.W., 2004. Order or chaos? An evaluation of the regulation of protein kinase CK2. Biochemistry and cell biology = Biochimie et biologie cellulaire 82, 681–93. doi:10.1139/o04-116

Pachernegg, S., Strutz-Seebohm, N., Hollmann, M., 2012. GluN3 subunit-containing NMDA receptors: not just one-trick ponies. Trends in neurosciences 35, 240–9. doi:10.1016/j.tins.2011.11.010

Paoletti, P., Ascher, P., Neyton, J., 1997. High-affinity zinc inhibition of NMDA NR1-NR2A receptors. The Journal of neuroscience : the official journal of the Society for Neuroscience 17, 5711–25.

Paoletti, P., Bellone, C., Zhou, Q., 2013. NMDA receptor subunit diversity: impact on receptor properties, synaptic plasticity and disease. Nature reviews. Neuroscience 14, 383–400. doi:10.1038/nrn3504

Paoletti, P., Neyton, J., 2007. NMDA receptor subunits: function and pharmacology. Current opinion in pharmacology 7, 39–47. doi:10.1016/j.coph.2006.08.011

Papadia, S., Soriano, F.X., Léveillé, F., Martel, M.-A., Dakin, K.A., Hansen, H.H., Kaindl, A., Sifringer, M., Fowler, J., Stefovska, V., McKenzie, G., Craigon, M., Corriveau, R., Ghazal, P., Horsburgh, K., Yankner, B.A., Wyllie, D.J.A., Ikonomidou, C., Hardingham, G.E., 2008. Synaptic NMDA receptor activity boosts intrinsic antioxidant defenses. Nature neuroscience 11, 476–87. doi:10.1038/nn2071

Papouin, T., Ladépêche, L., Ruel, J., Sacchi, S., Labasque, M., Hanini, M., Groc, L., Pollegioni, L., Mothet, J.-P., Oliet, S.H.R., 2012. Synaptic and extrasynaptic NMDA receptors are gated by different endogenous coagonists. Cell 150, 633–46. doi:10.1016/j.cell.2012.06.029

Parsons, C.G., Quack, G., Bresink, I., Baran, L., Przegalinski, E., Kostowski, W., Krzascik, P., Hartmann, S., Danysz, W., 1995. Comparison of the potency,

kinetics and voltage-dependency of a series of uncompetitive NMDA receptor antagonists in vitro with anticonvulsive and motor impairment activity in vivo. Neuropharmacology 34, 1239–58.

Parsons, M.P., Raymond, L.A., 2014. Extrasynaptic NMDA Receptor Involvement in Central Nervous System Disorders. Neuron 82, 279–293. doi:10.1016/j.neuron.2014.03.030

Philpot, B.D., Cho, K.K.A., Bear, M.F., 2007. Obligatory role of NR2A for metaplasticity in visual cortex. Neuron 53, 495–502. doi:10.1016/j.neuron.2007.01.027

Pohl, D., Bittigau, P., Ishimaru, M.J., Stadthaus, D., Hübner, C., Olney, J.W., Turski, L., Ikonomidou, C., 1999. N-Methyl-D-aspartate antagonists and apoptotic cell death triggered by head trauma in developing rat brain. Proceedings of the National Academy of Sciences of the United States of America 96, 2508–13.

Portera-Cailliau, C., Price, D.L., Martin, L.J., 1996. N-methyl-D-aspartate receptor proteins NR2A and NR2B are differentially distributed in the developing rat central nervous system as revealed by subunit-specific antibodies. Journal of neurochemistry 66, 692–700.

Prybylowski, K., Chang, K., Sans, N., Kan, L., Vicini, S., Wenthold, R.J., 2005. The synaptic localization of NR2B-containing NMDA receptors is controlled by interactions with PDZ proteins and AP-2. Neuron 47, 845–57. doi:10.1016/j.neuron.2005.08.016

Puddifoot, C., Martel, M.-A., Soriano, F.X., Camacho, A., Vidal-Puig, A., Wyllie, D.J.A., Hardingham, G.E., 2012. PGC-1α negatively regulates extrasynaptic NMDAR activity and excitotoxicity. The Journal of neuroscience : the official journal of the Society for Neuroscience 32, 6995–7000. doi:10.1523/JNEUROSCI.6407-11.2012

Punnakkal, P., Jendritza, P., Köhr, G., 2012. Influence of the intracellular GluN2 C-terminal domain on NMDA receptor function. Neuropharmacology 62, 1985–92. doi:10.1016/j.neuropharm.2011.12.018

Qiu, J., Tan, Y.-W., Hagenston, A.M., Martel, M.-A., Kneisel, N., Skehel, P.A., Wyllie, D.J.A., Bading, H., Hardingham, G.E., 2013. Mitochondrial calcium uniporter Mcu controls excitotoxicity and is transcriptionally repressed by neuroprotective nuclear calcium signals. Nature communications 4, 2034. doi:10.1038/ncomms3034

Quinlan, E.M., Philpot, B.D., Huganir, R.L., Bear, M.F., 1999. Rapid, experience-dependent expression of synaptic NMDA receptors in visual cortex in vivo. Nature neuroscience 2, 352–7. doi:10.1038/7263

Rachline, J., Perin-Dureau, F., Le Goff, A., Neyton, J., Paoletti, P., 2005. The micromolar zinc-binding domain on the NMDA receptor subunit NR2B. The

Journal of neuroscience : the official journal of the Society for Neuroscience 25, 308–17. doi:10.1523/JNEUROSCI.3967-04.2005

Rajadhyaksha, A., Barczak, A., Macías, W., Leveque, J.C., Lewis, S.E., Konradi, C., 1999. L-Type Ca(2+) channels are essential for glutamate-mediated CREB phosphorylation and c-fos gene expression in striatal neurons. The Journal of neuroscience : the official journal of the Society for Neuroscience 19, 6348–59.

Rammes, G., Rupprecht, R., Ferrari, U., Zieglgänsberger, W., Parsons, C.G., 2001. The N-methyl-D-aspartate receptor channel blockers memantine, MRZ 2/579 and other amino-alkyl-cyclohexanes antagonise 5-HT(3) receptor currents in cultured HEK-293 and N1E-115 cell systems in a non-competitive manner. Neuroscience letters 306, 81–4.

Ramoa, A.S., Alkondon, M., Aracava, Y., Irons, J., Lunt, G.G., Deshpande, S.S., Wonnacott, S., Aronstam, R.S., Albuquerque, E.X., 1990. The anticonvulsant MK-801 interacts with peripheral and central nicotinic acetylcholine receptor ion channels. The Journal of pharmacology and experimental therapeutics 254, 71–82.

Rauner, C., Köhr, G., 2011. Triheteromeric NR1/NR2A/NR2B receptors constitute the major N-methyl-D-aspartate receptor population in adult hippocampal synapses. The Journal of biological chemistry 286, 7558–66. doi:10.1074/jbc.M110.182600

Reisberg, B., Doody, R., Stöffler, A., Schmitt, F., Ferris, S., Möbius, H.J., 2003. Memantine in moderate-to-severe Alzheimer's disease. The New England journal of medicine 348, 1333–41. doi:10.1056/NEJMoa013128

Reynolds, I.J., Miller, R.J., 1988. Multiple sites for the regulation of the N-methyl-D-aspartate receptor. Molecular pharmacology 33, 581–4.

Riou, M., Stroebel, D., Edwardson, J.M., Paoletti, P., 2012. An alternating GluN1-2-1-2 subunit arrangement in mature NMDA receptors. PloS one 7, e35134. doi:10.1371/journal.pone.0035134

Roberts, A.C., Díez-García, J., Rodriguiz, R.M., López, I.P., Luján, R., Martínez-Turrillas, R., Picó, E., Henson, M.A., Bernardo, D.R., Jarrett, T.M., Clendeninn, D.J., López-Mascaraque, L., Feng, G., Lo, D.C., Wesseling, J.F., Wetsel, W.C., Philpot, B.D., Pérez-Otaño, I., 2009. Downregulation of NR3A-containing NMDARs is required for synapse maturation and memory consolidation. Neuron 63, 342–56. doi:10.1016/j.neuron.2009.06.016

Rodenas-Ruano, A., Chávez, A.E., Cossio, M.J., Castillo, P.E., Zukin, R.S., 2012. REST-dependent epigenetic remodeling promotes the developmental switch in synaptic NMDA receptors. Nature neuroscience 15, 1382–90. doi:10.1038/nn.3214

Roselli, F., Tirard, M., Lu, J., Hutzler, P., Lamberti, P., Livrea, P., Morabito, M.,

Almeida, O.F.X., 2005. Soluble beta-amyloid1-40 induces NMDA-dependent degradation of postsynaptic density-95 at glutamatergic synapses. The Journal of neuroscience : the official journal of the Society for Neuroscience 25, 11061–70. doi:10.1523/JNEUROSCI.3034-05.2005

Rosenberg, D., Artoul, S., Segal, A.C., Kolodney, G., Radzishevsky, I., Dikopoltsev, E., Foltyn, V.N., Inoue, R., Mori, H., Billard, J.-M., Wolosker, H., 2013. Neuronal D-serine and glycine release via the Asc-1 transporter regulates NMDA receptor-dependent synaptic activity. The Journal of neuroscience : the official journal of the Society for Neuroscience 33, 3533–44. doi:10.1523/JNEUROSCI.3836-12.2013

Rutter, A.R., Stephenson, F.A., 2000. Coexpression of postsynaptic density-95 protein with NMDA receptors results in enhanced receptor expression together with a decreased sensitivity to L-glutamate. Journal of neurochemistry 75, 2501–10.

Ryan, T.J., Emes, R.D., Grant, S.G., Komiyama, N.H., 2008. Evolution of NMDA receptor cytoplasmic interaction domains: implications for organisation of synaptic signalling complexes. BMC neuroscience 9, 6. doi:10.1186/1471-2202-9-6

Ryan, T.J., Kopanitsa, M. V, Indersmitten, T., Nithianantharajah, J., Afinowi, N.O., Pettit, C., Stanford, L.E., Sprengel, R., Saksida, L.M., Bussey, T.J., O'Dell, T.J., Grant, S.G.N., Komiyama, N.H., 2013. Evolution of GluN2A/B cytoplasmic domains diversified vertebrate synaptic plasticity and behavior. Nature neuroscience 16, 25–32. doi:10.1038/nn.3277

Sanz-Clemente, A., Gray, J.A., Ogilvie, K.A., Nicoll, R.A., Roche, K.W., 2013. Activated CaMKII couples GluN2B and casein kinase 2 to control synaptic NMDA receptors. Cell reports 3, 607–14. doi:10.1016/j.celrep.2013.02.011

Sanz-Clemente, A., Matta, J.A., Isaac, J.T.R., Roche, K.W., 2010. Casein kinase 2 regulates the NR2 subunit composition of synaptic NMDA receptors. Neuron 67, 984–96. doi:10.1016/j.neuron.2010.08.011

Schneider, L.S., Dagerman, K.S., Higgins, J.P.T., McShane, R., 2011. Lack of evidence for the efficacy of memantine in mild Alzheimer disease. Archives of neurology 68, 991–8. doi:10.1001/archneurol.2011.69

Seeman, P., Caruso, C., Lasaga, M., 2008. Memantine agonist action at dopamine D2High receptors. Synapse (New York, N.Y.) 62, 149–53. doi:10.1002/syn.20472

Shankar, G.M., Bloodgood, B.L., Townsend, M., Walsh, D.M., Selkoe, D.J., Sabatini, B.L., 2007. Natural oligomers of the Alzheimer amyloid-beta protein induce reversible synapse loss by modulating an NMDA-type glutamate receptor-dependent signaling pathway. The Journal of neuroscience : the

official journal of the Society for Neuroscience 27, 2866–75. doi:10.1523/JNEUROSCI.4970-06.2007

Sheng, M., Cummings, J., Roldan, L.A., Jan, Y.N., Jan, L.Y., 1994. Changing subunit composition of heteromeric NMDA receptors during development of rat cortex. Nature 368, 144–7. doi:10.1038/368144a0

Shih, P.-Y., Savtchenko, L.P., Kamasawa, N., Dembitskaya, Y., McHugh, T.J., Rusakov, D.A., Shigemoto, R., Semyanov, A., 2013. Retrograde synaptic signaling mediated by K+ efflux through postsynaptic NMDA receptors. Cell reports 5, 941–51. doi:10.1016/j.celrep.2013.10.026

Shin, A.H., Kim, H.J., Thayer, S.A., 2012. Subtype selective NMDA receptor antagonists induce recovery of synapses lost following exposure to HIV-1 Tat. British journal of pharmacology 166, 1002–17. doi:10.1111/j.1476-5381.2011.01805.x

Shipton, O.A., Paulsen, O., 2014. GluN2A and GluN2B subunit-containing NMDA receptors in hippocampal plasticity. Philosophical transactions of the Royal Society of London. Series B, Biological sciences 369, 20130163. doi:10.1098/rstb.2013.0163

Siegler Retchless, B., Gao, W., Johnson, J.W., 2012. A single GluN2 subunit residue controls NMDA receptor channel properties via intersubunit interaction. Nature neuroscience 15, 406–13, S1–2. doi:10.1038/nn.3025

Simon, R., Swan, J., Griffiths, T., Meldrum, B., 1984. Blockade of N-methyl-D-aspartate receptors may protect against ischemic damage in the brain. Science 226, 850–852. doi:10.1126/science.6093256

Soriano, F.X., Martel, M.-A., Papadia, S., Vaslin, A., Baxter, P., Rickman, C., Forder, J., Tymianski, M., Duncan, R., Aarts, M., Clarke, P., Wyllie, D.J.A., Hardingham, G.E., 2008. Specific targeting of pro-death NMDA receptor signals with differing reliance on the NR2B PDZ ligand. The Journal of neuroscience : the official journal of the Society for Neuroscience 28, 10696–710. doi:10.1523/JNEUROSCI.1207-08.2008

Sprengel, R., Suchanek, B., Amico, C., Brusa, R., Burnashev, N., Rozov, A., Hvalby, O., Jensen, V., Paulsen, O., Andersen, P., Kim, J.J., Thompson, R.F., Sun, W., Webster, L.C., Grant, S.G., Eilers, J., Konnerth, A., Li, J., McNamara, J.O., Seeburg, P.H., 1998. Importance of the intracellular domain of NR2 subunits for NMDA receptor function in vivo. Cell 92, 279–89.

Stanika, R.I., Pivovarova, N.B., Brantner, C.A., Watts, C.A., Winters, C.A., Andrews, S.B., 2009. Coupling diverse routes of calcium entry to mitochondrial dysfunction and glutamate excitotoxicity. Proceedings of the National Academy of Sciences of the United States of America 106, 9854–9. doi:10.1073/pnas.0903546106

Stanton, P.K., Jones, R.S.G., Mody, I., Heinemann, U., 1987. Epileptiform activity induced by lowering extracellular [Mg2+] in combined hippocampal-entorhinal cortex slices: Modulation by receptors for norepinephrine and N-methyl-d-aspartate. Epilepsy Research 1, 53–62. doi:10.1016/0920-1211(87)90051-9

Steigerwald, F., Schulz, T.W., Schenker, L.T., Kennedy, M.B., Seeburg, P.H., Kohr, G., 2000. C-Terminal Truncation of NR2A Subunits Impairs Synaptic But Not Extrasynaptic Localization of NMDA Receptors. J. Neurosci. 20, 4573–4581.

Strack, S., McNeill, R.B., Colbran, R.J., 2000. Mechanism and regulation of calcium/calmodulin-dependent protein kinase II targeting to the NR2B subunit of the N-methyl-D-aspartate receptor. The Journal of biological chemistry 275, 23798–806. doi:10.1074/jbc.M001471200

Supplisson, S., Bergman, C., 1997. Control of NMDA Receptor Activation by a Glycine Transporter Co-Expressed in Xenopus Oocytes. J. Neurosci. 17, 4580–4590.

Sutton, M.A., Ito, H.T., Cressy, P., Kempf, C., Woo, J.C., Schuman, E.M., 2006. Miniature neurotransmission stabilizes synaptic function via tonic suppression of local dendritic protein synthesis. Cell 125, 785–99. doi:10.1016/j.cell.2006.03.040

Talkowski, M.E., Rosenfeld, J.A., Blumenthal, I., Pillalamarri, V., Chiang, C., Heilbut, A., Ernst, C., Hanscom, C., Rossin, E., Lindgren, A.M., Pereira, S., Ruderfer, D., Kirby, A., Ripke, S., Harris, D.J., Lee, J.-H., Ha, K., Kim, H.-G., Solomon, B.D., Gropman, A.L., Lucente, D., Sims, K., Ohsumi, T.K., Borowsky, M.L., Loranger, S., Quade, B., Lage, K., Miles, J., Wu, B.-L., Shen, Y., Neale, B., Shaffer, L.G., Daly, M.J., Morton, C.C., Gusella, J.F., 2012. Sequencing chromosomal abnormalities reveals neurodevelopmental loci that confer risk across diagnostic boundaries. Cell 149, 525–37. doi:10.1016/j.cell.2012.03.028

Tang, T.T.-T., Badger, J.D., Roche, P.A., Roche, K.W., 2010. Novel approach to probe subunit-specific contributions to N-methyl-D-aspartate (NMDA) receptor trafficking reveals a dominant role for NR2B in receptor recycling. The Journal of biological chemistry 285, 20975–81. doi:10.1074/jbc.M110.102210

Thomas, C.G., Miller, A.J., Westbrook, G.L., 2006. Synaptic and extrasynaptic NMDA receptor NR2 subunits in cultured hippocampal neurons. Journal of neurophysiology 95, 1727–34. doi:10.1152/jn.00771.2005

Tovar, K.R., McGinley, M.J., Westbrook, G.L., 2013. Triheteromeric NMDA receptors at hippocampal synapses. The Journal of neuroscience : the official journal of the Society for Neuroscience 33, 9150–60. doi:10.1523/JNEUROSCI.0829-13.2013

Tovar, K.R., Westbrook, G.L., 1999. The incorporation of NMDA receptors with a

distinct subunit composition at nascent hippocampal synapses in vitro. The Journal of neuroscience : the official journal of the Society for Neuroscience 19, 4180–8.

Tovar, K.R., Westbrook, G.L., 2002. Mobile NMDA receptors at hippocampal synapses. Neuron 34, 255–64.

Traynelis, S.F., Hartley, M., Heinemann, S.F., 1995. Control of proton sensitivity of the NMDA receptor by RNA splicing and polyamines. Science (New York, N.Y.) 268, 873–6.

Tsai, G., Ralph-Williams, R.J., Martina, M., Bergeron, R., Berger-Sweeney, J., Dunham, K.S., Jiang, Z., Caine, S.B., Coyle, J.T., 2004. Gene knockout of glycine transporter 1: characterization of the behavioral phenotype. Proceedings of the National Academy of Sciences of the United States of America 101, 8485–90. doi:10.1073/pnas.0402662101

Tu, W., Xu, X., Peng, L., Zhong, X., Zhang, Wenfeng, Soundarapandian, M.M., Balel, C., Wang, M., Jia, N., Zhang, Wen, Lew, F., Chan, S.L., Chen, Y., Lu, Y., 2010. DAPK1 interaction with NMDA receptor NR2B subunits mediates brain damage in stroke. Cell 140, 222–34. doi:10.1016/j.cell.2009.12.055

Um, J.W., Nygaard, H.B., Heiss, J.K., Kostylev, M.A., Stagi, M., Vortmeyer, A., Wisniewski, T., Gunther, E.C., Strittmatter, S.M., 2012. Alzheimer amyloid-β oligomer bound to postsynaptic prion protein activates Fyn to impair neurons. Nature neuroscience 15, 1227–35. doi:10.1038/nn.3178

Valor, L.M., Charlesworth, P., Humphreys, L., Anderson, C.N.G., Grant, S.G.N., 2007. Network activity-independent coordinated gene expression program for synapse assembly. Proceedings of the National Academy of Sciences of the United States of America 104, 4658–63. doi:10.1073/pnas.0609071104

Von Engelhardt, J., Coserea, I., Pawlak, V., Fuchs, E.C., Köhr, G., Seeburg, P.H., Monyer, H., 2007. Excitotoxicity in vitro by NR2A- and NR2B-containing NMDA receptors. Neuropharmacology 53, 10–7. doi:10.1016/j.neuropharm.2007.04.015

Von Engelhardt, J., Doganci, B., Seeburg, P.H., Monyer, H., 2009. Synaptic NR2A-but not NR2B-Containing NMDA Receptors Increase with Blockade of Ionotropic Glutamate Receptors. Frontiers in molecular neuroscience 2, 19. doi:10.3389/neuro.02.019.2009

Wang, L.Y., Orser, B.A., Brautigan, D.L., MacDonald, J.F., 1994. Regulation of NMDA receptors in cultured hippocampal neurons by protein phosphatases 1 and 2A. Nature 369, 230–2. doi:10.1038/369230a0

Watanabe, M., Inoue, Y., Sakimura, K., Mishina, M., 1992. Developmental changes in distribution of NMDA receptor channel subunit mRNAs. Neuroreport 3, 1138–40.

Weick, J.P., Groth, R.D., Isaksen, A.L., Mermelstein, P.G., 2003. Interactions with PDZ proteins are required for L-type calcium channels to activate cAMP response element-binding protein-dependent gene expression. The Journal of neuroscience : the official journal of the Society for Neuroscience 23, 3446–56.

Wild, A.R., Akyol, E., Brothwell, S.L.C., Kimkool, P., Skepper, J.N., Gibb, A.J., Jones, S., 2013. Memantine block depends on agonist presentation at the NMDA receptor in substantia nigra pars compacta dopamine neurones. Neuropharmacology 73, 138–146. doi:10.1016/j.neuropharm.2013.05.013

Williams, K., Russell, S.L., Shen, Y.M., Molinoff, P.B., 1993. Developmental switch in the expression of NMDA receptors occurs in vivo and in vitro. Neuron 10, 267–78.

Wong, E.H., Kemp, J.A., Priestley, T., Knight, A.R., Woodruff, G.N., Iversen, L.L., 1986. The anticonvulsant MK-801 is a potent N-methyl-D-aspartate antagonist. Proceedings of the National Academy of Sciences of the United States of America 83, 7104–8.

Wrighton, D.C., Baker, E.J., Chen, P.E., Wyllie, D.J.A., 2008. Mg2+ and memantine block of rat recombinant NMDA receptors containing chimeric NR2A/2D subunits expressed in Xenopus laevis oocytes. The Journal of physiology 586, 211–25. doi:10.1113/jphysiol.2007.143164

Wroge, C.M., Hogins, J., Eisenman, L., Mennerick, S., 2012. Synaptic NMDA receptors mediate hypoxic excitotoxic death. The Journal of neuroscience : the official journal of the Society for Neuroscience 32, 6732–42. doi:10.1523/JNEUROSCI.6371-11.2012

Wu, G.Y., Deisseroth, K., Tsien, R.W., 2001. Activity-dependent CREB phosphorylation: convergence of a fast, sensitive calmodulin kinase pathway and a slow, less sensitive mitogen-activated protein kinase pathway. Proceedings of the National Academy of Sciences of the United States of America 98, 2808–13. doi:10.1073/pnas.051634198

Wyllie, D.J.A., Livesey, M.R., Hardingham, G.E., 2013. Influence of GluN2 subunit identity on NMDA receptor function. Neuropharmacology 74, 4–17. doi:10.1016/j.neuropharm.2013.01.016

Xia, P., Chen, H.V., Zhang, D., Lipton, S.A., 2010. Memantine preferentially blocks extrasynaptic over synaptic NMDA receptor currents in hippocampal autapses. The Journal of neuroscience : the official journal of the Society for Neuroscience 30, 11246–50. doi:10.1523/JNEUROSCI.2488-10.2010

Xue, J., Li, G., Laabich, A., Cooper, N.G., 2001. Visual-mediated regulation of retinal CaMKII and its GluR1 substrate is age-dependent. Brain research. Molecular brain research 93, 95–104.

Yang, K., Trepanier, C., Sidhu, B., Xie, Y.-F., Li, H., Lei, G., Salter, M.W., Orser,

B.A., Nakazawa, T., Yamamoto, T., Jackson, M.F., Macdonald, J.F., 2012. Metaplasticity gated through differential regulation of GluN2A versus GluN2B receptors by Src family kinases. The EMBO journal 31, 805–16. doi:10.1038/emboj.2011.453

You, H., Tsutsui, S., Hameed, S., Kannanayakal, T.J., Chen, L., Xia, P., Engbers, J.D.T., Lipton, S.A., Stys, P.K., Zamponi, G.W., 2012. Aβ neurotoxicity depends on interactions between copper ions, prion protein, and N-methyl-D-aspartate receptors. Proceedings of the National Academy of Sciences of the United States of America 109, 1737–42. doi:10.1073/pnas.1110789109

Young, A., Greenamyre, J., Hollingsworth, Z., Albin, R., D'Amato, C., Shoulson, I., Penney, J., 1988. NMDA receptor losses in putamen from patients with Huntington's disease. Science 241, 981–983. doi:10.1126/science.2841762

Yuan, H., Hansen, K.B., Zhang, J., Pierson, T.M., Markello, T.C., Fajardo, K.V.F., Holloman, C.M., Golas, G., Adams, D.R., Boerkoel, C.F., Gahl, W.A., Traynelis, S.F., 2014. Functional analysis of a de novo GRIN2A missense mutation associated with early-onset epileptic encephalopathy. Nature communications 5, 3251. doi:10.1038/ncomms4251

Yuzaki, M., Miyawaki, A., Akita, K., Kudo, Y., Ogura, A., Ino, H., Mikoshiba, K., 1990. Mode of blockade by MK-801 of N-methyl-d-aspartate-induced increase in intracellular Ca2+ in cultured mouse hippocampal neurons. Brain Research 517, 51–56. doi:10.1016/0006-8993(90)91006-3

Zeron, M.M., Hansson, O., Chen, N., Wellington, C.L., Leavitt, B.R., Brundin, P., Hayden, M.R., Raymond, L.A., 2002. Increased sensitivity to N-methyl-D-aspartate receptor-mediated excitotoxicity in a mouse model of Huntington's disease. Neuron 33, 849–60.

Zhai, S., Ark, E.D., Parra-Bueno, P., Yasuda, R., 2013. Long-distance integration of nuclear ERK signaling triggered by activation of a few dendritic spines. Science (New York, N.Y.) 342, 1107–11. doi:10.1126/science.1245622

Zhang, L., Zheng, X., Paupard, M.C., Wang, A.P., Santchi, L., Friedman, L.K., Zukin, R.S., Bennett, M. V, 1994. Spermine potentiation of recombinant N-methyl-D-aspartate receptors is affected by subunit composition. Proceedings of the National Academy of Sciences of the United States of America 91, 10883–7.

Zhang, S.-J., Zou, M., Lu, L., Lau, D., Ditzel, D.A.W., Delucinge-Vivier, C., Aso, Y., Descombes, P., Bading, H., 2009. Nuclear calcium signaling controls expression of a large gene pool: identification of a gene program for acquired neuroprotection induced by synaptic activity. PLoS genetics 5, e1000604. doi:10.1371/journal.pgen.1000604

Zhou, X., Hollern, D., Liao, J., Andrechek, E., Wang, H., 2013. NMDA receptor-

mediated excitotoxicity depends on the coactivation of synaptic and extrasynaptic receptors. Cell death & disease 4, e560. doi:10.1038/cddis.2013.82